

ABNORMAL HIPPOCAMPAL SYNAPTIC CONNECTIVITY IN SCHIZOPHRENIA

By

CLINT ERNEST YOUNG

B.Sc., The University of British Columbia, 1991

A THESIS SUBMITTED IN PARTIAL FULFILLMENT OF

THE REQUIREMENT FOR THE DEGREE OF

DOCTOR OF PHILOSOPHY

In

THE FACULTY OF GRADUATE STUDIES

(Graduate Program in Neuroscience)

We accept this thesis as conforming to the required standard

THE UNIVERSITY OF BRITISH COLUMBIA

January 22, 2001

Copyright Clint Ernest Young, 2001

In presenting this thesis in partial fulfilment of the requirements for an advanced degree at the University of British Columbia, I agree that the Library shall make it freely available for reference and study. I further agree that permission for extensive copying of this thesis for scholarly purposes may be granted by the head of my department or by his or her representatives. It is understood that copying or publication of this thesis for financial gain shall not be allowed without my written permission.

Department of Psychiatry

The University of British Columbia
Vancouver, Canada

Date April 27 / 2001

ABSTRACT

The thesis was designed to address three major questions about the pathogenesis of schizophrenia. First, given findings of abnormal organisation of layer II and III neurons of the schizophrenic entorhinal hippocampus, would the perforant pathway ERC→hippocampal circuitry be altered? The investigation began by using improved methods of nonfluorescent immunocolocalisation and quantitative immunohistochemistry to assess the distribution and amount of presynaptic protein immunoreactivity [ir] (synaptophysin and SNAP-25; markers of synaptic density) in schizophrenia with normal controls. The perforant pathway termination zones in schizophrenia showed unchanged amounts of synaptophysin (an indirect indicator of synapses globally) and decreased amounts of SNAP-25 (enriched in a subset of synapses), suggesting that (a subset of) circuits from the entorhinal cortex to the hippocampus may be disconnected in schizophrenia. Second, given findings suggesting abnormal development in schizophrenia, would specific regions of the dentate gyrus (which have a different developmental profile) have altered circuitry in schizophrenia? Using optimised immunohistochemical image analysis of presynaptic proteins, schizophrenia showed that the number of terminals (as assessed by fractional area of immunostaining) was similarly increased for both limbs as gauged by synaptophysin ir and was more prominently reduced in the (later forming) internal limb than the (earlier forming) external limb of the dentate gyrus with SNAP-25 ir, which is consistent with the notion that schizophrenia may be a prenatal defect at 39-40 weeks gestational age (or earlier) when the two limbs should be

identical – although differential postnatal properties between the limbs is also plausible. Thirdly, given that most schizophrenics are exposed to antipsychotic drugs (APDs), could the changes in presynaptic proteins seen here in schizophrenia be attributed to APD treatment? Using an approach to immunohistochemical image analysis parallel to the studies of schizophrenia, we studied presynaptic proteins (synaptophysin and SNAP-25) in rats exposed to typical APDs (haloperidol, chlorpromazine, and trifluoperazine). Analysis of the ERC→hippocampal circuit after APD exposure generally revealed changes in presynaptic protein different in distribution and amount from that seen in schizophrenia. The results of this thesis indicate that schizophrenia may be a defect that results in aberrant synaptic reorganisation possibly arising from a prenatal developmental problem or from postnatal influences.

TABLE OF CONTENTS

ABSTRACT	ii
TABLE OF CONTENTS	iv
LIST OF TABLES	vi
LIST OF FIGURES	vii
CHAPTER I ABNORMAL HIPPOCAMPAL SYNAPTIC CONNECTIVITY IN SCHIZOPHRENIA	1
I.1. HIPPOCAMPUS IN SCHIZOPHRENIA.....	5
I.2. MECHANISM OF ILLNESS (DEVELOPMENTAL)	15
I.3. EFFECTS OF ANTIPSYCHOTIC DRUGS ON SYNAPTIC CONNECTIVITY	25
I.4. MEASURING SYNAPTIC CONNECTIVITY	28
I.5. OBJECTIVE.....	35
CHAPTER II INTENSITY AND DISTRIBUTION OF PRESYNAPTIC PROTEIN	
IMMUNOREACTIVITY IN HIPPOCAMPUS IN SCHIZOPHRENIA	37
II.1. OVERVIEW.....	37
II.2. MATERIALS & METHODS	38
II.3. RESULTS.....	68
II.4. CONCLUSION	79
CHAPTER III MECHANISMS OF ILLNESS IN SCHIZOPHRENIA: GRANULE CELL LAYER	
DEVELOPMENT OF DENTATE GYRUS	80
III.1. OVERVIEW.....	80
III.2. MATERIALS & METHODS	81
III.3. RESULTS.....	88
III.4. CONCLUSION	95
CHAPTER IV ANTI-PSYCHOTIC DRUG TREATMENT	96
IV.1. OVERVIEW.....	96
IV.2. MATERIALS & METHODS	96
IV.3. RESULTS.....	104
IV.4. CONCLUSION	122
CHAPTER V DISCUSSION	124
V.1. OVERVIEW.....	124
V.2. ASPECTS OF DENTATE DEVELOPMENT: LIMBS AND GRANULE CELLS.....	131
V.3. SYNAPTIC CHANGES FROM APD TREATMENT	142
V.4. LIMITATIONS	144
V.5. SUMMARY	147
REFERENCES	148

APPENDIX I: AUTOFLUORESCENCE ARTIFACTS.....176
A. THE BASIS OF AUTOFLUORESCENCE & ATTEMPTS TO BLOCK AUTOFLUORESCENCE176

LIST OF TABLES

Table I-1	Entorhinal projections to hippocampus.....	11
Table I-2	Effects of Haloperidol on presynaptic mRNA	27
Table II-1	Human brains studied.....	60
Table V-1	Summary of Overall Hippocampus: Changes in presynaptic protein.....	124
Table V-2	Summary of Dentate Gyrus: Changes in presynaptic proteins.....	125
Table V-3	Changes in Entorhinal cortical layers in schizophrenia	127
Table V-4	Dentate Granule Cells: Deep versus Superficial Granule cells	136

LIST OF FIGURES

Figure I-1	Perforant pathway inputs from entorhinal cortex to hippocampus.....	14
Figure I-2	Cellular layers of the dentate gyrus.....	22
Figure I-3	Developmental sequence of the two limbs of the dentate gyrus.....	23
Figure I-4	Development across the span of the granule cell layer.....	24
Figure II-1	Quantification with ELISA system using a spectrophotometer.....	41
Figure II-2	Quantification with immunohistochemical system using a CCD camera.....	41
Figure II-3	Spectral response curve for the CCD camera.....	44
Figure II-4	Colour wheel: optical relationship among colours.....	44
Figure II-5	Example of an immunostain biological standard.....	48
Figure II-6	High magnification images of immunostained biological standard.....	48
Figure II-7	OD step tablets.....	53
Figure II-8	Relationship between grey pixel value and OD.....	53
Figure II-9	Relationship between antigen amount and OD for synaptophysin immunostaining.....	56
Figure II-10	Relationship between antigen amount and OD for SNAP-25 immunostaining.....	57
Figure II-11	Relationship between grey pixel value and DAB parameters.....	58
Figure II-12	Graph demonstrating calculation of the optimal DAB incubation time.....	58
Figure II-13	Regions and layers of an immunostained human hippocampus.....	63
Figure II-14	Schizophrenic hippocampus: altered levels of presynaptic-ir.....	71
Figure II-15	AEC codistribution of synaptophysin and MBP.....	73
Figure II-16	AEC codistribution of NeuN and GFAP.....	74
Figure II-17	Different sequential AEC processing for codistribution of NeuN and GFAP.....	75
Figure II-18	AEC codistribution of synaptophysin and SNAP-25 in control hippocampus.....	77
Figure II-19	AEC codistribution of synaptophysin and SNAP-25 in schizophrenic hippocampus.....	78
Figure III-1	Full extent of both dentate limbs sampled at 20x magnification.....	85
Figure III-2	Outlining the granule cell layer at 20x magnification.....	85
Figure III-3	Subdividing the granule cell layer into five parts.....	86
Figure III-4	Segmenting an immunostained image into stained/unstained regions.....	87
Figure III-5	Schizophrenic GCL: SNAP-25 analysis.....	89
Figure III-6	Schizophrenic GCL: Synaptophysin analysis.....	90
Figure IV-1	Regions and layers of an immunostained rat hippocampus.....	101
Figure IV-2	Sample images taken from both dentate limbs.....	101

Figure IV-3	Outlining the granule cell layer at 40x magnification.....	102
Figure IV-4	Rat hippocampus: Haloperidol treatment on presynaptic proteins	106
Figure IV-5	Rat hippocampus: Chlorpromazine treatment on presynaptic proteins	107
Figure IV-6	Rat hippocampus: Trifluoperazine treatment on presynaptic proteins	108
Figure IV-7	Rat GCL: Haloperidol effects on SNAP-25 ir.....	112
Figure IV-8	Rat GCL: Haloperidol effects on Synaptophysin ir.....	113
Figure IV-9	Rat GCL: Chlorpromazine effects on SNAP-25 ir	116
Figure IV-10	Rat GCL: Chlorpromazine effects on Synaptophysin ir	117
Figure IV-11	Rat GCL: Trifluoperazine effects on SNAP-25 ir	120
Figure IV-12	Rat GCL: Trifluoperazine effects on Synaptophysin ir	121
Figure V-1	Summary: Schizophrenia and APD effects on SNAP-25 ir	130
Figure V-2	Summary: Schizophrenia and APD effects on Synaptophysin ir	131

Chapter I ABNORMAL HIPPOCAMPAL SYNAPTIC CONNECTIVITY IN SCHIZOPHRENIA

OVERVIEW

Schizophrenia is a syndrome (cluster or constellation of signs and symptoms) affecting the patient's ability to test reality, and affecting the cognitive and emotional aspects in patients, resulting in inappropriate emotions (autism, ambivalence, loose associations, flat affect), and disturbed cognitions (delusions, hallucinations, thought disorders, feeling of external control).

There is a 1% lifetime risk of developing schizophrenia (Hare 1987) such that the disease can strike any time between early teens to late 70s, the majority of cases having an onset of between 15-45. Generally, for men the peak onset is 27 years of age while women have a later peak onset of 30 (and a smaller peak of 45); although both sexes are affected equally.

What is known as schizophrenia today was first characterised a little more than 100 years ago when in 1896 Emil Kraepelin (Kraepelin, Barclay et al. 1919) separated what he then called *dementia praecox* from other disorders like mood disorder and another illness recently characterised by his good friend Alois Alzheimer. By looking at the long-term outcomes of hundreds of patients, Kraepelin observed that *dementia praecox* was a dementia (a decline in memory or other cognitive function in comparison with the patient's previous level of functioning) that occurred precociously (early in adolescent life), was progressively deteriorating (of cognition and function), and without remission ultimately leading to a dramatic loss of intellect – making it very similar to Alzheimer's

disease except that Alzheimer's mainly occurred in the elderly. Dementia praecox was also very different from manic-depressive disorder which has no dementia, later onset, was without progressive deterioration, and had a fluctuating course (remissions and relapses).

Eugene Bleuler objected to Kraepelin's definition of this illness because Bleuler saw that dementia was not an inevitable outcome of the disease, that in some patients the disease struck in adulthood, and he observed occasional remissions. Bleuler wanted to emphasise the cognitive impairment, the loose and disorganised thinking in this disorder – so in 1911 he coined the term "schizophrenia," which is Greek meaning a "schism" or splitting of the mind from reality (Bleuler 1950). He believed schizophrenia had four fundamental symptoms, called the "four A's":

- Autism
- Ambivalence
- loose Associations
- blunt Affect

German psychiatrist Kurt Schneider in 1959 wanted, instead, to emphasize other symptoms as diagnostic indicators of schizophrenia, so he created a list of "1st rank symptoms" (Schneider 1959). One of these, in the absence of organic disease, persistent affective disorder, or drug intoxication, was sufficient for a diagnosis of schizophrenia:

- primary delusions (unshakeable belief inconsistent with the patient's educational and cultural background that is fully formed and has no connection with previous events)
- 3rd person auditory hallucinations (running commentaries on the patient's actions or thoughts, or arguments about the patient)
- thought insertion, withdrawal, broadcasting
- feelings of external control over the patient's emotions, behaviours, and thoughts.

The Diagnostic and Statistical Manual (DSM) of the American Psychiatric Association currently provides the most widely used system for diagnosing and classifying schizophrenia in North America and in the international research community. DSM's diagnosis of schizophrenia represents a convergence of all these views incorporating Kraepelin's course, Bleuler's fundamental symptoms, and Schneider's emphasis on delusions and hallucinations. Under DSM-IV criteria, to be diagnosed with schizophrenia, one needs all of the following:

- psychosis lasting longer than a month
- loss of function greater than six months
- not due to mood disorder nor organic cause
- deteriorating social or occupational function
- if autistic, prominent hallucinations and delusions.

In terms of research implications, the study of the schizophrenia syndrome can proceed only by first identifying the patient population. The validity and replicability of the diagnosis therefore fundamentally affects the validity and reliability of any research into this disorder.

Although research has given greater insights into the impact of symptoms and the nature of the deficits associated with schizophrenia, the pathophysiology and causes of this illness are still not clearly understood. An increasingly popular notion is that schizophrenia is a neurodevelopment disorder (Pilowsky, Kerwin et al. 1993; Bunney, Potkin et al. 1995; Harrison 1995; Knable and Weinberger 1995; Arnold, Franz et al. 1996; Weinberger 1999) concerning a "non-lethal" disturbance during fetal development. Specifically, this model suggests that an insult occurs during the second trimester of pregnancy when differentiation and growth of the fetal central nervous system (CNS) is at its height. During this period, a minor insult to the CNS may have profound

effects. Damage to the CNS may occur as a result of maternal exposure to viruses/toxins, poor nutrition, birth injury/hypoxia, hemorrhage, an inborn error of gene expression or any combination of the above.

According to the neurodevelopmental model, obvious symptoms of schizophrenia are not evident in early childhood although subtle impairments of attention, motor incoordination and affective expression have been documented (Jones, Rodgers et al. 1994; David, Malmberg et al. 1997; Jones and Dones 1997; Malmberg, Lewis et al. 1998). In late adolescence or young adulthood, the so-called "latent lesion" becomes active as affected brain regions mature. Thereafter, the signs and symptoms of schizophrenia appear.

The search for the neuropathological basis of schizophrenia has received new impetus from the technical advances in neuroimaging and molecular neurosciences, leading to the consensus that the pathology appears to be most consistently observed in the medial temporal lobe, together with interconnected regions including the prefrontal cortex and cingulate gyrus.

Research into the role of the hippocampus in schizophrenia can be divided into four basic approaches: neuroimaging (using CT/MRI/PET scans), neuropsychological (testing temporohippocampal function), animal models (focusing on changes in behaviour and neuropathology that may give insight into schizophrenia), and pathological (using post-mortem tissue). The findings suggest that schizophrenia involves a defect in the plasticity of hippocampal circuitry and connectivity, a defect possibly based on abnormal neuronal development.

This thesis focuses on three main objectives:

1. to investigate if specific hippocampal circuits are altered in schizophrenia;
2. to see if a pattern of synaptic change in the developmentally organised subregions of the hippocampus (specifically the dentate gyrus) can help elucidate the timing of abnormal neuronal development in schizophrenia; and,
3. to study the effects of typical antipsychotic drugs on synaptic connectivity.

In examining synaptic connectivity in schizophrenia, I measured the intensity and distribution of presynaptic proteins (synaptophysin and SNAP-25) with quantitative immunohistochemistry in postmortem brain tissue.

I.1. HIPPOCAMPUS IN SCHIZOPHRENIA

I.1.A. BACKGROUND: Altered hippocampal connectivity in schizophrenia

The hippocampal formation has been a centerpiece of investigation in schizophrenia. Using such methods as neuroimaging, neuropsychological testing, animal models, and pathological research, studies have implicated abnormal circuitry and connectivity of the hippocampus in schizophrenia.

I.1.A.i. Hippocampus: Neuroimaging

A range of structural brain abnormalities have been found in schizophrenia using neuroimaging techniques. Computed tomographic [CT] scanning and magnetic resonance imaging [MRI] have shown that the population of patients with schizophrenia as a whole have ventricular and cortical sulcal enlargement as well as loss of gray matter volume (Ward, Friedman et al. 1996;

Lawrie and Abukmeil 1998). Positron emission tomography [PET] demonstrates functional abnormalities such as frontal hypometabolism(Chua and McKenna 1995).

I.1.A.i.a. Structural

Supporting the hypothesis that structural changes preferentially affect the temporal lobes are MRI findings of reduced temporal lobe volume and reduced hippocampal gray matter volume in schizophrenia(Lawrie and Abukmeil 1998; McCarley, Wible et al. 1999; Wright, Rabe-Hesketh et al. 2000). Most of the CT scan studies found no correlation between ventricular or cortical sulcal enlargement and the disease duration(Chua and McKenna 1995) and no significant difference in ventricular size in follow-up studies(Nasrallah, Andreasen et al. 1986; Illowsky, Juliano et al. 1988; Andreasen, Swayze et al. 1990), although one study found a stepwise progressive ventricular enlargement in a small subgroup of chronic deteriorating schizophrenic patients(Woods, Yurgelun-Todd et al. 1990).

I.1.A.i.b. Functional PET, MRIs

The findings of functional imaging studies for temporal lobe dysfunction in schizophrenia are inconsistent(Friston and Frith 1995; Velakoulis and Pantelis 1996); there have been reports of increased right-sided activity, increased left-sided activity, decreased left-sided activity, bilateral increases in function, and bilateral hypofunctioning. Recent studies have demonstrated reduced hippocampal N-acetylaspartate (NAA) with no change in hippocampal volume in schizophrenia, suggesting neuronal dysfunction or damage in the hippocampus rather than neuronal loss(Deicken, Pegues et al. 1999; Soares and Innis 1999)

I.1.A.ii. Hippocampus: Neuropsychological

Disturbances in the organisation or development of the temporal lobe may underlie certain aspects of the symptoms of schizophrenia. In particular, recent studies have shown neuropsychological and *in vivo* brain disturbances in the medial temporal lobe in schizophrenia, specifically the hippocampus. Schizophrenia patients showed neuropsychological deficits in tests related to temporohippocampal function (learning and memory) (Gruzelier, Seymour et al. 1988; Saykin, Gur et al. 1991; Goldberg, Torrey et al. 1994; Saykin, Shtasel et al. 1994; Rubin, Holm et al. 1995). A search to correlate MRI temporal lobe volume with neuropsychological deficits related to hippocampal dysfunction has yielded contradictory results (Nestor, Shenton et al. 1993; Seidman, Yurgelun-Todd et al. 1994). Studies have, however, found that anterior hippocampal volume (Bilder, Bogerts et al. 1995) and superior temporal gyrus volume (Vita, Dieci et al. 1995) correlated with neuropsychological deficits in tests related to frontal system function (abstraction, verbal fluency, and motor) suggesting a possible defect in an integrated functional system that includes both frontal and temporohippocampal components.

I.1.A.iii. Hippocampus: Animal Models

Early attempts to model schizophrenia have predominantly used either pharmacological perturbations in the striato-limbic DA activity or primary prefrontal lesions to modify subcortical DA activity (Borison and Diamond 1978; McKinney and Moran 1981). Hippocampectomized adult animals exhibited attentional deficits, recognition memory deficits, stereotyped behaviour, hyperactivity, poor habituation, and resistance to extinction (Schmajuk 1987; Chambers, Moore et

al. 1996). A recent attempt to model schizophrenia demonstrated locomotor hyperactivity and deficits in prepulse inhibition in socially isolated animals with parallel reductions in synaptic connectivity in the dentate gyrus(Varty, Marsden et al. 1999). Taken together, these data support the proposal that hippocampal dysfunction might occur in schizophrenia.

I.1.A.iv. Hippocampus: Pathology (post-mortem studies)

I.1.A.iv.a. Neuronal morphometric findings

In postmortem studies, schizophrenics showed left temporal horn enlargement, which is consistent with loss in the surrounding temporolimbic structures(Bogerts, Meertz et al. 1985; Brown, Colter et al. 1986; Crow, Ball et al. 1989; Heckers, Heinsen et al. 1990). As well, reductions in volumes of cross-sectional areas of the hippocampus, amygdala, and parahippocampal gyrus(Bogerts, Meertz et al. 1985; Colter, Battal et al. 1987; Falkai, Bogerts et al. 1988; Stevens, Altshuler et al. 1988; Jeste and Lohr 1989; Altshuler, Casanova et al. 1990), and reduced hippocampal volume are reported(Brown, Colter et al. 1986; Jeste and Lohr 1989; Bogerts, Falkai et al. 1990).

Postmortem investigations have revealed a variety of structural abnormalities in several cortical limbic regions of schizophrenic brain that connect to the hippocampus, including the prefrontal cortex(Benes, Davidson et al. 1986), anterior cingulate region(Benes, Majocho et al. 1987; Benes, Sorensen et al. 1992), and the entorhinal area(Jakob and Beckmann 1986; Falkai, Bogerts et al. 1988; Falkai, Schneider-Axmann et al. 2000).

The findings of cytoarchitectural abnormalities of the hippocampus in schizophrenia are inconsistent (Dwork 1997; Harrison 1999; Weinberger 1999). Many negative studies (Christison, Casanova et al. 1989; Benes, Sorensen et al. 1991; Arnold, Franz et al. 1995) exist alongside positive reports (Kovelman and Scheibel 1984; Altshuler, Conrad et al. 1987; Conrad, Abebe et al. 1991; Jonsson, Luts et al. 1997; Zaidel, Esiri et al. 1997) of disarray of hippocampal pyramidal neurons. In terms of hippocampal neuron density, there have been reports of decreases (Jeste and Lohr 1989; Jonsson, Luts et al. 1997; Zaidel, Esiri et al. 1997; Benes, Kwok et al. 1998), increases (Zaidel, Esiri et al. 1997), and no change (Kovelman and Scheibel 1984; Falkai and Bogerts 1986; Benes, Sorensen et al. 1991; Heckers, Heinsen et al. 1991; Arnold, Franz et al. 1995). Decreased mean size of hippocampal pyramidal neurons is described (Benes, Sorensen et al. 1991; Arnold, Franz et al. 1995; Zaidel, Esiri et al. 1997) as well as no change in mean size (Christison, Casanova et al. 1989; Benes, Kwok et al. 1998).

These results indicate that in the vast majority of cases, schizophrenia is probably not associated with conspicuous abnormalities of hippocampal cytoarchitecture. If the synaptic circuitry is altered in schizophrenia, a more sensitive technique other than a crude standard histological approach is required to detect the subtle changes in synaptic connectivity (see I.4 Measuring Synaptic Connectivity).

Synaptic, axonal and dendritic findings

The axonal profile of dentate granule cells (mossy fibres) using modified Timm's silver stain revealed both an increase (Goldsmith and Joyce 1995) and no change (Adams, DeMasters et al.

1995) in mossy fibre staining intensity in schizophrenia. The synaptic profile of the hippocampus using presynaptic proteins expression have found decreased synapsin I protein(Browning, Dudek et al. 1993), no change in synaptophysin protein(Browning, Dudek et al. 1993), decreased synaptophysin mRNA and protein(Eastwood, Burnet et al. 1995; Eastwood and Harrison 1995; Eastwood and Harrison 1999), and decreased complexin (I and II) mRNA and protein(Harrison and Eastwood 1998; Eastwood and Harrison 2000). The dendritic profile of the hippocampus using immunoreactivity for the dendritic protein microtubule-associated protein 2 [MAP2] showed a decrease in total MAP2 [MAP2-T] expression specific to the subiculum and entorhinal cortex(Arnold, Lee et al. 1991) and showed an increase in non-phosphorylated MAP2 [MAP2-NP] restricted to the left CA1 and subiculum subregions(Cotter, Kerwin et al. 1997). Dendritic morphology in terms of MAP-2 immunoreactive dendritic length showed an increase for total MAP-2 in CA1, CA4 and subicular regions and an increase for MAP-2NP in CA1, CA2, CA3 and subicular regions(Cotter, Wilson et al. 2000). Dendritic morphology using rapid Golgi impregnation revealed decreased spine density and aborization of apical dendrites in the subiculum of schizophrenics(Rosoklija, Toomayan et al. 2000), raising the possibility that the main synaptic inputs from the entorhinal cortex to this region may also be affected.

These results indicate that both the intrinsic and extrinsic circuitry of the hippocampus are probably altered in schizophrenia.

I.1.A. HYPOTHESIS: Altered hippocampal connectivity in schizophrenia

The major synaptic connection into the hippocampus comes from the perforant pathway of the entorhinal cortex [ERC], specifically originating from ERC layer II and layer III neurons (**Figure I-1**).

Originally described by Ramon y Cajal (1911), the essential ERC→hippocampal perforant pathway organisation is strikingly constant among species (Witter, Wouterlood et al. 2000), where the perforant pathway from the ERC perforates the subiculum en route to the dentate gyrus (DG), CA3, and CA1. ERC layer II neurons send projections to directly innervate the dentate outer molecular layer [OML] and CA3 molecular layer (Steward and Scoville 1976; Witter and Amaral 1991; Witter, Wouterlood et al. 2000). ERC layer III neurons send projections to CA1 molecular layer and subiculum (Steward and Scoville 1976; Witter and Amaral 1991; Witter, Wouterlood et al. 2000).

Intracellular tracing studies in the rat also provide evidence for other ERC→hippocampus projections (see Table I-1). ERC layer II neurons send a few collaterals to the subiculum (Tamamaki and Nojyo 1993). ERC layer III neurons send projections via the alvear pathway to directly innervate the stratum oriens of CA1-CA3 (Buzsaki, Penttonen et al. 1995; Deller, Adelman et al. 1996). ERC layer IV-VI neurons send projections via a novel DG pathway to directly innervate the dentate inner molecular layer [IML], cell bodies of granule cells and GABAergic neurons in the dentate gyrus (Deller, Martinez et al. 1996).

Table I-1

The ERC projections to the hippocampus: Perforant, Alvear, and DG pathways

E R C	II	Perforant path →	dentate OML → CA3 → CA1 → subiculum →	E R C
			CA3 molecular layer →	
			Subiculum →	
	III	Perforant path →	Subiculum →	
			CA1 molecular layer →	
			Alvear path →	
	IV-VI	DG path→	proximal dendrites and cell bodies of granule cells and GABAergic neurons → CA3 → CA1 → subiculum →	

Studies have found abnormal lamination and cellular disarray of entorhinal cortex layer II and layer III neurons in schizophrenia (Jakob and Beckmann 1986; Jakob and Beckmann 1989; Arnold, Hyman et al. 1991; Jakob and Beckmann 1994; Arnold, Franz et al. 1995; Arnold, Ruscheinsky et al. 1997; Falkai, Honer et al. 1999; Falkai, Schneider-Axmann et al. 2000) although this was not replicated in other studies (Heinsen, Gossmann et al. 1996; Akil and Lewis 1997; Krimer, Herman et al. 1997). A few studies have also found reduced pyramidal number and size (Jakob and Beckmann 1994) and abnormal pyramidal orientation (Arnold, Hyman et al. 1991) in entorhinal cortex layer IV-VI in schizophrenia. I hypothesised then that synaptic connectivity would be decreased in the perforant pathway termination fields of the schizophrenic hippocampus.

Specifically, I hypothesized the intensity and distribution of synaptophysin and SNAP-25 (markers of synaptic connectivity) immunoreactivity would be decreased in the molecular layer of the cornu ammonis CA1-CA4 and the dentate outer molecular layer (see I.4 Measuring Synaptic Connectivity).

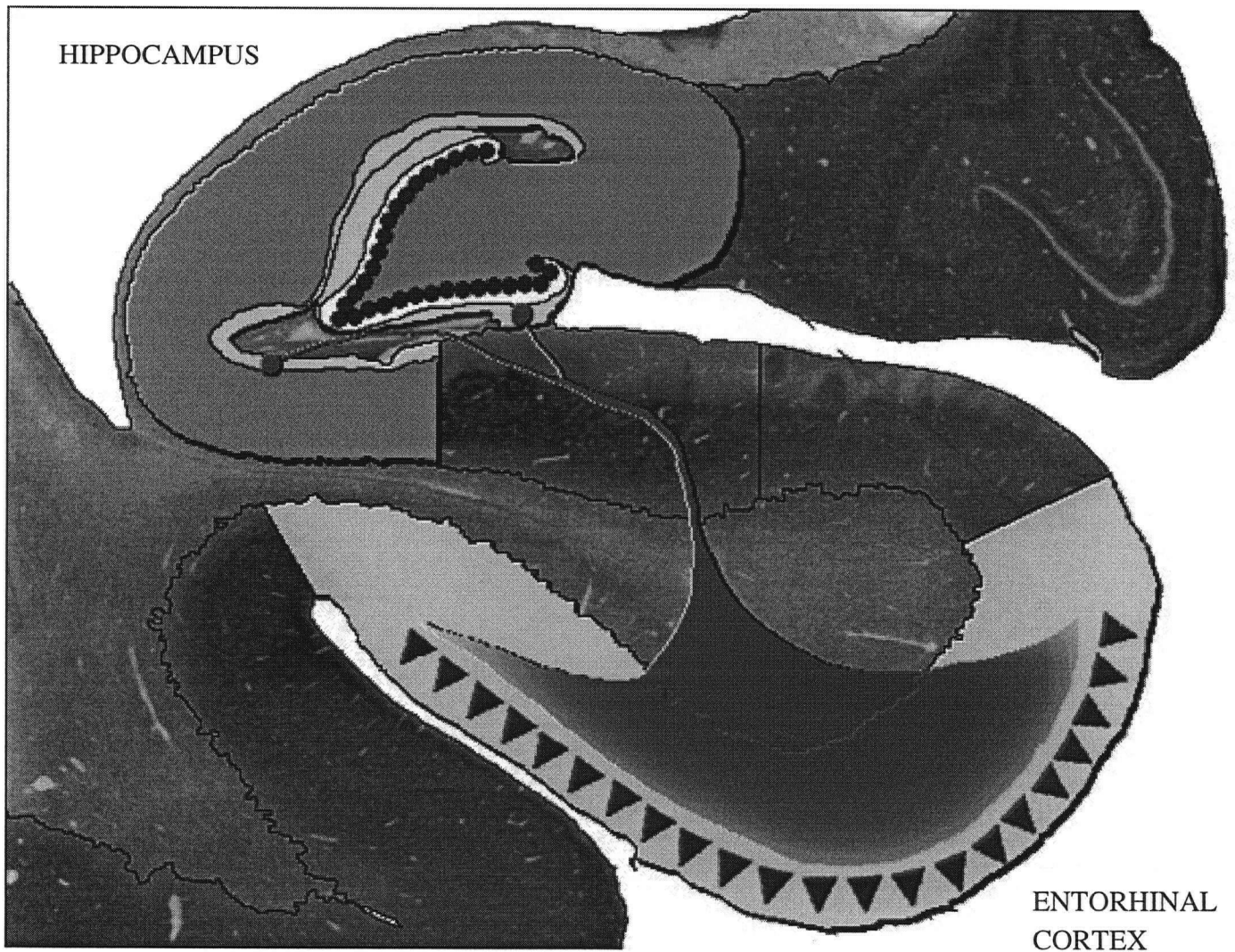


Figure I-1

Layer II and layer III neurons of the entorhinal cortex provide the major source of input into the hippocampus via the perforant pathway synapsing onto the molecular layer of the cornu ammonis and the outer molecular layer of the dentate gyrus.

I.2.MECHANISM OF ILLNESS (DEVELOPMENTAL)

I.2.A. BACKGROUND: Abnormal development in schizophrenia

Neuroimaging, neuropsychological testing, animal models, and post-mortem investigations form the foundation of the hypothesis that schizophrenia is caused by aberrant neurodevelopment which is present in the fetus and has observable, but relatively mild, effects throughout childhood and adolescence to emerge with such destructive effects in young adults. It has been proposed that in schizophrenia certain neural systems are destined from early development to malfunction to produce the illness. This potential, however, cannot be realised until a certain stage of postnatal brain development is reached. Prior to this they either do not malfunction to a clinically significant degree, or their malfunctioning can be compensated for by other systems.

Developmental: Neuroimaging

The majority of CT and MRI scan studies support the view that brain pathology, at least in the majority of schizophrenics, is not progressive and probably predates the onset of the typical clinical symptoms. Ventricular enlargement and reduced temporolimbic structure volumes have been observed in CT and MRI scans at the beginning of the disease before the patients had substantial amounts of neuroleptic drugs (Schulz, Koller et al. 1983; Bogerts, Ashtari et al. 1990; Degreef, Ashtari et al. 1991), suggesting that in schizophrenia, anatomical changes in the adult brain are non-progressive and occurred prior to the onset of illness. This is an important difference to the well known degenerative brain diseases such as Alzheimer's, Pick's, Parkinson's and

Huntington's disease, and supports the neuropathological findings that schizophrenia may be a disorder of brain development.

Developmental: Neuropsychological

If the brains of patients with schizophrenia have not developed normally, it is reasonable to expect that subtle abnormalities of neural function would be apparent early in life. Both genetic "high risk" observational and birth-cohort studies provide support for a development disturbance in infants prior to the onset of the illness.

In prospective genetic "high-risk" studies involving groups of subjects born to mothers with schizophrenia, high-risk subjects had "pandepvelopmental retardation" with delays in achieving psycho-motor milestones and poor integration of CNS functioning (Fish 1977), poorer cognitive and motor dysfunction (Fish, Marcus et al. 1992), lower psychomotor scores (Marcus, Auerbach et al. 1981), persistent attentional dysfunction (Erlenmeyer-Kimling and Cornblatt 1992; Erlenmeyer-Kimling, Squires-Wheeler et al. 1995; Erlenmeyer-Kimling, Adamo et al. 1997), poorer social skills and greater disciplinary problems at school (Parnas, Schulsinger et al. 1982). Two "high risk" studies suggest that these premorbid deficits associated with schizophrenia have a physical basis in abnormal brain development. In one, high-risk infants had greater sulcal enlargement as adults (Cannon, Mednick et al. 1994). In another, high-risk subjects showed subtle deficits (poorer motor skills and had a higher rate of neuromotor abnormalities) that tended to disappear after two years of age (Walker, Savoie et al. 1994), suggesting that the maturation of the neural systems related to such motor behaviours was at least delayed.

In general-population birth-cohort studies, children who later developed schizophrenia compared with controls had significant developmental delays in walking and talking (Jones, Rodgers et al. 1994; Jones and Dones 1997), poorer scores on cognitive tests (Jones, Rodgers et al. 1994; Jones and Dones 1997), abnormalities in coordination and clumsiness (Done, Crow et al. 1994; Jones and Dones 1997), poorer educational achievement (Done, Crow et al. 1994; Jones and Dones 1997), lower IQ (David, Malmberg et al. 1997), and a lack of sociability and sensitivity in childhood and adolescence (Malmberg, Lewis et al. 1998).

As well, onset of symptoms in schizophrenia typically occurs near adolescence, a period coinciding with myelination of the pathway connecting the entorhinal cortex to the hippocampus (Benes 1989; Arnold and Trojanowski 1996). The timing of development of neuropsychological problems coincides with an anatomical substrate, the coupling of the entorhinal-hippocampal circuit.

Developmental: Animal Models

Although animal models appear to mimic broadly the symptoms of schizophrenia, they have paid insufficient attention to the neurodevelopmental insult and the developmental time-course of the symptoms associated with this mental disorder. To date, there have been two groups tracing the time-course of behavioural changes from infancy through adulthood in animals with an early lesion of the hippocampus. One group (Lipska, Jaskiw et al. 1992; Lipska, Jaskiw et al. 1993; Lipska, Swerdlow et al. 1995) studying rodents demonstrated that the behavioural effects of an early lesion of the hippocampus – increased responsiveness to stress and exaggerated exploratory behaviour – may remain silent until puberty and is consistent with a neurodevelopmental model of

schizophrenia. Another group(Beauregard and Bachevalier 1996) studying nonhuman primates showed that the neuromotor and behavioural effects of a neonatal hippocampal lesion – increased locomotor stereotypies and decreased social interaction – remained relatively silent in infancy and became more profound as the animals reached adulthood.

Developmental: Pathology (post-mortem studies)

The pathological differences found in the brains of patients with schizophrenia include larger ventricles, reduced brain weight and length, disorganisation of cortical neurons and reduced number neuronal number in the medial temporal lobe, reduced neuronal number in other cortical areas, and absence of gliosis or neurodegenerative change. These changes fit the pattern expected in a disorder of brain development(Harrison 1999).

Although the brains of patients with schizophrenia have larger ventricles, exhaustive studies have failed to reveal neuropathological evidence of neurodegenerative changes and, in particular, reveal a marked absence of the reactive or activated glial cells (gliosis) that characterize most known neurodegenerative processes. An important neurohistological indicator of a progressive degenerative or inflammatory brain disease is gliosis which means increased densities or absolute numbers of reactive glial cells, especially astrocytes. Gliosis has been described qualitatively in periventricular and temporo limbic structures(Stevens 1982), brainstem(Fisman 1975), corpus callosum(Nasrallah, McCalley-Whitters et al. 1983) and diffusely distributed in brains of schizophrenics(Bruton, Crow et al. 1990). As Bogerts (1993) comments, a major problem with these qualitative studies of gliosis is that they do not allow a quantitative-statistical comparison of

glial cell densities. By counting stained reactive astrocytes with GFAP (glial fibrillary acidic protein), later quantitative studies (Benes, Davidson et al. 1986; Falkai and Bogerts 1986; Roberts, Colter et al. 1986; Casanova, Stevens et al. 1987; Roberts, Colter et al. 1987; Falkai, Bogerts et al. 1988; Stevens, Altshuler et al. 1988; Crow, Ball et al. 1989; Pakkenberg 1990; Benes, McSparren et al. 1991; Arnold, Franz et al. 1996) found no evidence of gliosis in medial temporal lobe, cingulate gyrus or hypothalamic periventricular regions suggesting that schizophrenia may be disorder of brain development.

In the last decade, the developmental basis for schizophrenia has been supported by neuroanatomical studies, and summarised in several recent reviews (Pilowsky, Kerwin et al. 1993; Bunney, Potkin et al. 1995; Harrison 1995; Knable and Weinberger 1995; Arnold, Franz et al. 1996; Weinberger 1999). Histological studies on areas of the medial temporal lobe described anomalies of cortical lamination patterns in hippocampal and parahippocampal regions in schizophrenics, interpreted as resulting from defective neuronal migration in development (Jakob and Beckmann 1986; Kovelman and Scheibel 1986; Jakob and Beckmann 1989; Arnold, Hyman et al. 1991). Alternatively, they could represent abnormalities of the distribution of normal variation in cytoarchitecture, which still supports a developmental abnormality. A significant increase in volume of the lateral and third ventricles in schizophrenics may also reflect altered brain development since it is present in early stages of the disease and does not progress over time.

I.2.B. DENTATE GYRUS: Model of developmental organisation

Cortical dysfunction is a prominent characteristic of schizophrenia where prefrontal-hippocampal functional connectivity may be especially impaired. The molecular events that account for the functional maturation of these systems are probably complex, and may involve stabilization of synapses, leveling off of the growth of dendritic trees, and other processes related to the refinement of cortical connectivity, all of which seem to plateau in early adult life.

The dentate gyrus can be used as a possible developmental model of schizophrenia since the structure and placement of granule cells within the dentate gyrus follows a developmentally timed sequence. One study found the width the granule cell layer decreased in schizophrenia (McLardy 1975). The dentate gyrus is one of the simplest and most distinctive of all cortical structures in the mammalian brain and consists essentially of just two cellular layers: an outer layer of granule cells which constitute the principal cell type in the region and a deeper polymorphic zone (CA4) in which a variety of local and projection interneurons reside (**Figure I-2**).

During development of the human fetal dentate gyrus, two developmental gradients are apparent: the limbs of the granule cell layer evince differences in cell density and organisation prenatally (Arnold and Trojanowski 1996), while the span or width of the granule cell layer continues to develop postnatally (Rakic and Nowakowski 1981; Eckenhoff and Rakic 1988; Eriksson, Perfilieva et al. 1998). The two limbs are initially anatomically different early in gestation with the (early forming) external limb being more condensed and more organised than the (later forming) internal limb (**Figure I-3**). The limbs become anatomically identical towards term.

Meanwhile, unlike most other neuronal populations in the CNS, human granule neurons are generated postnatally throughout life from a population of continuously dividing progenitor cells residing in the subgranular zone of the dentate gyrus (Eriksson, Perfilieva et al. 1998). Although some granule cells arise directly from progenitor cells lining the neuroepithelium of the lateral ventricle, many are generated from a proliferative population located within the future CA4 of the dentate gyrus. From this proliferative region, granule cells migrate short distances and settle their layer in an outside-in sequence. As a result of this neurogenic gradient, early-born granule cells reside in the outer portion of the GCL and later-born granule cells occupy the inner portion of the layer (**Figure I-4**).

I.2.C. HYPOTHESIS: Abnormal development in schizophrenia

I hypothesized that the timing of abnormalities in neural development in schizophrenia might be illuminated through analysis of the pattern of synaptic connectivity seen in the developmentally organized subregions of the dentate gyrus. If schizophrenia is a problem of abnormal prenatal development, then one might expect a different pattern of connectivity between the two limbs of the dentate gyrus, while a predominantly postnatal problem might show differences in the span of the granule cell layer.

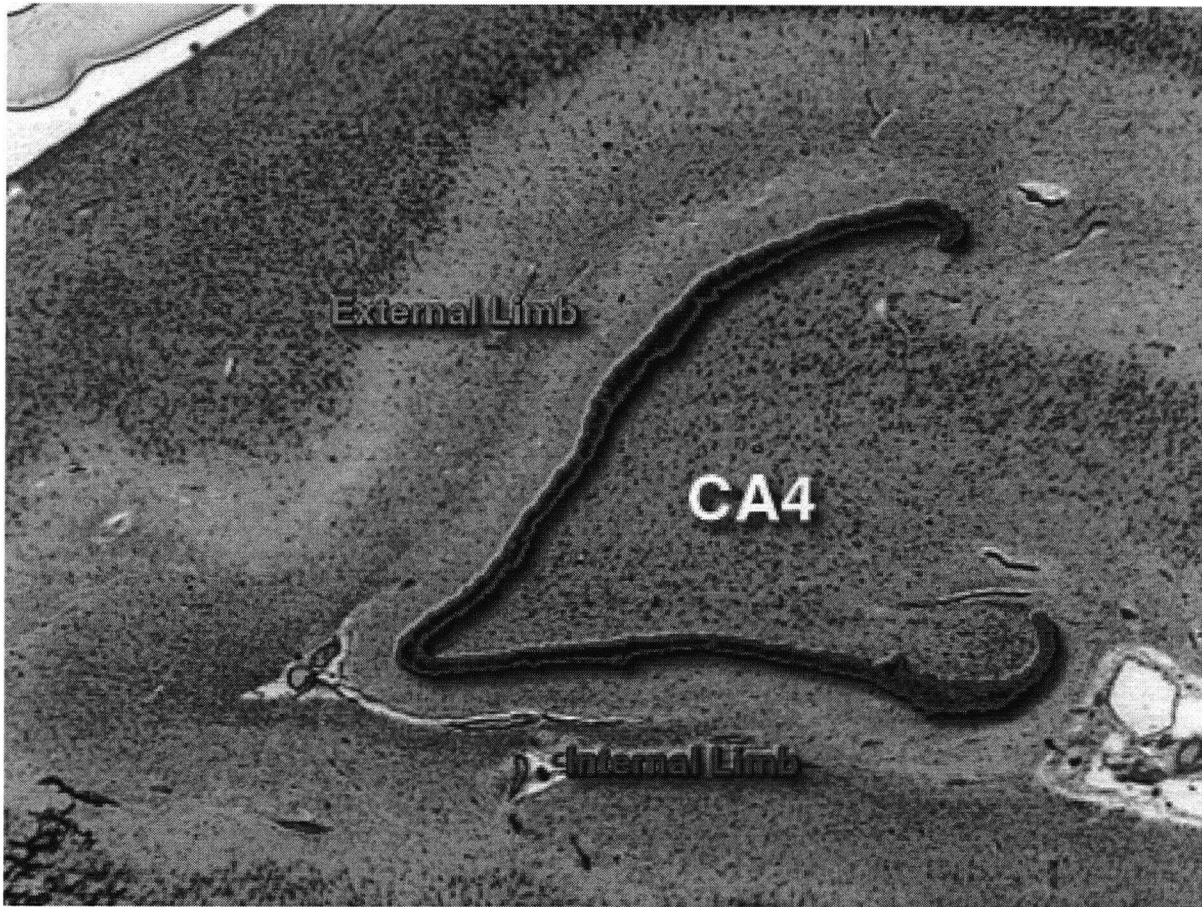


Figure I-2

The dentate gyrus consists essentially of just two cellular layers: 1) an outer layer of granule cells which constitute the principle cell type forming the two limbs of the dentate gyrus (external and internal) and 2) a deeper polymorphic zone (CA4) in which a variety of local and projection interneurons reside.

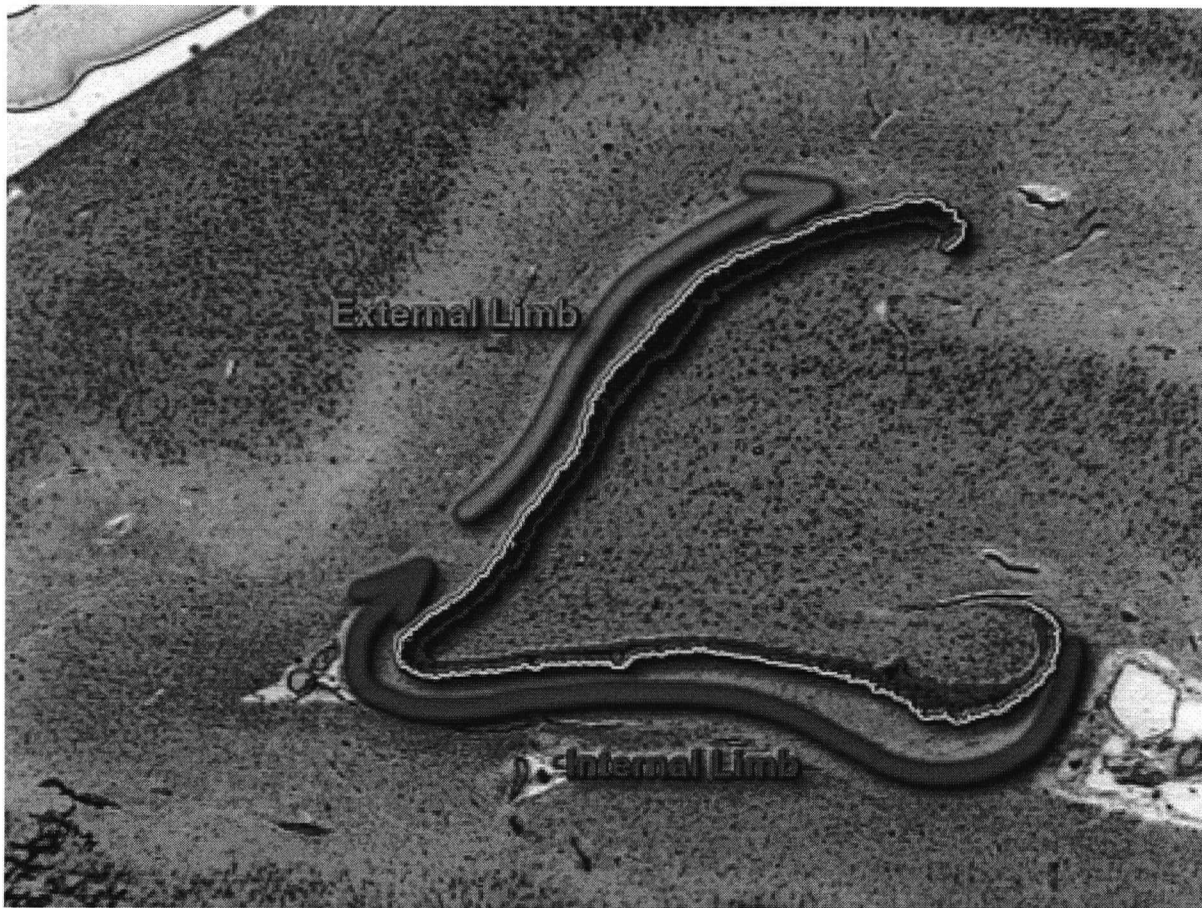


Figure I-3

The dentate gyrus of the hippocampus is made of two limbs, an external limb and an internal limb (seen in relief). The structure and placement of granule cells within the dentate gyrus follows a developmentally timed sequence. In the first phase of development, the earliest generated granule cells travel along the molecular border to create an outer shell (yellow), or skeleton, for the granule layer. The earliest born granule cells settle first in the external limb and then later in the internal limb, such that a developmental time gradient (orange-red arrows) is created along the outer shell where granule cells have greater ages and greater differentiation as one moves from the internal limb to the external limb.

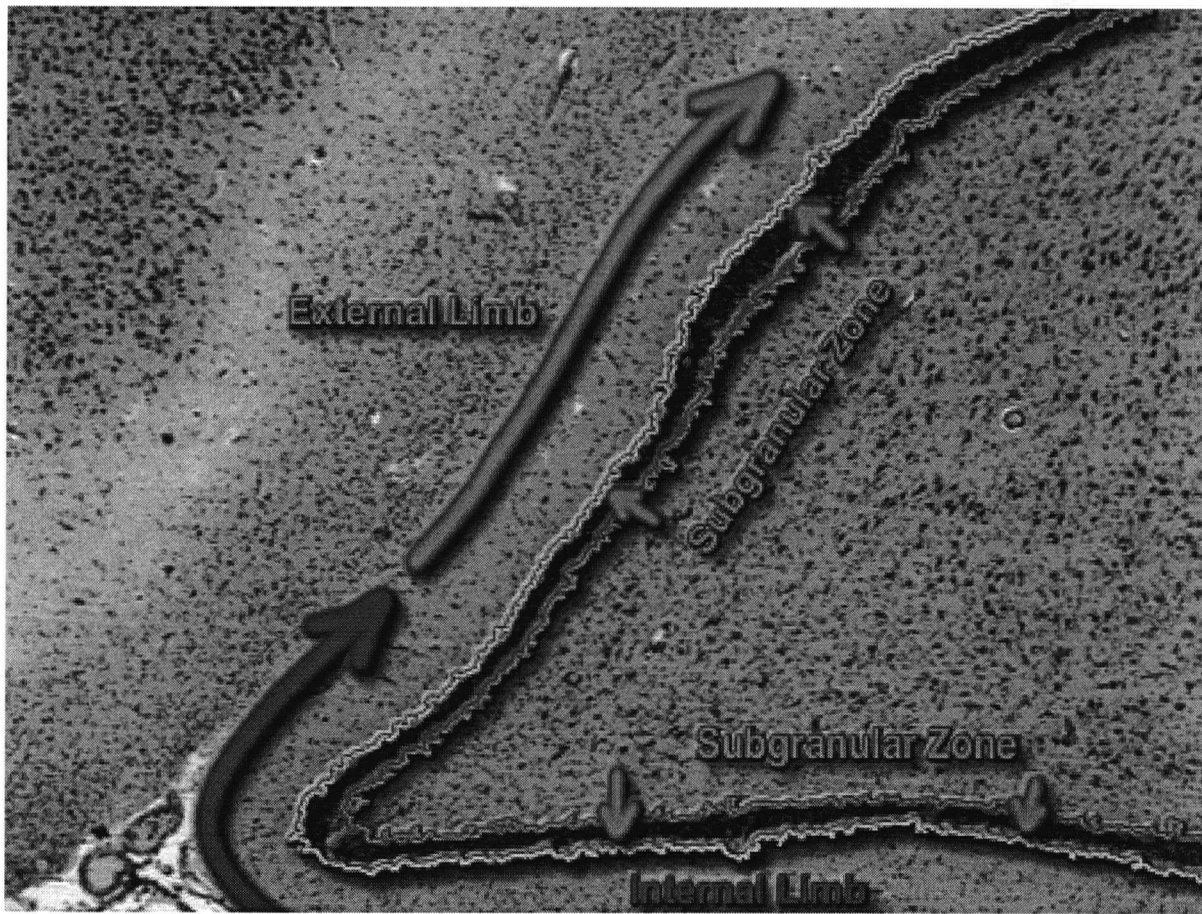


Figure I-4

In the second developmental phase, newly generated granule cells at the polymorph border (specifically at the subgranular zone, green) settle beneath the outer shell of granule cells at the molecular border, such that another developmental time gradient (green arrows) is created across the span of the granule cell layer where granule cells have greater ages and greater differentiation as one moves across the granule cell layer from the polymorph border (green outline) to the molecular border (yellow outline).

I.3.EFFECTS OF ANTIPSYCHOTIC DRUGS ON SYNAPTIC CONNECTIVITY

I.3.A. BACKGROUND: APD effects on synaptic connectivity

In addition to their neurochemical effects, antipsychotic drugs [APD] produce structural brain changes, altering both pre- and post-synaptic elements in neuronal circuitry(Harrison 1999). The results of molecular and immunocytochemical studies of synapses in APD treated animals show the greatest morphological changes in the basal ganglia, notably the caudate nucleus with the nucleus accumbens unaffected.

APD effects on neurons

Neuronal density was found to be decreased in the striatum in some rat studies of antipsychotic administration(Pakkenberg, Fog et al. 1973; Nielsen and Lyon 1978; Jeste, Lohr et al. 1992), and unchanged in others(Fog, Pakkenberg et al. 1976; Jeste, Lohr et al. 1998). Neuronal size was increased in the caudate(Benes, Paskevich et al. 1985), but unchanged in the substantia nigra(Benes, Paskevich et al. 1983) and medial prefrontal cortex(Benes, Paskevich et al. 1985). In the hippocampus, haloperidol treatment in rats resulted in increased neurogenesis in the dentate gyrus granule cells(Dawirs, Hildebrandt et al. 1998). A recent primate study(Selemon, Lidow et al. 1999) found no change in neuronal density as well as a laminar-specific gliosis and hypertrophy of layer V in the prefrontal cortex of chronic drug-treated monkeys.

APD effects on synapses

In electron microscopy studies, rats treated with haloperidol have shown increased vesicle size(Takeichi 1985), decreased number of vesicles(Ihara, Sato et al. 1986), spines(Kelley, Gao et al.

1997), and asymmetrical axospinous synapses(Roberts, Gaither et al. 1995) in the striatum. As well, an increased number of axon terminals was observed in the caudate(Benes, Paskevich et al. 1985; Meshul, Janowsky et al. 1992; See, Chapman et al. 1992) with decreased number of asymmetrical synapses and spines(Benes, Paskevich et al. 1985; Vincent, McSparren et al. 1991). In prefrontal cortex, an increase in number of symmetrical synapses was described(Vincent, McSparren et al. 1991). In the hippocampus, haloperidol treatment resulted in no changes in ultrastructure(Uranova, Orlovskaya et al. 1991).

Studies of synaptophysin mRNA and protein in rats have shown increases(Eastwood, Burnet et al. 1994; Eastwood, Heffernan et al. 1997; Marin and Tolosa 1997) or no change(Nakahara, Nakamura et al. 1998) in the striatum and frontal cortex after haloperidol treatment, increases in the striatum after chlorpromazine treatment(Eastwood, Burnet et al. 2000), and no change in the hippocampus after haloperidol treatment(Eastwood, Burnet et al. 1995; Eastwood, Heffernan et al. 1997). SNAP-25 mRNA was unchanged in the striatum and frontal cortex after haloperidol treatment in rats(Nakahara, Nakamura et al. 1998). The mRNA of other presynaptic proteins (syntaxin 1A, rab3a, synaptobrevin, and synaptotagmin) were increased in the nucleus accumbens and unchanged in the prefrontal cortex, striatum, substantia nigra and ventral tegmental area after haloperidol treatment(Nakahara, Nakamura et al. 1998). Olanzapine treatment increased complexin I mRNA in the striatum and frontal cortex. Olanzapine and haloperidol exposure decreased the abundance of complexin II mRNA relative to complexin I mRNA in striatum and frontal cortex. Chlorpromazine increased complexin II mRNA in the frontal cortex(Eastwood, Burnet et al. 2000).

Table I-2

Effects of Haloperidol exposure on Presynaptic mRNA levels

	Hippocampus	Frontal Cortex or Striatum	Accumbens
Synaptophysin	no Δ [1,2]	\uparrow [1,2,4] no Δ [5]	no Δ [5]
SNAP-25		no Δ [5]	no Δ [5]
Syntaxin		no Δ [5]	\uparrow [5]
Synaptobrevin		no Δ [5]	\uparrow [5]
Synaptotagmin		no Δ [5]	\uparrow [5]
Rab3		no Δ [5]	\uparrow [5]
Complexin I	no Δ [3]	OLZ \uparrow [3]	
Complexin II	no Δ [3]	\downarrow [3] OLZ \downarrow [3] CPZ \uparrow Frontal Cx only [3]	

¹Eastwood, Burnet et al. 1995²Eastwood, Heffernan et al. 1997³Eastwood, Burnet et al. 2000⁴Marin and Tolosa 1997⁵Nakahara, Nakamura et al. 1998

These results indicate that APD exposure causes the greatest changes of presynaptic mRNA levels either in the frontal cortex or basal ganglia, notably the nucleus accumbens. Overall, changes in presynaptic proteins following APD treatment appear to be minimal compared to mRNA, with few if any differences from controls.

I.3.B. HYPOTHESIS: APD effects on synaptic connectivity

Given that the symptoms of schizophrenia can be ameliorated and treated with antipsychotic drugs, I hypothesised that typical APD treatment would produce a pattern of synaptic change – as assessed with synaptophysin and SNAP-25 immunoreactivity (see I.4 Measuring Synaptic

Connectivity) in the hippocampus different from the pattern of changes in schizophrenia and, simultaneously, revealing possible regions of therapeutic effect.

I.4. MEASURING SYNAPTIC CONNECTIVITY

To assess synaptic connectivity I quantified the intensity and distribution of presynaptic protein (synaptophysin and SNAP-25) immunostaining. Neurotransmission requires the docking of synaptic vesicles to the presynaptic plasma membrane. Presynaptic proteins are involved in the molecular mechanisms of synaptic vesicle docking and membrane fusion. Three proteins, vesicle associated membrane protein (VAMP), syntaxin, and synaptosomal associated proteins of 25 kDa (SNAP-25) form a SNARE (soluble N-ethylmaleimide-sensitive factor attachment protein receptor) core complex that is known to be essential for synaptic transmission (Scheller 1995; Fernandez-Chacon and Sudhof 1999). Choice of presynaptic proteins used in these studies was based on the limited availability of monoclonal antibodies that were amenable to immunohistochemical visualisation in paraffin-embedded human brain.

I.4.A. Presynaptic proteins: Synaptophysin and SNAP-25

BACKGROUND: Synaptophysin

Synaptophysin is a 38-kDa protein of the synaptic vesicle with four predicted transmembrane domains. It is widely expressed in neurons and some neuroendocrine tissues (Wiedenmann and Franke 1985; Buckley, Floor et al. 1987; Sudhof, Lottspeich et al. 1987; Sudhof, Lottspeich et al. 1987; Cowan, Linial et al. 1990; Leube 1994; Leube, Leimer et al. 1994).

Immuno-electron microscopy and biochemical studies indicate that synaptophysin is limited to

small electron-translucent synaptic vesicles(Wiedenmann and Franke 1985; Navone, Jahn et al. 1986), although nonneuronal homologues of synaptophysin have been described(Knaus, Marqueze-Pouey et al. 1990; Zhong, Hayzer et al. 1992; Leube, Leimer et al. 1994). Three studies show that synaptophysin contribute to synaptic vesicle secretion: 1) synaptophysin expression was required for calcium-dependent glutamate secretion observed in *Xenopus* oocytes that had been injected with total cellular mRNA from rat cerebellum(Alder, Lu et al. 1992), 2) synaptophysin antibodies injected in *Xenopus* blastomeres resulted in a decreased amplitude of evoked synaptic currents and a decreased frequency of spontaneous synaptic currents in neurons(Alder, Xie et al. 1992), 3) overexpression of synaptophysin in *Xenopus* blastomeres showed opposite results to the antibody injection study along with a decrease in delay time between stimulation and secretion(Alder, Kanki et al. 1995). Together, these results suggest that synaptophysin increases the availability or probability of exocytosis without effecting a change in mean quantal size. A biochemical study(Edelmann, Hanson et al. 1995; Woodman 1997) has shown that synaptophysin interacts with VAMP-2 and may modulate the SNARE complex, described below. Mutant mice lacking the synaptophysin I gene showed normal synaptic transmission, no detectable changes in synaptic plasticity or the probability of release, and no changes in the structure and protein composition of the mutant brains except for a decrease in VAMP-2(McMahon, Bolshakov et al. 1996). These results suggest that synaptophysin's function may be redundant, or that it has a more subtle function as yet unknown.

BACKGROUND: SNAP-25

The 25-kDa protein SNAP-25 was originally characterised by its neuronal specific expression and differential expression by a specific subset of synapses(Oyler, Higgins et al. 1989; Bark and Wilson 1994). Localised to axons and nerve terminals(Garcia, McPherson et al. 1995), SNAP-25 is a component of the 20S SNARE complex implicated in vesicle docking and fusion. It has two distinct isoforms (a and b) created by alternative RNA splicing and is differentially expressed during neuronal development(Catsicas, Larhammar et al. 1991; Oyler, Polli et al. 1991; Bark 1993; Bark and Wilson 1994; Bark, Hahn et al. 1995). The alternative isoforms of SNAP-25 may play distinct roles in vesicular fusion events required for membrane addition during axonal outgrowth and for release of neuromodulatory peptides and neurotransmitters(Bark, Hahn et al. 1995). Homologues have been identified in a diversity of organisms, including yeast(Catsicas, Larhammar et al. 1991; Bark 1993; Risinger, Blomqvist et al. 1993; Risinger and Larhammar 1993; Bark and Wilson 1994; Brennwald, Kearns et al. 1994). The SNAP-25 protein is thought to associate with the presynaptic plasma membrane via fatty acylation of cysteine residues(Hess, Slater et al. 1992) and is a substrate for specific clostridial neurotoxins whose action inhibits neurotransmitter release(Blasi, Chapman et al. 1993; Schiavo, Santucci et al. 1993; Binz, Blasi et al. 1994). In addition to a role in neurotransmitter release, SNAP-25 was implicated in the process of neurite extension during development(Osen-Sand, Catsicas et al. 1993). Although selective inhibition of SNAP-25 expression prevents neurite elongation, it is not known whether this effect is

due to a distinct role of SNAP-25 in this process or whether the lack of SNAP-25 significantly impaired vesicular release generally important in supplying membrane to the lengthening neurite.

The mouse mutation coloboma (Cm/+) has a contiguous gene defect on mouse chromosome 2 which includes the gene encoding SNAP-25(Hess, Collins et al. 1994) and results in reduced levels of SNAP-25 protein and mRNA(Hess, Jinnah et al. 1992). The coloboma mouse also exhibits delayed neurobehavioural developmental milestones(Heyser, Wilson et al. 1995), reduced theta rhythmic activity, hyperactivity, and learning defects(Raber, Mehta et al. 1997), suggesting that reduced SNAP-25 levels may lead to neuromotor dysfunctions similar to those seen in schizophrenia.

I.4.B. Presynaptic proteins: Immunohistochemical quantification

Synaptic density is an important parameter of brain structure and function. Its measurement is of interest in studies of neurodevelopment and in the brain's response to injury or disease. Present accepted methods of estimating the density of synapses can be divided into three groups: (a) the conventional direct ones, based on quantification of synapses identified with the electron microscope (EM)(DeGroot and Bierman 1986; Calverly, Bedi et al. 1988; Bertoni-Freddari, Fattoretti et al. 1989), (b) immunochemical quantification of synapse-associated proteins in brain homogenates and fractions by Western blot(Masliah, Terry et al. 1991), dot-blot(Jahn, Schiebler et al. 1984), radioimmunoassay(Perdahl, Adolfsson et al. 1984; Stridsberg, Lundqvist et al. 1994), and ELISA(Wiedenmann, Rehm et al. 1988; White, Simmons et al. 1993), and (c) the recent indirect method of immunohistochemical quantification of synapse-associated proteins by laser confocal imaging(Lichtman, Sunderland et al. 1989; Masliah, Terry et al. 1990; Mossberg, Arvidsson et al.

1990; Masliah, Ellisman et al. 1992; Masliah, Mallory et al. 1993; Varty, Marsden et al. 1999) or light microscopy optical density(Masliah, Terry et al. 1989; Masliah, Terry et al. 1990; Masliah, Terry et al. 1991; Heinonen, Soininen et al. 1995; Davies, Schweitzer et al. 1998; Looney, Dohan et al. 1999), and immunoautoradiography(Eastwood and Harrison 1995). The conventional electron microscopy method is time-consuming, requires specialized tissue processing and facilities, is susceptible to perimortem artifacts, and is limited in the size of the area studied, hampering investigation of synaptic density in human brain. The immunochemical method requires homogenising brain samples and, therefore, lacks the ability to study microscopic regions or layers in detail. Partly in response to these limitations, the detection and measurement of presynaptic terminal proteins has become established as an alternative means to investigate synapses in human brain. By using immunohistochemistry (IHC) and subsequent image analysis (IA) – collectively termed IHC-IA – the relative abundance of synaptophysin has become an established way of indirectly assessing synaptic density in postmortem brain(Masliah, Terry et al. 1990; Masliah, Terry et al. 1991; Calhoun, Jucker et al. 1996), while the abundance and distribution of SNAP-25 has become an indirect method of assessing synaptic density in a specific subset of synapses and a putative method of tracking the progress of the developing brain(Oyler, Polli et al. 1991).

Synaptophysin immunoreactivity changes during synaptogenesis, lesion-induced synaptic reorganisation, and following cerebral ischaemia(Cabalka, Hyman et al. 1992). Where available, electron microscopy data are generally in agreement with these alterations in synaptophysin immunoreactivity in each situation(Steward and Vinsant 1983; Davies, Mann et al. 1987; Bertoni-

Freaddari, Fattoretti et al. 1989; DeKosky and Scheff 1990; Scheff and Price 1993), supporting the use of synaptophysin as an indicator of synaptic density. The onset of SNAP-25 mRNA and protein expression was found to correspond to the time of synaptogenesis and was differentially expressed by neuronal subpopulations (Catsicas, Larhammar et al. 1991). SNAP-25 immunoreactivity increased during development (Mayanil and Knepper 1993) and the cellular localization of SNAP-25 immunoreactivity concomitantly shifted from axons and cell bodies to presynaptic terminals (Oyler, Polli et al. 1991), suggesting that the SNAP-25 protein shifts in subcellular localization during development and may play a role in the establishment and stabilization of specific presynaptic terminals in brain.

Although quantifying synaptophysin staining intensity does not allow for any differentiation between synapse type or neurotransmitter identity, it enables an estimate of presynaptic terminal density over a wide expanse of the neuropil (Masliah, Terry et al. 1990; Cabalka, Hyman et al. 1992; Eastwood and Harrison 1995), and has been used to demonstrate the synaptic loss following experimentally induced lesions such as perforant path transection and entorhinal cortex ablations (Masliah, Fagan et al. 1991; Cabalka, Hyman et al. 1992; Kirkby and Higgins 1998), the synaptic loss of Alzheimer's disease (Masliah, Terry et al. 1989; Masliah, Terry et al. 1990; Terry, Masliah et al. 1991; Heinonen, Soininen et al. 1995) and of temporal lobe epilepsy-associated hippocampal sclerosis (Honer, Beach et al. 1994; Davies, Schweitzer et al. 1998; Looney, Dohan et al. 1999).

The intensity of SNAP-25 immunostaining is a useful marker of major hippocampal pathways and axonal plasticity, and has been used to demonstrate synaptic loss following experimentally induced lesions such as perforant path transection and entorhinal cortex ablations (Geddes, Hess et al. 1990; Patanow, Day et al. 1997).

While there appears to be a correlation between decreased synaptic protein immunoreactivity and loss of synaptic density in degenerative disorders and animal lesion studies, when studying schizophrenia one must consider that any changes in synaptic protein immunoreactive does not necessarily mean a change in synaptic terminal density, but could instead be reflective of the amount of synaptic protein per terminal.

I.5. OBJECTIVE

The objective of this thesis is to investigate hippocampal neuronal connectivity in schizophrenia through the study of presynaptic proteins (synaptophysin and SNAP-25).

Investigating presynaptic proteins in schizophrenia may provide insight into specific altered patterns of connectivity and mechanisms of illness. Investigating presynaptic proteins in animals treated with antipsychotic drugs may provide insight into actions of antipsychotic drugs in schizophrenia.

Hypotheses:

1. Given findings of abnormal organisation of the layer II and III neurons of the schizophrenic entorhinal cortex, presynaptic proteins will be decreased in the perforant pathway termination fields of the schizophrenic hippocampus.
2. Given findings suggesting abnormal development in schizophrenia, presynaptic proteins will be altered in specific regions of the dentate gyrus which have a different developmental profile.
3. Typical antipsychotic drugs (APD) will produce a pattern of presynaptic protein levels in the rat hippocampus different from the pattern of changes in schizophrenia, thereby showing that altered presynaptic protein levels in schizophrenia are not attributed to APD exposure, and revealing possible areas of therapeutic effect.

Each chapter will address a specific aim:

Chapter 2: Altered pattern of hippocampal neuronal connectivity in Schizophrenia

The aim is to use immunohistochemistry and image analysis (IHC-IA) to quantify the distribution and amount of synaptophysin and SNAP-25 in postmortem whole hippocampus of 12 cases of schizophrenia and 12 controls.

Chapter 3: Mechanisms of Illness in Schizophrenia (development)

The aim is to use IHC-IA to investigate subregions of the dentate gyrus (which have a different developmental profile) and determine if this is altered in schizophrenia; namely, to quantify the amount of synaptophysin and SNAP-25: a) in the internal and external limbs of the granule cell layer (GCL) in the dentate gyrus; and, b) across the span of the GCL.

Chapter 4: Effects of Typical antipsychotic drugs on synaptic connectivity

To study the effects of low, medium, and high potency APDs on presynaptic proteins in the hippocampus of four groups of rats (n=6) given daily injections of either trifluoperazine (6 mg/kg), chlorpromazine (10 mg/kg), haloperidol (1 mg/kg), or vehicle over three weeks.

Chapter II INTENSITY AND DISTRIBUTION OF PRESYNAPTIC PROTEIN IMMUNOREACTIVITY IN HIPPOCAMPUS IN SCHIZOPHRENIA

II.1. OVERVIEW

Schizophrenia is a severe mental illness characterised by hallucinations, delusions, disordered thought processes, and reduced ability to function in society. Pathological abnormalities appear to be most consistently observed in the medial temporal lobe. Given the abnormal lamination and cellular disarray of entorhinal cortex layer II neurons in schizophrenia (Jakob and Beckmann 1986; Jakob and Beckmann 1989; Arnold, Hyman et al. 1991; Jakob and Beckmann 1994; Arnold, Franz et al. 1995; Arnold, Ruscheinsky et al. 1997; Falkai, Honer et al. 1999; Falkai, Schneider-Axmann et al. 2000) which provide a major input into the hippocampus via the perforant pathway, I hypothesised that presynaptic proteins (markers of synaptic connectivity) would be decreased in the perforant pathway termination fields of the schizophrenic hippocampus. To study the intensity and distribution of presynaptic protein immunoreactivity (synaptophysin and SNAP-25), I used improved methods of immunohistochemical image analysis and of colocalisation at the visible light microscopy level.

II.2. MATERIALS & METHODS

II.2.A. Immunohistochemistry Image Analysis

Quantitative immunohistochemistry (densitometry) is the process of immunostaining for a specific (presynaptic) protein and quantifying the non-soluble reaction product with the aid of a video-microscope system to assess the amount of that particular product present in a stained tissue. In other words, densitometric measurement of immunohistochemical staining by an enzymatic color reaction can be used as a quantitative method of detecting antigen content in brain sections. I chose the avidin-biotin-peroxidase complex (ABC) detection method in combination with the diaminobenzidine [DAB] chromagen since the ABC method is the most sensitive among several other detection methods, such as the standard peroxidase-anti-peroxidase (PAP) method and indirect immunoperoxidase procedure (Hsu, Raine et al. 1981), and DAB appears to be more sensitive than other chromagens (Trojanowski, Obrocka et al. 1983).

In investigating the validity of quantifying synaptophysin immunostain intensity as an indicator of synaptic connectivity, (Calhoun, Jucker et al. 1996) found that synaptophysin immunohistochemical densitometry failed to confirm the consistent stereological findings of a difference in total number of synaptophysin-ir presynaptic boutons in the dentate gyrus molecular layers compared to the stratum oriens. His image analysis technique, however, was based on the formula $OD = -\log(\text{greyscale value}/255)$ which is not meaningful (see II.2.C.ii) and probably accounts for his failure to corroborate stereological findings with quantitative synaptophysin

immunohistochemistry. Using my approach, I have consistently found a robust difference between synaptophysin staining intensity between the dentate molecular layers and stratum oriens in both rat and humans, suggesting this parameter is a useful indicator of synaptic connectivity.

Unlike the widely accepted method of enzyme-linked immunosorbent assay (ELISA) where a linear relationship exists between OD signal and antigen concentration, current practices to quantify immunohistochemistry do not use a set of (biological) antigen standards to obtain a calibration curve. Instead, a non-biological (plastic(Masliah, Terry et al. 1990) or nitrocellulose based(Peretti-Renucci, Feuerstein et al. 1991; Melloni, Hemmendinger et al. 1993)) standard is widely used. This method does not, however, take into account the complex optical and physical properties of antibody-antigen binding in biological tissue. In this context, one aim of this thesis is to test the validity of quantifying immunohistochemistry by developing standards of predetermined antigen content adaptable to immunohistochemical quantification with antibodies reactive with the presynaptic proteins synaptophysin and SNAP-25. I attempted to model the quantification of immunohistochemistry using the theories underlying the basis of ELISA.

II.2.B. Overview of Spectrophotometry

To begin, ELISA is the process of immunostaining for a specific (presynaptic) protein and quantifying the soluble reaction product (2,2'-azino-di-(3-ethylbenzthiazoline-6-sulfonate) [ABTS]) with the aid of a spectrophotometer to assess the amount of that particular product present in a tissue homogenate. Photometry is the measurement of light. Spectrophotometry is the

measurement of the amount of transmitted light at a single known, defined wavelength passing through a medium. When a beam of light passes through a medium, generally the incident light intensity (I_0) will always be greater than the intensity of the light emerging from the other side of the sample (I). The incident light beam is reduced in intensity by reflections in the air, scattering by any particulate matter suspended in the medium, and direct absorption of light by the material itself. In normal circumstances, the absorption process is the major factor involved. The amount of light absorbed at a particular wavelength is given the term absorbance, or optical density [OD], and is dependent on (i) the concentration of absorber, (ii) the path length of the absorbing medium, and (iii) a factor dependent upon the physical nature of the material itself. Algebraically, this dependence is described by the Beer-Lambert law (Vivino ; Straughan and Walker 1976; Mize, Holdefer et al. 1988; Sommer 1989; Wygant and Nelson):

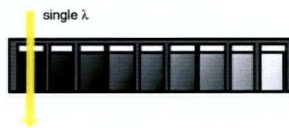
$$\{1\} OD(\lambda) = -\log(I/I_0) = k(\lambda) * C * L$$

where $OD(\lambda)$ is defined as the optical density (or absorbance) at the wavelength λ , $k(\lambda)$ is a constant (depends on physical nature of the medium) at the wavelength λ , L is the path length of the absorbing medium, and C is the concentration of the absorber (Figure II-1). The ratio (I/I_0) is defined as the transmittance or transmission (T). Thus,

$$\{2\} OD(\lambda) = -\log T$$

If the path length is held constant, then (based on a defined wavelength) the optical density can be thought of as the equivalent to concentration of light absorbing substance.

ELISA SYSTEM



Spectrophotometer

$$OD(\lambda) = k(\lambda) * C * L$$

Figure II-1

ELISA quantification uses a spectrophotometer to detect and measure the light at a particular wavelength absorbed by samples in the wells of a microplate. The Beer-Lambert law describes the relationship between the light absorbance and the concentration of the absorber.

OD(λ) optical density (or absorbance) at wavelength λ

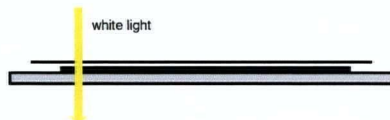
k(λ) constant (depends on physical nature of the medium) at wavelength λ

L pathlength of the absorbing medium

C concentration of the absorber

When an equal volume of sample is placed in the well of a microplate, the pathlength (L) becomes a constant, making the OD(λ) directly proportional to the concentration (C) of the absorber.

IMMUNOHISTOCHEMICAL SYSTEM



CCD Camera

$$OD(\lambda) \neq \text{grey pixel value}$$

Figure II-2

For immunostained sections of uniform thickness (where the pathlength L is constant), the OD should theoretically be directly proportional to the concentration of the light absorbing DAB if measured by a spectrophotometer at a particular wavelength. Immunohistochemical quantification uses, however, full spectrum light (instead of a single wavelength) thus preventing the application of the Beer-Lambert law. Also, the CCD camera outputs grey pixel values which are not directly equivalent to OD values.

For immunostained sections with uniform thickness (i.e. L is a constant), the OD should theoretically be directly proportional to the concentration of the light absorbing DAB stain. The Beer-Lambert Law does not, however, directly apply for immunohistochemical image analysis (Figure II-2) since, unlike the conditions used in ELISA quantification, immunohistochemical quantification uses a) full spectrum light (instead of a single wavelength) and b) a charge-coupled device (CCD) camera (instead of a spectrophotometer). To better quantify immunohistochemistry at the light microscope level, I made adjustments and calibrations during image capture conditions to ensure that the Beer-Lambert Law would apply when quantifying immunohistochemistry with a CCD camera, and I made attempts at improving methods of quantifying presynaptic proteins using immunohistochemical image analysis.

II.2.C. Overview of the CCD camera

II.2.C.i. Single Wavelength of Light: Using a light filter for B&W image capture

My lab uses a black-and-white Sony CCD video camera which is best at detecting grey toned (achromatic) images. It can still be used, however, for capturing chromatic coloured specimens such as those found in immunohistochemistry according to the CCD camera's spectral response [SR] curve (an indicator of the camera's sensitivity to varying wavelengths of light). The spectral response curve for my CCD camera is seen in Figure II-3.

If, at the y-axis, the "normalised spectral sensitivity" [NSS] is equal to 1.0 (as when capturing a purely grey toned, achromatic image), then the camera is at its most sensitive and at its best in distinguishing changes in light intensity. Using my CCD camera's SR curve, the orange-brown peroxidase-DAB coloration (approximate wavelength range of 600 nm(Pappolla 1988)) seen in immunostained specimens can be detected with a NSS of about 0.84. To improve the NSS when capturing images of DAB stained sections, one needs to use a (complementary) colour filter that, when added, will result in a black and white, or grey toned, image.

The spectrum of colours can be subdivided diagrammatically as a "colour wheel" (Figure II-4A) comprised of neutral colours (black, white, greys), primary colours (red, blue, yellow) and secondary colours (green, orange, purple). Complementary colours are those that are opposite each other on the colour wheel which in pigments (e.g. paints, inks, and stains) add to black. The complementary colour of the orange-brown DAB staining colour is blue; in other words, DAB

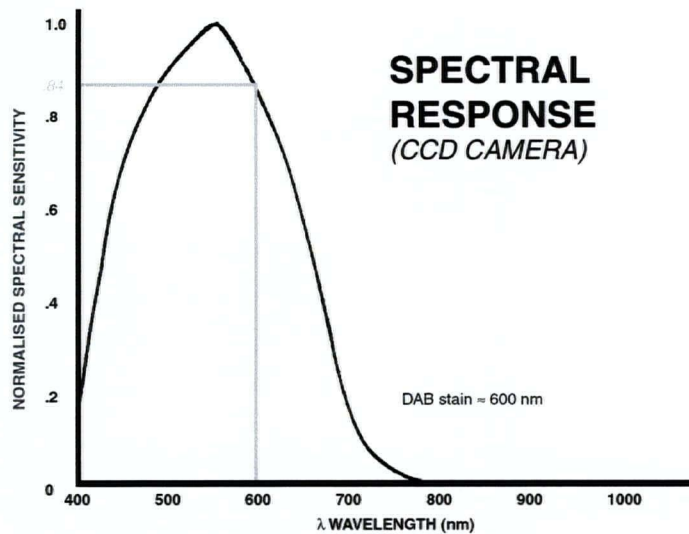


Figure II-3

My B&W Sony CCD camera is most sensitive at detecting purely grey toned, achromatic images. In detecting coloured images, the CCD camera's sensitivity changes according to the wavelength of light. The "Normalised Spectral Sensitivity" at the y-axis is maximal for achromatic images (NSS = 1.0), near maximal for yellow-green images ($\lambda \approx 550$ nm, NSS $\approx .95$), and moderate for the orange-brown DAB coloration ($\lambda \approx 600$ nm, NSS $\approx .84$).

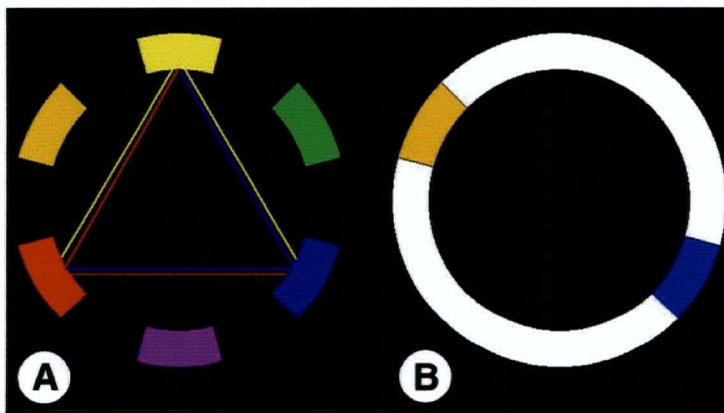


Figure II-4

The "colour wheel" (A) indicates the relations among colours. The primary colours (red, yellow, and blue) form a triad. The secondary colours (green, orange, and purple) are mixtures of two primary colours. Any two colours that lie directly opposite each other on the colour circle are called complementary colours which in pigments combine to black. The complementary colour of the orange-brown DAB stain is blue (B). Thus, DAB stained sections will appear grey toned when a blue filter is added.

stained sections will appear grey toned when a blue filter is added (Figure II-4B). Based on the spectral properties found in commercially available LEE Filters (Chromatic Edition), the HT 363 Special Medium Blue filter was selected for its narrow transmittance band centred around the blue spectrum (450 nm, which appropriately complements the orange-brown DAB stain(Pappolla 1988)). As well as optimising the CCD's detection of the stained image, using the HT 363 Blue filter also fulfils one of the conditions for the Beer-Lambert Law; namely, that the transmitted light be of one single defined wavelength.

II.2.C.ii. OD-grey value relationship: Calibration using Non-biological OD standard

Unlike a spectrophotometer, a CCD camera does not give readouts in purely OD units(Vivino); instead, CCD cameras output pixel or grey values where the level of staining is assigned a grey value ranging from 0 (no staining) to 256 (highly intense staining). Specifically, CCD cameras have been designed to be linear with respect to light transmission; namely, the grey values are an indication of the amount of light transmission:

$$\{3\} \text{ Grey value}[I] = k * I$$

Where I is the amount of transmitted light through a sample registered by the CCD camera and k is a constant (dependent on the physical and optical qualities of the camera).

Since one can obtain the optical density of a sample knowing the amount of incident and transmitted light, some have attempted to use a CCD camera and take the negative log of the grey value {3} but this is not meaningful since:

$$-\log(\text{Grey value}[I]) = -\log(k*I) \neq -\log(I/I_0)$$

To convert the CCD camera's grey levels to meaningful OD values, one needs also to obtain the grey value of the light incident on the sample:

$$\{4\} \text{ Grey value}[I_0] = k * I_0$$

Dividing Grey value[I] by Grey value [I₀] gives transmission:

$$(\text{Grey value}[I]/\text{Grey value}[I_0]) = (k * I)/(k * I_0) = I/I_0$$

By taking the negative log of (grey value [I]/grey value [I₀]), a CCD camera can be used to determine OD values:

$$\{5\} \text{ OD (CCD camera)} = -\log(\text{grey value}[I]/\text{grey value}[I_0]) = -\log(I/I_0)$$

Due to limitations of the imaging software program NIH Image, which is unable to perform this calculation on a pixel-by-pixel basis, I chose to calibrate the grey values using the widely used OD step tablet.

Made of a continuous strip of thin plastic, the typical OD step tablet has twenty steps, or grey levels, with known OD values for each division (Figure II-5A). Custom designed slides (Figure II-5B) totaling thirty-six steps, or grey levels, were created which had a wider lower range and which had more easily distinguishable OD steps compared to the standard OD step tablet. In the custom designed slide, the OD of each dot was determined using an ELISA microplate reader's spectrophotometer set at a wavelength of 405nm (blue); the size of the grey dots having the exact dimension of the ELISA microplate cell. By capturing images of this custom designed OD tablet using the same image capture settings as when imaging immunostained sections with the CCD camera, one can calibrate grey values to OD using this non-biological standard (Figure II-6).

II.2.D. Attempts at Improving Methods of Quantifying Presynaptic Proteins

The standard practise of using a non-biological standard to calibrate grey scale images of immunostained sections to OD units relies, however, on the assumption that the observed reaction product from antigen-antibody binding has a 1:1 stoichiometry. In fact, the antibody-antigen binding in biological tissue follows a complex cascade of interactions such that when DAB visualisation occurs, the concentration of light absorbing DAB particles may not be linearly related to the antigen concentration, casting doubts on the accuracy of using a non-biological (optical density) calibration. In this context, I attempted to develop a biological standard, a standard scale of antigens adaptable to immunoenzymatic coloration procedures.

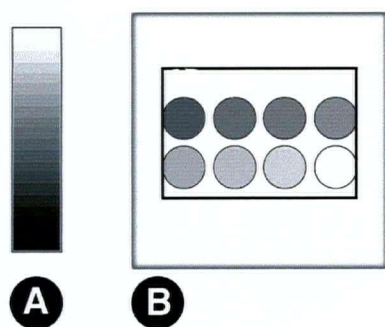


Figure II-5

Made of a continuous strip of plastic, commercially available Kodak OD step tablets (A) typically have eighteen steps, or grey levels, with known OD values. Using this step tablet becomes problematic since, the steps being physically positioned side-by-side, the steps become less distinguishable as the grey levels become darker. To facilitate ease of use and to widen the lower OD range, I created custom designed slides (B) with dots of different grey level that are easily discernible. Using an ELISA microplate reader's spectrophotometer, the OD of each dot was determined; the size of the dots matched the exact dimension of the ELISA microplate cell.

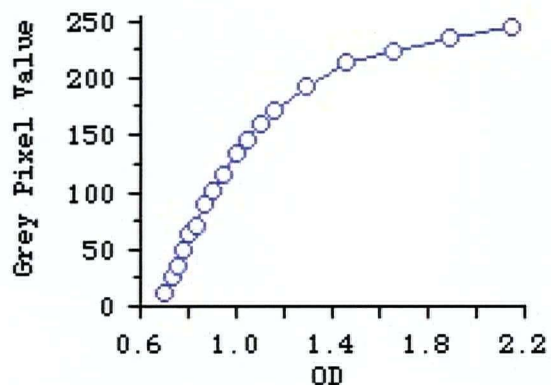


Figure II-6

Grey pixel values from the CCD camera were calibrated to OD units by capturing images of the custom designed OD slides resulting in a curvilinear relationship. A linear relationship exists at the low signal range between grey pixel values and optical density from approximately grey level values of 0 to 150.

II.2.D.i.a. Biological Standard: Matrix preparation

Other investigators have developed standards using a variety of substrate materials, including agarose(Nabors, Songu-Mize et al. 1988), brain paste(Biegon and Wolff 1986), gelatin(Millar and Williams 1982; Schipper, Werkman et al. 1984), polyacrylamide films(Streefkerk and Van der Ploeg 1973), agar beads(Streefkerk, Van der Ploeg et al. 1975; Pool, Madlener et al. 1984), and tissue embedding compound OCT(Huang, Chen et al. 1996). Similar to (Nabors, Songu-Mize et al. 1988) I compared several artificial media (gelatin, agar, and gelatin-agar) for use as a standard and found bactoagar (Difco) to be the best inert matrix in terms of pellucidity and malleability. I also applied a chemical activation technique widely used in affinity chromatography. Unlike Nabors *et al.* (1988) who used the toxic chemical cyanogen bromide (CNBr) for activation, I used the safer chemical periodic acid (HIO_4 , Sigma) which caused oxidation of cis-vicinal hydroxyl groups of bactoagar to generate aldehyde functions which react with primary amines of the antigen/protein(Parikh, March et al. 1974; Wilchek and Miron 1974; Porath and Axen 1976; Penke, Zarandi et al. 1986). Activation involved stirring dry bactoagar in 1% (w/v) periodic acid-anhydrous ethanol for 30 minutes at room temperature. After removing the periodic acid by washing the wet bactoagar with excess anhydrous ethanol, a 12% activated-bactoagar (w/v) slurry was formed by adding distilled water and heated until thoroughly melted. An equal volume of antigen solution was added to weight of the melted activated-bactoagar liquid and thoroughly mixed by sonication. The coupling process was accelerated by the elevated heat

and agitation caused by sonication. The antigen-bactoagar matrix was allowed to gel at room temperature, placed in a 4°C TBS bath for storage until cut into cube form and placed in a liquid 3% (unactivated) bactoagar mold with other antigen-bactoagar cubes of different antigen concentrations, creating a single manageable (calibration) block with eight to twelve embedded cubes (Figure II-7). This calibration block was readily amenable to immunohistochemistry and was either immediately sectioned with a vibratome, or embedded in paraffin before being sectioned with a microtome.

Initial attempts at developing a biological standard used diluted concentrations of homogenised formalin fixed human control cortex placed in the bactoagar matrix but immunostained calibration standards looked particulate under high magnification (**Figure II-8A**) because the antigen source had been formalin fixed before being homogenated, physically preventing thorough homogenisation. I then compared several unfixed antigen sources (differentiated PC12 cells, bovine synaptosome preparations, purified GST-fusion proteins) for use as a standard and found purified synaptosome preparations from bovine cortex to be the best source in terms of quantity and availability.

Briefly, synaptosomes were prepared as follows: a crude synaptosome fraction was isolated based on a minor modification of the method described by Kadota and Kadota (1973) which was adapted from procedures developed by Gray & Whittaker (1962) and Whittaker *et al.* (1964). Cortex (10 g wet weight) dissected from fresh bovine brains were homogenised in 10 mL ice-cold buffered 0.32M sucrose solution (1mM MgCl₂, 1mM NaHCO₃, 0.5mM CaCl₂) and the homogenate

diluted to 100 mL with buffered 0.32M sucrose solution before centrifugation. This material was pelleted (1000 g for 10 minutes), the supernatant saved, and the pellet resuspended by homogenisation in 0.32M sucrose solution and pelleted again. The remaining pellet was discarded and the combined supernates were pelleted (14,500 g for 10 minutes). This pellet (approx. 1 mL) was resuspended in 5 mL of 0.32M sucrose solution and placed on top of a gradient consisting of 5 mL 0.8M sucrose and 5 mL 1.2M sucrose. The gradient was centrifuged for 60 minutes at 14,500 g. The band at the 0.8/1.2M interface was collected, diluted 1:10 with ice-cold distilled water (1 mM MgCl₂, 1 mM NaHCO₃, 0.5 mM CaCl₂), and pelleted by centrifugation (14,500 g for 10 minutes). The pellet containing crude synaptosomes was used as the antigen source for the biological standard. Calibration blocks prepared from the bovine synaptosomes resulted in calibration standards with a homogeneous immunostaining pattern (**Figure II-8B**). The calibration block also contained a cube made from activated bactoagar which had not been coupled to antigen to test the specificity of the immunohistochemical reaction.

The agarose matrix was ideal for immunohistochemical procedures since it could be cut as free floating thick (50 to 200 μm) vibratome sections, or paraffin embedded for thin (from 3 μm to 20 μm) microtome sections. When processed for immunohistochemistry, the agar-antigen matrix provided a 128-fold antigen range with staining intensities nearly approaching the highest staining levels attainable in any human specimen.

When thin (10 μm) sections of the bactoagar-homogenate were immunostained for synaptophysin and SNAP-25, the grey pixel value was determined at both a low and a high

magnification, using a CCD camera-constant source lightbox (Northern Light, Ontario) and a CCD camera-microscope configuration, respectively. Using my custom designed non-biological OD slides, the CCD camera grey pixel values were also converted to OD units for each configuration.

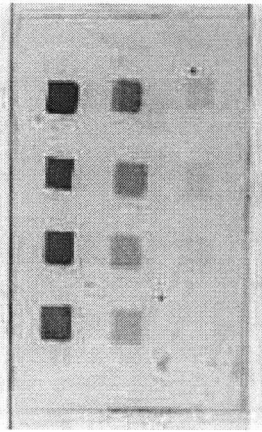


Figure II-7

Example of an immunostained biological standard. The cubes were created through serial dilution of the antigen source by halves. The cube with the highest antigen content (upper left) stains darkest while cube with lower content (move down columns and then across rows) stain lighter.

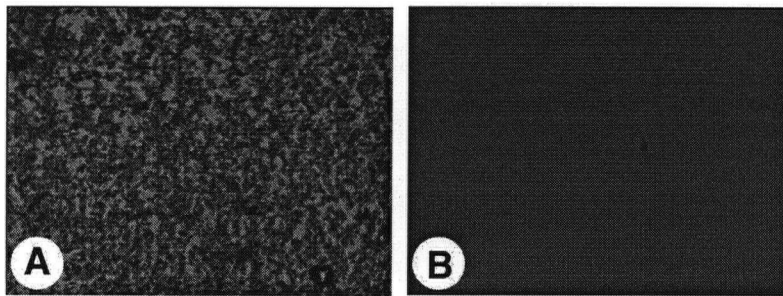


Figure II-8

High magnification 20x images of an immunostained biological standard prepared from formalin fixed human cortex (A) and from purified synaptosomes (B). The formalin fixed antigen source shows clumping and a non-homogenous distribution because formalin fixation prevented the antigen from being thoroughly and evenly mixed. The purified synaptosome antigen source resulted in a homogenous distribution in the bactoagar matrix.

The concentration of antigen showed a curvilinear relationship in terms of grey level and of optical density for both synaptophysin and SNAP-25 immunostained standards. For both synaptophysin and SNAP-25, there was an asymptotic curvilinear relationship between antigen concentration and immunostain OD signal (**Figure II-9** and **Figure II-10**). Since my CCD camera is nearly linear to OD at the low grey level range (\leq grey value of 150), the relationship between antigen amount and OD parallels the findings between antigen amount and grey level. While a log transformation of antigen concentration versus signal (grey or OD) produced a curvilinear relationship over the full range provided by the antigen standard, a linear relationship was found within the range closest to that found in human immunostained sections (inset of **Figure II-9** and **Figure II-10**). For synaptophysin immunostaining, the relevant range found in human sections spanned a 16-fold range of antigen concentration. For SNAP-25 immunostaining, the relevant range spanned an 8-fold range of antigen concentration. The highest signal in the biological standard, however, never equaled nor exceeded the highest signal found in human immunostained sections meaning that the biological standard could handle only the lower range of immunostaining.

2.1.A.iii.b. Optimising antibody-substrate factors

The calibration block allowed us to run controlled experiments to determine the optimal conditions for the immunohistochemical procedure; namely, the optimal concentration of DAB and the optimal DAB incubation time. Uniformly thick sections of the agar-antigen standard were processed identically but, in the developing of the DAB substrate, varying concentrations of freshly prepared DAB (0.00375, 0.0075, 0.015, 0.03, 0.06 and 0.12%) and varying incubation times (2, 4,

8, 16, and 32 minutes) were used (**Figure II-11**). The grey signal range for the stained agar-antigen matrix increased with increasing DAB concentrations, peaking near 0.015% when higher DAB concentrations caused the signal of the highest antigen concentration to become indistinguishable from the signal of the next highest antigen step. The widest grey signal range for a stained agar-antigen matrix occurred at DAB concentrations of 0.015 and 0.03%. The velocity of the DAB reaction begins to plateau for the high range of antigen concentrations at a DAB concentration of 0.03% or higher.

The minimum length of time t_{\min} to wait until the velocity of the DAB reaction reaches its nadir is the time point when the DAB signal begins to plateau for the highest antigen concentration (**Figure II-12**). Focusing on the kinetics of the 0.03% DAB reaction, t_{\min} was determined as approximately eight to ten minutes.

Using these optimised parameters of DAB concentration (0.03%) and DAB incubation time (eight minutes), immunohistochemical image analysis of synaptophysin and SNAP-25 immunoreactivities was performed on postmortem hippocampal samples from cases of schizophrenia and controls.

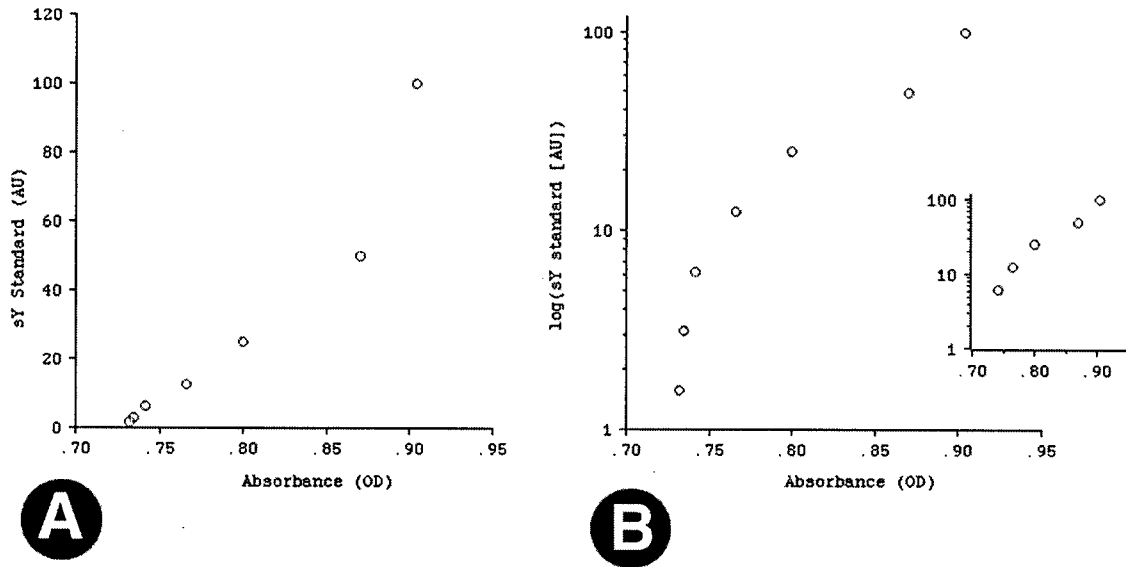


Figure II-9

Relationship between concentration of brain protein (in arbitrary units [AU]) and optical density [OD] signal in a thin (10 μm) biological standard immunostained for synaptophysin image captured at a high magnification (20x microscope objective). A curvilinear asymptotic relationship exists between antigen level and OD signal (A) such that small changes in the higher OD level range translates into dramatically high changes in antigen levels. While a curvilinear relationship remains between OD signal and the log transformation of antigen amount (B), linearity is present within the range closest to the human synaptophysin immunostained thin (10 μm) sections (inset) representing a 16-fold antigen range. (Low magnification images gave similar results as these high magnification findings.)

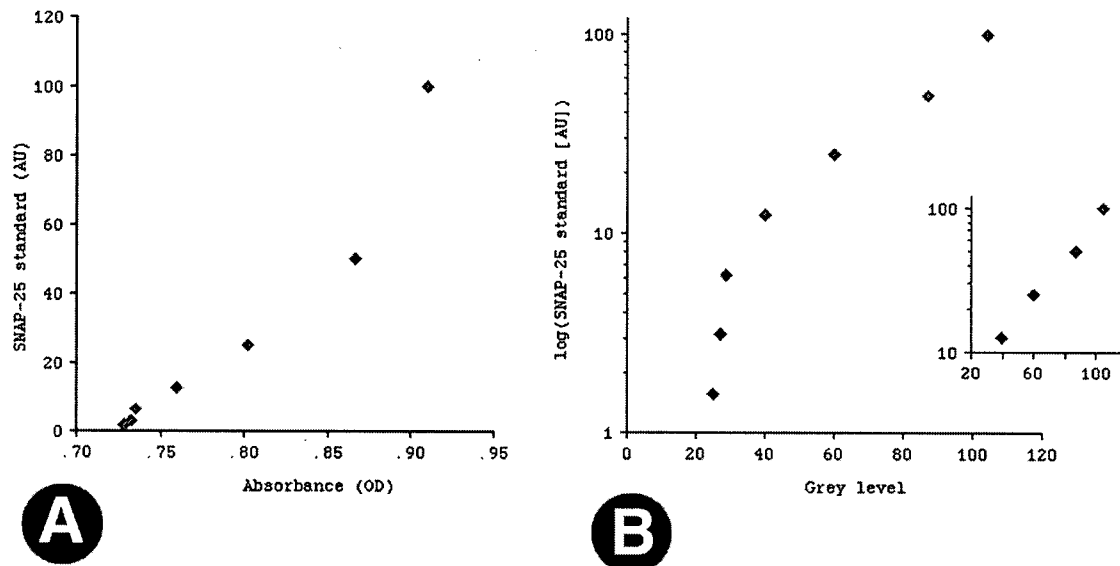


Figure II-10

Relationship between concentration of brain protein (in arbitrary units [AU]) and optical density [OD] signal in a thin (10 μm) biological standard immunostained for SNAP-25 image captured at a high magnification (20x microscope objective). Like the relationship in synaptophysin, SNAP-25 has a curvilinear asymptotic relationship between antigen level and OD signal. A linearity is shown between OD signal and the log transformation of antigen amount (B) within the range closest to the human SNAP-25 immunostained thin (10 μm) sections (inset) representing an 8-fold antigen range. (Low magnification images gave similar results as these high magnification findings.)

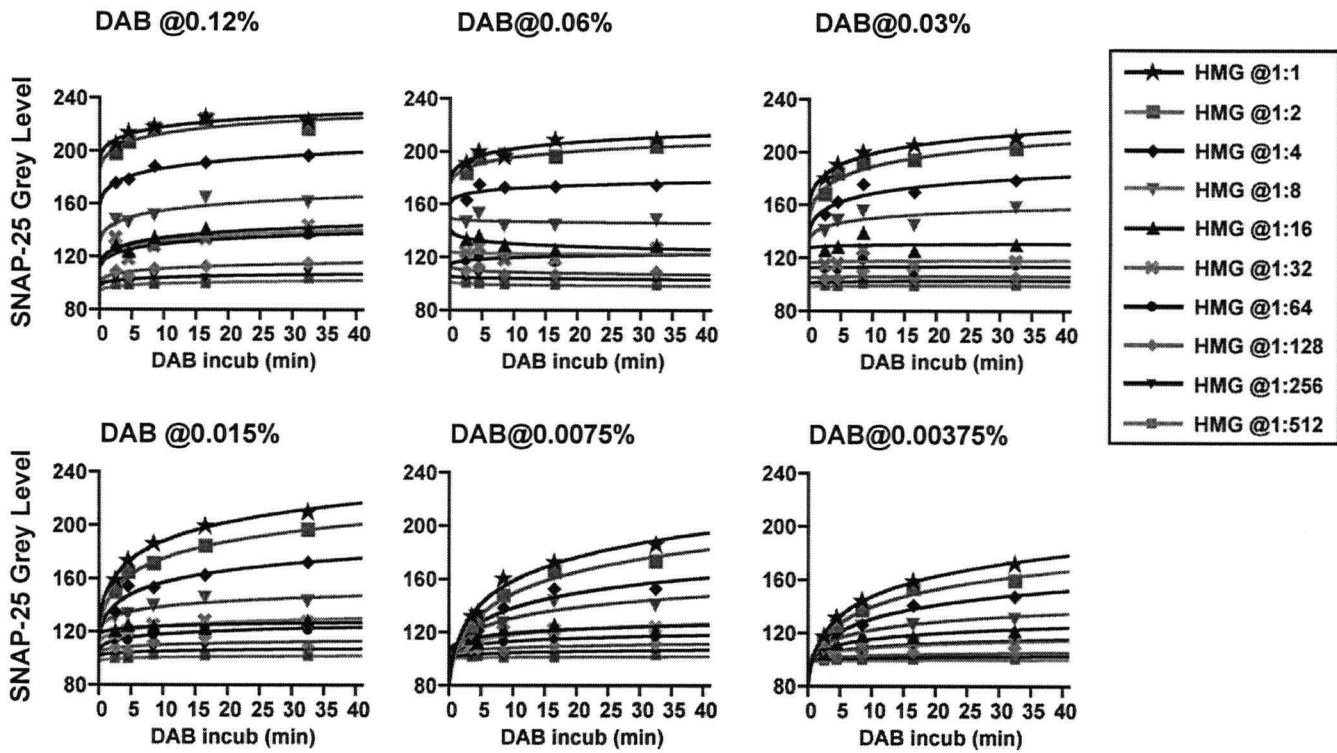


Figure II-11

Relationship between grey value and DAB parameters (concentration and incubation time) in thick (100 μm) biological standards for SNAP-25 immunostaining. The grey signal range increases with increasing DAB concentration, reaching a maximum at 0.015% DAB.

Relationship between grey value and DAB parameters (concentration and incubation time) in thick (100 μm) biological standards for SNAP-25 immunostaining. The grey signal range increases with increasing DAB concentration, reaching a maximum at 0.015% DAB.

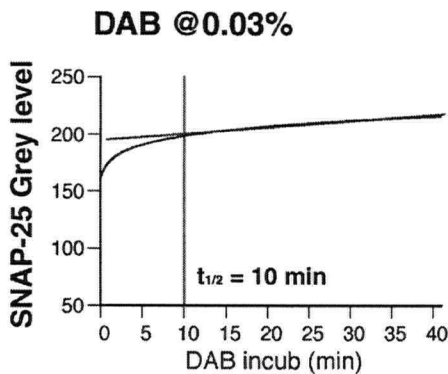


Figure II-12

In determining t_{min} the minimum length of time to wait until the velocity of the DAB reaction is at its lowest I focused on the kinetics of the 0.03% DAB reaction. The time point when the DAB signal begins to plateau for the highest antigen concentration was calculated as between 8 and 10 minutes.

II.2.E. Schizophrenia Samples

II.2.E.i. Case Selection and Clinical Summaries

Paraffin-embedded sections of the hippocampus at or anterior to the lateral geniculate nucleus were available from a sample of 12 schizophrenic patients (eight males and four females) and 12 controls (nine males and three females). Details of individual cases appear in Table II-1.

All of the control hippocampi were from the left side, 7 of 12 schizophrenic were from the left side.

The mean age of schizophrenic patients (56.8 years, SD 9.4) did not differ from controls (54.4 years, SD 16.8) nor did mean postmortem interval (8.6 h, SD 6.7; controls 13.6 h, SD 5.3).

Following fixation in 10% neutral buffered formalin for ~2 weeks, blocks of the hippocampus were removed, paraffin embedded and cut at a thickness of 3 μ m for immunohistochemistry. Specimens were reviewed by a forensic pathologist and/or neuropathologist and found to be free of neurological disease. No clinically relevant neuropathology was found in the specimens for this study. Diagnoses were made according to DSM-III-R criteria following chart review by a research psychiatrist.

Monoclonal antibodies reactive with synaptophysin (EP10) and SNAP-25 (SP12) were used.

Table II-1
Human brains studied

Diagnosis	Illness subtype	Sex	Age (years)	PMI (hrs)	Cause of Death
Schizophrenia	paranoid	M	66	18.0	pneumonia
Schizophrenia	catatonic	M	49	7.0	not recorded
Schizophrenia	disorganized	F	61	2.0	thrombocytopenic purpura
Schizophrenia	disorganized	M	68	6.0	pulmonary tuberculosis, diabetes
Schizophrenia	paranoid	M	48	8.7	not recorded
Schizophrenia	paranoid	F	51	8.7	sudden death, cause uncertain
Schizophrenia	paranoid	F	36	5.0	pulmonary tuberculosis
Schizophrenia	disorganized	M	57	4.0	myocardial infarction
Schizophrenia	catatonic	M	65	8.0	bowel obstruction
Schizophrenia	disorganized	M	56	23.0	bronchopneumonia
Schizophrenia	disorganized	M	65	4.0	pneumonia
Schizophrenia	paranoid	F	60	9.0	pulmonary aspergilliosis
Control		M	57	15.5	coronary vascular disease
Control		F	70	11.0	coronary vascular disease
Control		F	73	22.0	bowel obstruction, tumor
Control		M	29	14.0	accidental multiple trauma
Control		M	59	7.5	myocardial infarction, diabetes
Control		M	33	9.0	transected aorta, accident
Control		M	58	6.5	coronary vascular disease
Control		M	41	17.5	acute myocardial infarction
Control		M	68	11.5	coronary vascular disease
Control		F	68	17.0	coronary vascular disease
Control		M	29	10.0	transected aorta, accident
Control		M	68	22.0	acute myocardial infarction

II.2.E.ii. Immunohistochemistry

Sections were deparaffinized by sequential immersion in xylene and decreasing concentrations of alcohol followed by Tris-buffered saline (TBS: 10 mM Tris-HCl, 140 mM NaCl, pH 7.4). This was followed by incubation in TBS plus 0.2% Triton X-100 with 3% hydrogen peroxide for 30 min. Non-specific immunoreactivity was blocked by incubation in TBS-5% nonfat powdered milk for 1 hr at room temperature [RT]. Primary antibodies (tissue culture supernatant EP10 and SP12) diluted 1:10 in TBS-milk were then added and incubated overnight at 4°C. Slides were then washed in TBS (five times for 5 min) at RT. Biotinylated goat anti-mouse immunoglobulin G plus M (Jackson Immunolabs) diluted 1:500 in TBS was then added for 1 hr at RT. Following a TBS wash (five times for 5 min) at RT, peroxidase-conjugated streptavidin (Jackson Immunolabs) was added in a dilution of 1:1000 in TBS for 30 min at RT. After sections were washed in TBS (five times for 5 min) at RT, sections were incubated in freshly prepared 0.03% diaminobenzidine (Sigma), 0.015% hydrogen peroxide in 0.1M Trizma-base, pH 7.4. The reaction was terminated after 8 min, the slides then dried, dehydrated by serial immersion in increasingly concentrated alcohol solutions and finally xylene, then coverslipped using Permount. A common reference section was used as a positive control for EP10 and SP12 staining for each run of immunohistochemistry. In addition, for a negative control, tissue culture medium conditioned by the parent, nonsecreting myeloma cell line was substituted for the primary antibody on an additional section.

2.1.B.iii. Imaging and Image Analysis

Images of the whole hippocampus were collected blinded to diagnosis using my Sony CCD video camera, Nikon lens, and a Northern Light constant source lightbox. As per 2.1.A., imaging conditions were optimised to ensure appropriate compliance with the Beer-Lambert Law; namely, a single wavelength filter (Lee Chromalux HT 363) centred around 450 nm and a custom designed series of monochrome slides for calibrating grey scale intensities to OD values were utilised. A reference sample was imaged at the beginning and end of each session to ensure consistency of technique.

Hippocampal regions of interest were demarcated (**Figure II-13**) with the help of a neuropathologist (Dr.T.G.Beach) using an atlas (Duvernoy, 1988). Ammon's horn subregions were defined by characteristics of the pyramidal cell layer including width (seen on adjacent Nissl-stained sections) and terminations of afferent projections such as the mossy fibres (synaptic immunostained sections). From the OD converted grey scale image, regions were outlined using NIH Image v.1.45 (Rasband 1996), and the mean pixel intensity was calculated. For synaptophysin, white matter values were subtracted from grey matter image values on the same section. Since SNAP-25 is present in axons to a small but variable extent, this correction was not applied to SNAP-25 immunostaining. Instead, the background value from the negative control section was subtracted from the image values. Run-to-run variability in staining intensity of sections from the same case was 9% for synaptophysin, and 2% for SNAP-25.

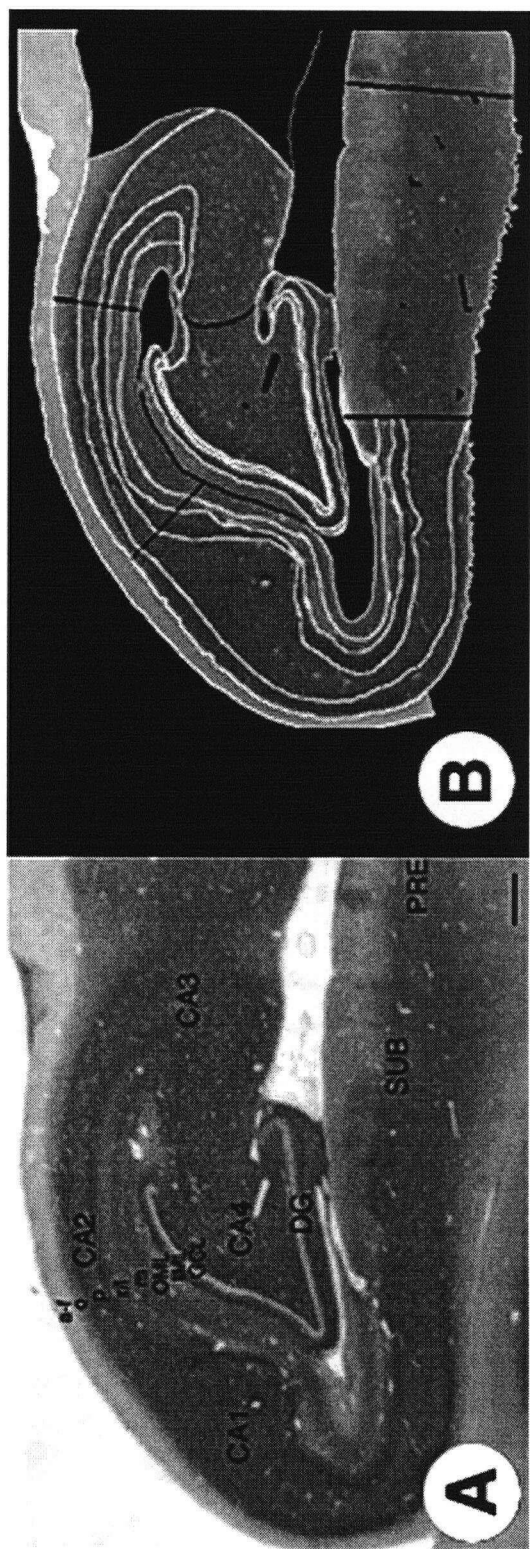


Figure 2-13 Example of a SNAP-25 immunostained human hippocampus (A). Regions and layers were demarcated (B) with aid of a brain atlas (Duvernoy, 1988) and a neuropathologist.

2.1.B.iv. Statistical Analysis

For analysis of hippocampal regions of interest on immunostained sections, repeated-measures analysis of variance (ANOVA) was used for data sets obtained from CA1-CA3, and the dentate gyrus. Significant interactions between diagnosis and subregion, and the additional regions not included in the repeated-measures analyses were studied with analysis of variance using age and postmortem interval as covariates for each subregion. Bonferroni corrections were applied for multiple comparisons (eight initial regions [presubiculum, subiculum, alveus-fimbria, CA1, CA2, CA3, CA4 and the dentate gyrus], followed by three [in the dentate gyrus: outer molecular layer, inner molecular layer, and the granule cell layer] or four subregions [in the CA: oriens, pyramidal, radiatum/lacunosum, and the molecular layer] for significant interaction effects). Two sections from cases of schizophrenia and one control section stained poorly with antibody EP10 and these were omitted from analyses of synaptophysin immunoreactivity. All sections stained well for SNAP-25 immunoreactivity with antibody SP12.

II.2.F. Colocalisation Of Presynaptic Proteins

In studying the co-distribution of synaptophysin and SNAP-25 in the regions and layers of the hippocampus, I hoped to better understand the possible role of each presynaptic protein in the well-defined circuitry of the hippocampus. Given that synaptophysin is expressed in all presynaptic terminals while SNAP-25 is expressed in a specific subset of synapses and axons, colocalisation of these two presynaptic proteins was hypothesised to reveal overlap in synaptic terminals with a wider distribution for synaptophysin and to reveal only SNAP-25 in axons.

II.2.G. Colocalisation with visible light microscopy: AEC Colocalisation

Studies of colocalisation of antigens often use immunofluorescent techniques. There are, however, limitations to these approaches in human brain fixed in formalin due to autofluorescence. I used several strategies (described in Appendix 1) to limit autofluorescence without success. There are advantages to chromogen-based strategies for colocalisation (Taylor 1978; Valnes and Brandtzaeg 1982). These include: application on fixed and paraffin-embedded tissue specimens, the bright-field microscopical observation, and the production of (semi) permanent coloured precipitates (Taylor 1978; Valnes and Brandtzaeg 1982).

By taking advantage of the physical property of the staining substrate AEC (which is soluble to alcohol and can therefore be washed off), I have developed a sequential double immunolabelling technique using the same immunoenzymatic system. The reliability of the method presented here was established in two model systems where I separately showed: (1) no overlap in the two AEC

stains (of non-overlapping antigens, synaptophysin and myelin basic protein) at a low magnification and (2) no overlap in the two AEC stains (of non-overlapping antigens NeuN and GFAP) at a higher magnification. Once the reliability of the method was shown, I used this AEC colocalisation method to study the co-distribution of synaptophysin and SNAP-25.

Antibodies

Monoclonal antibodies reactive with synaptophysin (SP15, mouse immunoglobulin M) and myelin-basic protein (SMI-94, mouse immunoglobulin G, Sternberger) were chosen for the low magnification colocalisation studies because no overlap is expected from these markers of presynaptic contacts and myelin, respectively. A monoclonal neuronal nuclei antibody (NeuN, mouse immunoglobulin G, Chemicon) and a polyclonal glial fibrillary acidic protein antibody (GFAP, rabbit immunoglobulin G and M, gift from Dr. S. Yen, Albert Einstein College of Medicine) were used for the microscopic study because no overlap is expected from these markers of neurons and astrocytes, respectively. Monoclonal antibodies reactive with synaptophysin (SP15, mouse immunoglobulin M) and SNAP-25 (SP12, mouse immunoglobulin G) were used for the synaptic colocalisation study in the hippocampus from two controls and two schizophrenics.

AEC Colocalisation Immunohistochemistry

Human paraffin sections were deparaffinized by sequential immersion in xylene and decreasing concentrations of alcohol followed by TBS. This was followed by incubation in TBS plus 0.2% Triton X-100 with 3% hydrogen peroxide for 30 min. Non-specific immunoreactivity was blocked by incubation in TBS-5% nonfat, powdered milk for 1 hr at RT. The paired antibodies

diluted in TBS-milk (1:10 SP15, 1:100 MBP; 1:100 NeuN, 1:500 GFAP; 1:10 SP15, 1:10 SP12) were both added simultaneously and co-incubated overnight at 4°C. (For NeuN, antigen heat retrieval was performed(Wolf, Buslei et al. 1996)). Briefly, after deparaffinization, sections were placed in a pH 5.4 citric acid bath at 95°C for 10 minutes followed by immunohistochemical procedures above.) Slides were then washed in TBS (five times for 5 min) at RT. A peroxidase-conjugated subclass/species-specific secondary antibody (Jackson Immunolabs) diluted 1:500 in TBS was then added for 1 hr at RT to probe for one of the two primary antibodies. Following a TBS wash (five times for 5 min) at RT, sections were incubated in freshly prepared 0.03% aminoethyl carbazole (Sigma), 0.015% hydrogen peroxide in 0.1M acetate buffer, pH 5.4. When the reaction was terminated after 8 min, the slides were then dried and coverslipped using mineral oil.

Images of the whole hippocampus were collected using a Sony CCD video camera, Nikon lens and a Northern Light constant source lightbox. Microscopic images of the granule cell layer of the dentate gyrus were captured using the Sony CCD video camera in combination with the 40x objective of an Olympus BH2 microscope. To improve the standard immunocytochemical technique, a Lee Chromalux Primary Green filter centred at 510 nm was used to complement the red AEC reaction product and to optimise the response characteristics of the camera.

After image capture, the coverslip was removed and the AEC stain cleared by sequential immersion in increasing concentrations of alcohol followed by immersion in xylene to remove the mineral oil.

This was followed by incubation in TBS with 6% hydrogen peroxide for 30 min to inactivate the enzymatic ability of the peroxidase linked to the first secondary antibody. Slides were then washed in TBS (five times for 5 min) at RT. A biotinylated subclass/species-specific secondary antibody (Jackson Immunolabs) diluted 1:500 in TBS was then added for 1 hr at RT to probe for the other of the paired primary antibodies. Following a TBS wash (five times for 5 min) at RT, peroxidase-conjugated streptavidin (Jackson Immunolabs) was added in a dilution of 1:1000 in TBS for 30 min at RT. Following a TBS wash (five times for 5 min) at RT, sections were incubated in freshly prepared 0.03% aminoethyl carbazole (Sigma), 0.015% hydrogen peroxide in 0.1M acetate buffer, pH 5.4. When the reaction was terminated after 8 min, the slides were then dried and coverslipped using mineral oil.

Images were obtained under standardised conditions as before and formatted using the same NIH Image and Adobe Photoshop software parameters for each set of images.

Controls included executing all steps throughout but in which tissue culture medium replaced one or both primary antibodies and included reversing the order of application of subclass/species specific secondary antibodies.

II.3. RESULTS

II.3.A. Schizophrenia

Initial analyses of 18 different grey matter regions indicated no statistically significant correlation between SNAP-25 immunostain intensity and age. Significant negative correlations were observed for synaptophysin immunostain intensity and age for the presubiculum and

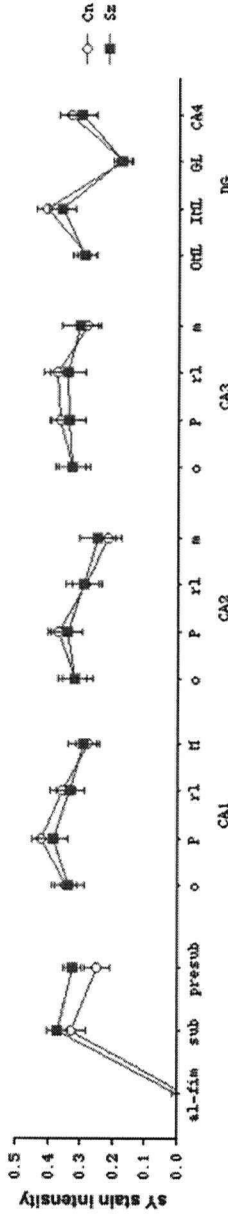
subiculum ($r = 0.44-0.55$, $P = 0.04$, uncorrected for multiple comparisons). Significant positive correlations were observed for SNAP-25 immunoreactivity and postmortem interval for presubiculum and CA1 and CA2 pyramidal layers ($r = 0.41-0.52$, $P = 0.03$; $r = 0.44-0.55$, $P = 0.03-0.05$, uncorrected for multiple comparisons). No correlations between synaptophysin immunoreactivity and postmortem interval were observed.

In images of the overall hippocampus, although mean synaptophysin immunostain intensity tended to be lower in most regions in schizophrenia, no significant differences were observed (**Figure 2-14A**). Significant reductions in mean SNAP-25 immunostain intensity were observed in the subiculum ($F=9.876$, $df=1$, $p=.0051$), CA1 ($F=12.414$, $df=1$, $p=.0021$), CA2 ($F=14.259$, $df=1$, $p=.0013$), and the dentate gyrus ($F=14.259$, $DF=1$, $P=.0013$) in schizophrenia (**Figure 2-14B**); the significant level was set at $0.05/8$, or $p=.0063$ for 8 comparisons. Analyses of individual subregions were covaried for age and postmortem interval. Significant reductions were observed in multiple subregions, including the oriens ($F=9.426$, $df=1$, $p=.0060$), radiatum-lacunosum ($F=8.353$, $df=1$, $p=.0091$), and molecular layers ($F=10.897$, $df=1$, $p=.0036$) of CA1; the oriens ($F=13.998$, $df=1$, $p=.0014$), pyramidal ($F=13.486$, $df=1$, $p=.0016$), radiatum-lacunosum ($F=14.143$, $df=1$, $p=.0013$), and molecular layers ($F=10.854$, $df=1$, $p=.0038$) of CA2; the inner ($F=9.292$, $df=1$, $p=.0063$), outer ($F=7.053$, $df=1$, $p=.0152$), and granule cell layers ($F=15.911$, $df=1$, $p=.0007$) of the dentate gyrus; the significant level was set at $0.05/4$, or $p=.0125$ for the four subregions within CA layers, and at $0.05/3$, or $p=0.0167$ for the three subregions within the dentate gyrus. No significant differences were observed in the presubiculum, CA3, CA4, or alveus-fimbria.

When the comparisons were restricted to the subset of cases of schizophrenia with available left side sections, the results were the same as for the overall group for both synaptophysin and SNAP-25. Because there were no right side sections available for controls, this comparison was not possible; however, no left to right side differences in immunostaining were observed in schizophrenia.

ALTERED PRESYNAPTIC-IR IN THE SCHIZOPHRENIC HIPPOCAMPUS

A. Synaptophysin Immunoreactivity



B. SNAP-25 Immunoreactivity

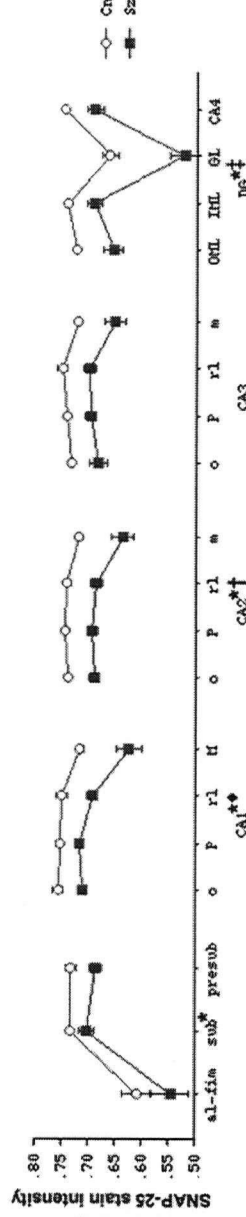
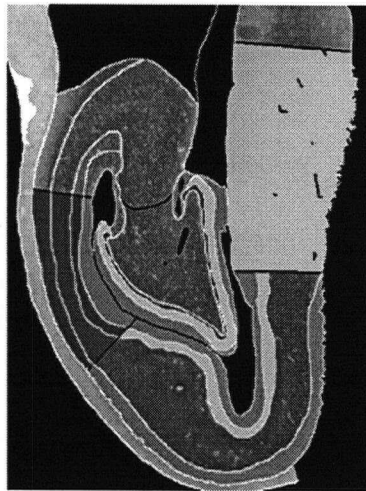


Figure 2-14 In images of the overall hippocampus, although mean synaptophysin staining intensity (A) tended to be lower in most regions in schizophrenia, no significant differences were observed. SNAP-25 staining intensity (B) was significantly reduced in regions such as the subiculum, CA1, CA2 and the dentate gyrus (main effect of diagnosis on SNAP-25 immunoreactivity: * $p < 0.05$, † $p < 0.005$, ‡ $p < 0.0001$). The statistical significance of SNAP-25 reductions in individual subregions is represented diagrammatically (diagram B). Analyses were covaried for age and postmortem interval.

CA1-4
Al-fim
Sub
Presub
o
p
r
l
m
DG
OML
IML
GL

Ammons region
alveus fimbria
subiculum
presubiculum
oriens layer
pyramidal layer
radiatum-lacunosum layer
molecular layer
Dentate gyrus
outer molecular layer
inner molecular layer
granule cell layer

2.2.B. COLOCALISATION

2.2.B.i. *Effectiveness of AEC Colocalisation Immunohistochemistry*

Using the AEC colocalisation method, I showed little overlap at the low magnification level between synaptophysin (a marker of synaptic connectivity) and MBP (a marker of myelin) (**Figure II-15**) and I showed no overlap at the higher magnification level between neuronal nuclei (NeuN, a marker of neurons) and GFAP (a marker of astrocytes) (**Figure II-16**). Reversing the order of AEC immunostaining did not change the distribution pattern and still resulted in little overlap in the antibody pairs studied (**Figure II-17**).

Having demonstrated the effectiveness of this method, I proceeded to examine the colocalisation of synaptophysin and SNAP-25 in the hippocampus of two controls and two schizophrenics.

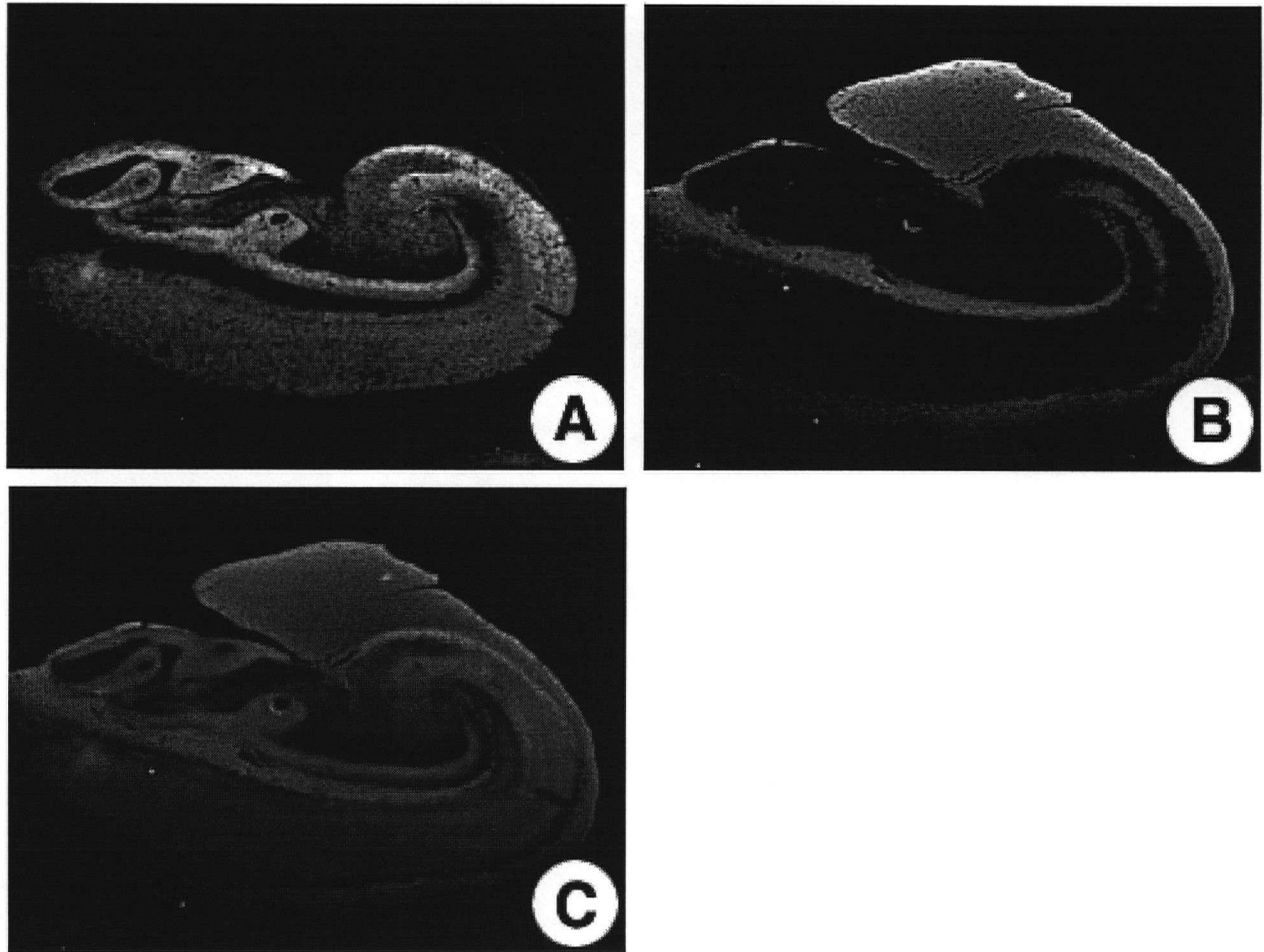


Figure II-15

Result of double AEC immunostaining for synaptophysin and MBP in normal human hippocampus. Synaptophysin expression (A) was confined to grey matter regions where synaptic contacts reside while MBP expression (B) was restricted to the heavily myelinated white matter regions. Overlapping the two images (C) shows little overlap between synaptophysin (red) and MBP (green)—except in the terminal zone of the mossy fibres in CA3 where the granule cells send their axonal and synaptic projections—illustrating the reliability of this method in colocalising at the panoramic (or gross magnification) level.

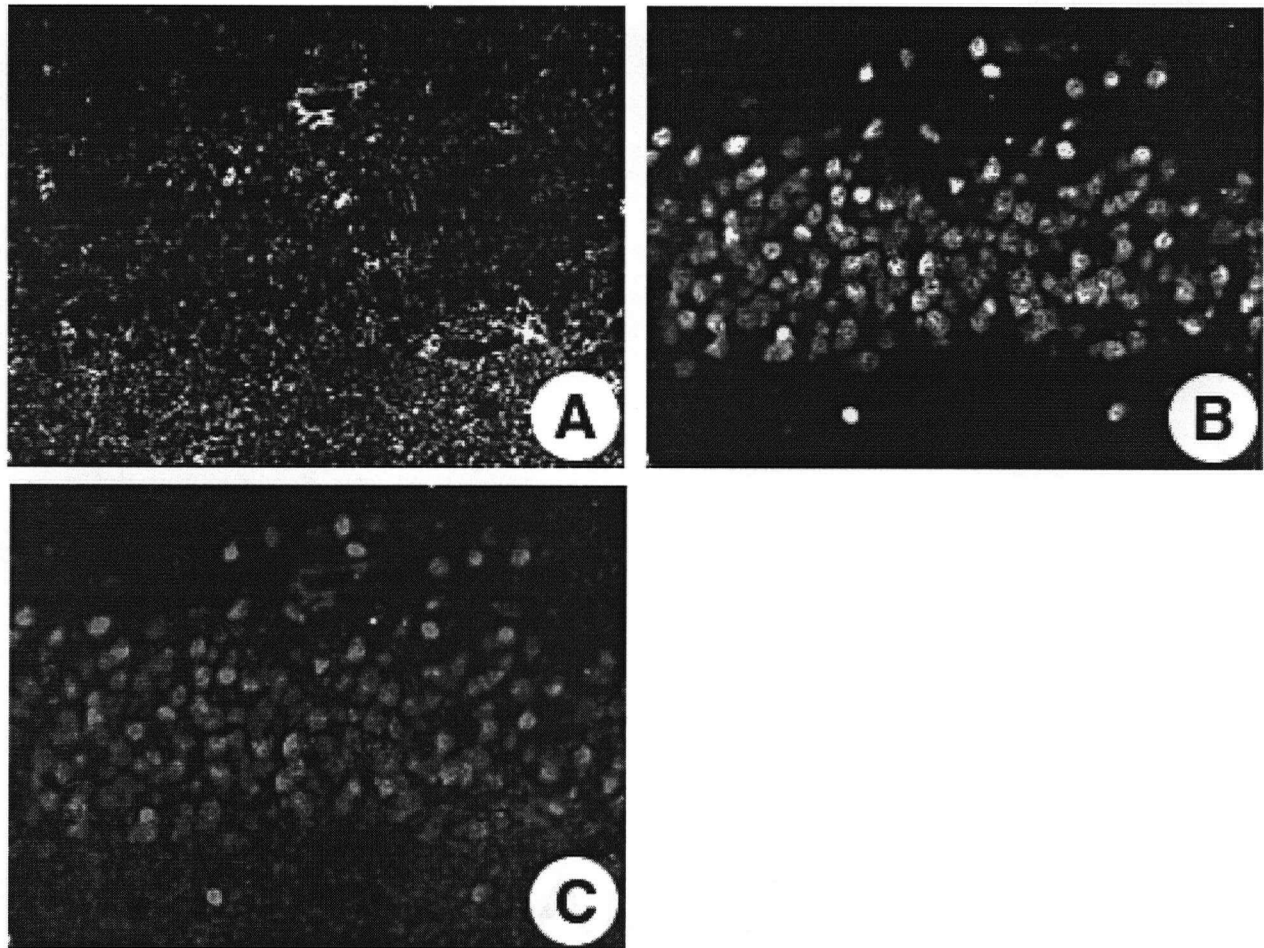


Figure II-16

Result of double AEC immunostaining for NeuN and GFAP in normal human hippocampus. GFAP expression (A) is restricted to astrocytes and processes, the majority of which reside in the molecular layer with some processes penetrating through the span of the granule cell layer. NeuN expression (B) is confined mainly to the neurons in the granule cell layer with some expression in isolated neurons in the molecular layer of the dentate gyrus. When sequentially probing for GFAP (A) and then NeuN (B), overlapping the two images (C) shows no overlap between GFAP (red) and NeuN (green), illustrating the reliability of this method in colocalising at the microscopic level.

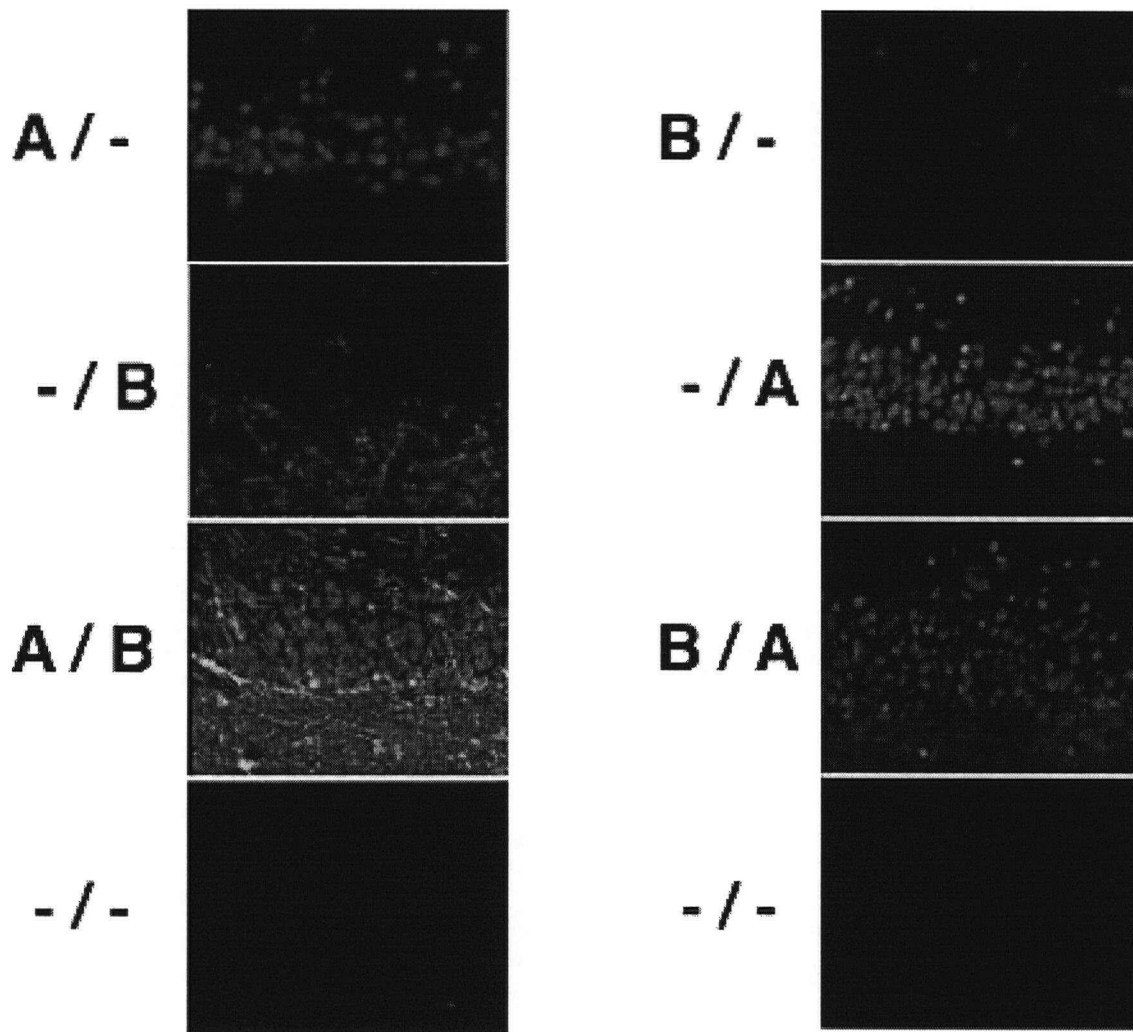


Figure II-17

Result of AEC double immunostaining (A = NeuN, B = GFAP) in different sequential orders. The left column shows paired antibody combination with NeuN (red) visualised first and then GFAP (green). The right column shows the reverse order with GFAP (red) visualised first and then NeuN (green). The sequence of visualisation had no effect on the (non-overlapping) distribution pattern between NeuN and GFAP.

II.3.B. Presynaptic colocalisation in controls and in schizophrenia

A double immunostaining study was performed to determine the extent of regional overlap between hippocampal synaptophysin and SNAP-25 in controls and in schizophrenia. In controls, relative to synaptophysin, SNAP-25 immunostain intensity was increased in the oriens, radiatum-lacunosum, and CA4 (**Figure II-18**). In schizophrenia, relative to synaptophysin, SNAP-25 immunostain intensity was reduced in the radiatum-lacunosum and terminal regions of perforant pathway afferents, elevated in CA4, in the terminal zone of the mossy fibres in CA3 and in the alveus fimbria (**Figure II-19**).

These findings suggest that SNAP-25 may be more abundant in subsets of terminals, with discrete patterns of distribution.

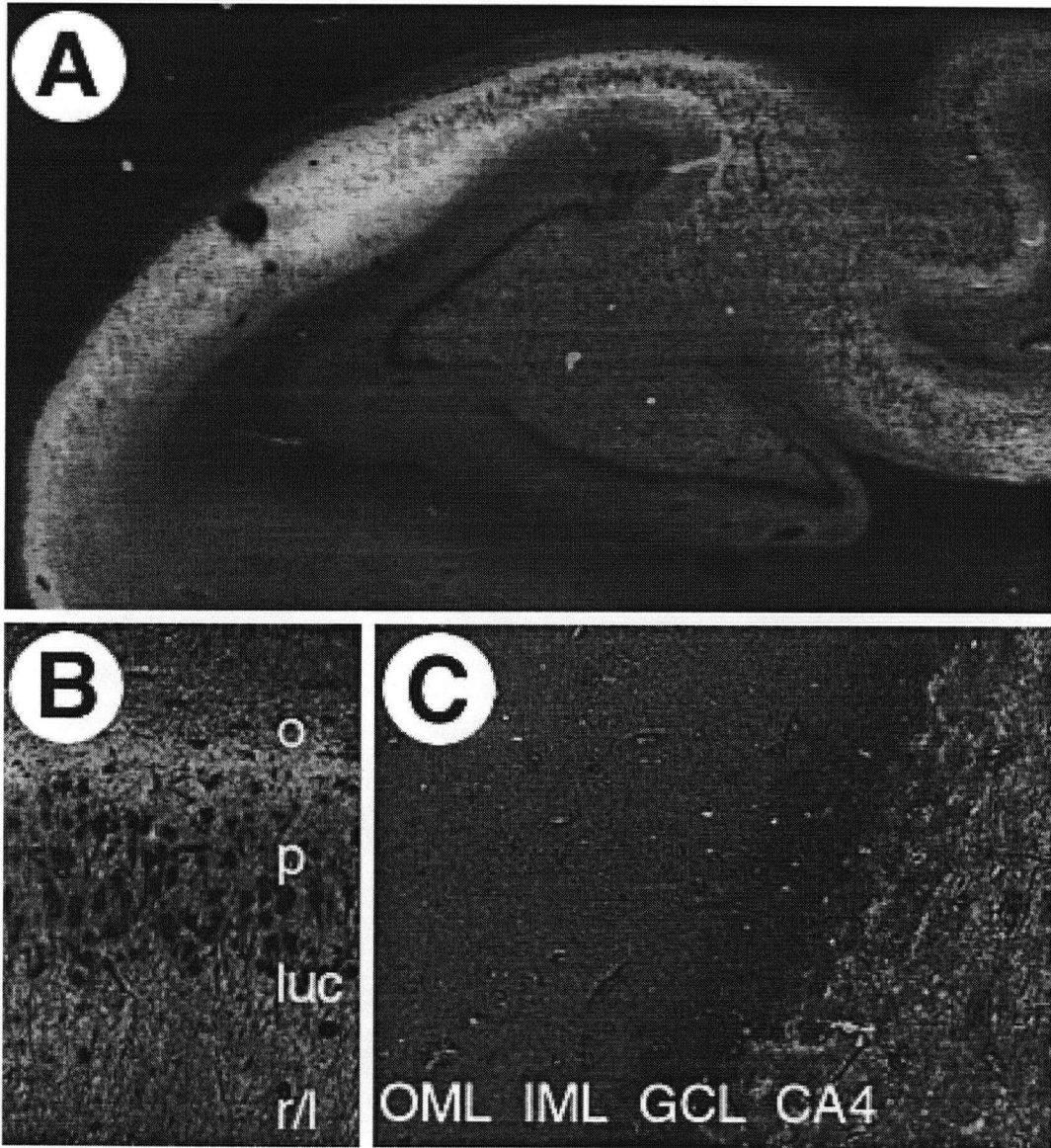


Figure II-18

Result of double AEC immunostaining for synaptophysin (red) and SNAP-25 (green) in control hippocampus. In A, relative increases of SNAP-25 compared to synaptophysin signal in the Ammon's horn, notably in the oriens and the radiatum-lacunosum, are seen. SNAP-25 was relatively elevated in the alveus (B) and decreased throughout the area surrounding CA3 pyramidal neurons (B). Higher magnification view of the dentate gyrus (C) illustrates generally low levels of SNAP-25 in the molecular layer and elevated levels in the polymorph layer.

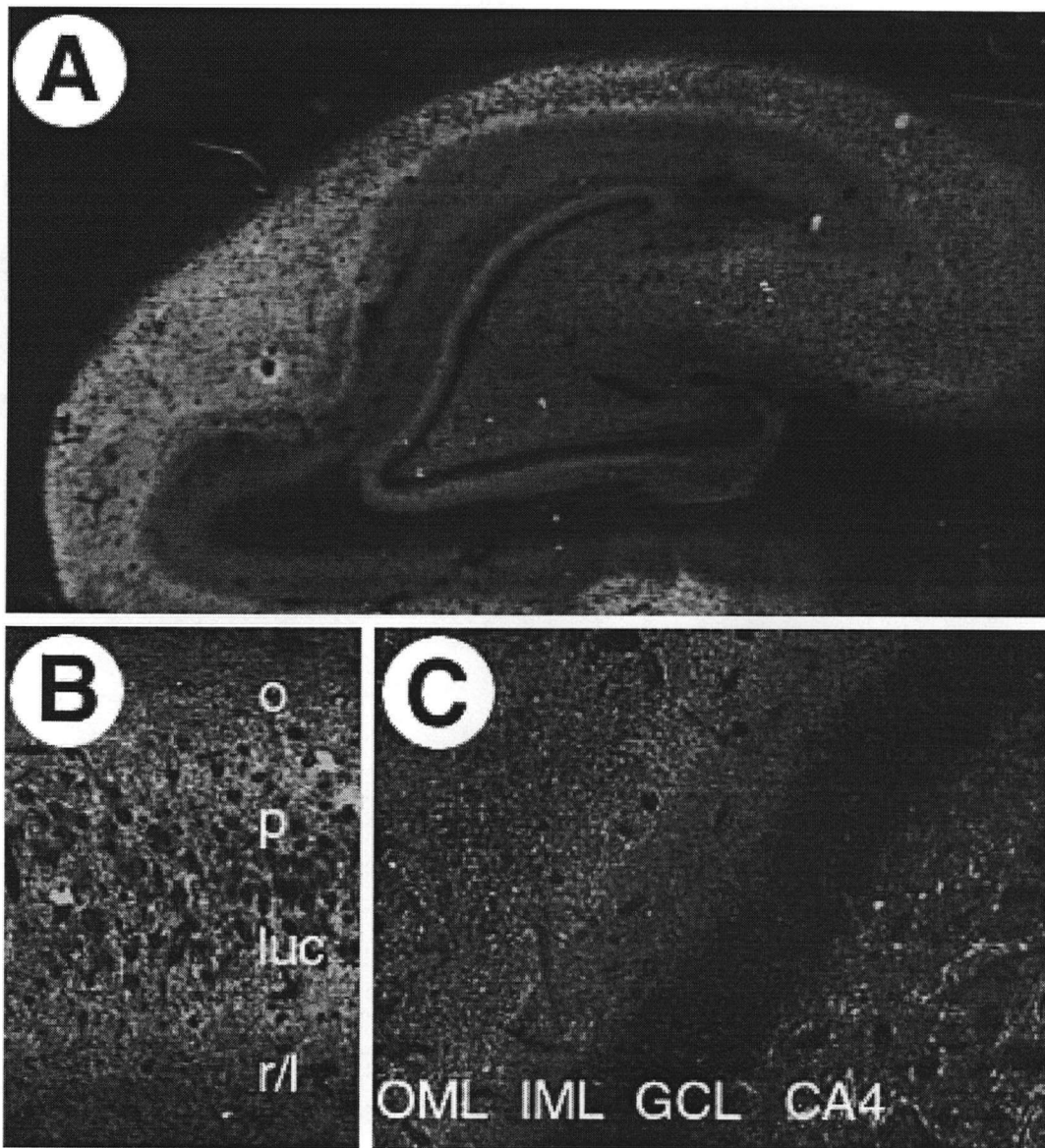


Figure II-19

Result of double AEC immunostaining for synaptophysin (red) and SNAP-25 (green) in schizophrenic hippocampus. In A, relative loss of SNAP-25 compared to synaptophysin signal was observed in the Ammon's horn and dentate gyrus molecular layer. SNAP-25 was relatively increased in the alveus (B) and in the mossy fibre terminals at the base of the CA3 pyramidal cells (B). Higher magnification view of the dentate gyrus (C) illustrates relative loss of SNAP-25 in the molecular layer.

II.4. CONCLUSION

In this chapter, analyses of the overall hippocampus revealed no change in synaptophysin immunostain intensity with a concomitant reduction of SNAP-25 immunostain intensity in perforant pathway termination zones (subiculum, molecular layer of CA1 and CA2, and the outer molecular layer of the dentate gyrus) in schizophrenia. The present data is consistent with my hypothesis that a subset of circuits from the entorhinal cortex to the hippocampus is disconnected in schizophrenia.

Since specific subregions of the dentate gyrus and the granule cell layer have different development profiles, the changes seen in the dentate gyrus provided impetus for a closer examination into the hypothesis that a developmental pattern of synaptic change in this area might be seen in schizophrenia.

Chapter III MECHANISMS OF ILLNESS IN SCHIZOPHRENIA: GRANULE CELL LAYER DEVELOPMENT OF DENTATE GYRUS

III.1. OVERVIEW

In the last decade, the developmental basis for schizophrenia has been supported by neuroanatomical studies (Pilowsky, Kerwin et al. 1993; Bunney, Potkin et al. 1995; Harrison 1995; Knable and Weinberger 1995; Arnold, Franz et al. 1996; Harrison 1999). Histological studies of the cortical lamination patterns in hippocampal and parahippocampal regions suggest defective neuronal migration or cortical organisation in development (Jakob and Beckmann 1986; Kovelman and Scheibel 1986; Jakob and Beckmann 1989; Arnold, Hyman et al. 1991). Therefore I hypothesised that presynaptic proteins (markers of synaptic connectivity) in specific subregions of the dentate gyrus (which have a different developmental profile) would be altered in schizophrenia.

In the human fetal dentate gyrus, two developmental gradients are apparent: the limbs of the granule cell layer evince differences in cell density and organisation prenatally (Arnold and Trojanowski 1996), while the span of the granule cell layer continues to increase postnatally (Rakic and Nowakowski 1981; Eckenhoff and Rakic 1988; Eriksson, Perfilieva et al. 1998). The two limbs are initially anatomically different early in gestation with the (early forming) external limb being more condensed and more organised than the (later forming) internal limb (**Figure I-3**) and with the limbs becoming more anatomically identical towards term. Concomitantly during development and throughout adulthood, newly formed granule cells at the proliferative zone near the polymorph border migrate into and across the granule cell layer towards the molecular border. This creates a

gradient across the span of the granule cell layer with granule cell age increasing as one moves from the polymorph to the molecular edge (**Figure I-4**).

I hypothesized that the timing of abnormalities in neural development in schizophrenia might be resolved according to the pattern of abnormal synaptic immunoreactivity seen in the developmentally organized subregions of the dentate gyrus. Namely, if schizophrenia is problem of abnormal prenatal development, then one would expect a different pattern of connectivity between the two limbs of the dentate gyrus, while a postnatal problem would show differences in the span of the granule cell layer.

Using optimised immunohistochemical image analysis, I studied presynaptic proteins (synaptophysin and SNAP-25) in these two developmentally organised components of the dentate gyrus: one, the limbs of the dentate gyrus and the other, the span of the granule cell layer.

III.2. MATERIALS & METHODS

III.2.A. Immunohistochemical Image Analysis

Images of the granule cell layer of the dentate gyrus from immunostained sections (2.1.B.i.) were collected using the 20x objective of an Olympus microscope. The full extent of the granule cell layer of both limbs of the dentate gyrus in each section was sampled by obtaining multiple images, avoiding areas with convolutions (**Figure III-1**). The granule cell layer in both limbs was outlined manually (**Figure III-2**) using NIH Image software v.1.45 (Rasband 1996) and the span of the layer divided into five segments (**Figure III-3**): two border regions (molecular [M] and

polymorph [P]) and three regions in-between (a,b,c). For analysis, Brain Image software v.2.0 (Abrams, 1995) was used for thresholding and for parameter measures.

III.2.B. Threshold Selection method: Otsu filter

Selecting an adequate threshold of grey level for extracting objects from their background is important for proper image analysis. A methodological investigation revealed that while subjective decisions for determining the appropriate threshold by observer judgement are highly variable depending on the weighted preference for stain intensity and/or image characteristics, automatic selection of immunostained regions is problematic when staining intensity is low and near background levels (Jago, Steel et al. 1991). Since the degree of presynaptic immunostaining in my samples was markedly higher than background for both synaptophysin and SNAP-25, I decided that the use of an automated method for threshold determination was appropriate.

For analysis with Brain Image software, I used a nonparametric and automated method of threshold selection formulated by (Otsu 1979) which is based on the global properties of an image's histogram. The Otsu filter set the optimal threshold value distinguishing immunostained elements from background for each image allowing subtraction of unstained areas such as blood vessels and cell somas (**Figure III-4**) from positively immunostained areas.

III.2.C. Parameters measured: Mean Intensity & Fractional area of immunostaining

The width of the granule cell layer was measured to gauge possible granule cell loss or proliferation. As well, in the present study, the parameters measured (stain intensity and fractional

area of immunostaining) are those commonly utilised within the field of immunohistochemical quantification of synaptophysin and SNAP-25.

3.1.C.i.) Intensity of immunostaining

Technical aspects of measurement of intensity were discussed in sections 2.1.A.. The intensity of immunostaining can be interpreted as the amount of synaptic protein per terminal. Changes in immunostaining intensity may imply a disruption in the regulation of presynaptic proteins. Since SNAP-25 is an essential for neurotransmission and plasticity, altered SNAP-25 immunostaining intensity in this context may relate to alterations in neurotransmitter release and synaptic functioning.

3.1.C.ii.) Fractional area of immunostaining

Previous investigators have used confocal and quantitative electron microscope studies of synaptophysin percentage area stained as an indicator of global presynaptic terminal number. For instance, this technique has been used to demonstrate decreases in numerical density, average area, and surface density of synaptic contacts with increasing age (Bertoni-Freddari, Fattoretti et al. 1989; Masliah, Mallory et al. 1993). The percentage area stained by SNAP-25 would be an indicator of a specific subset of presynaptic terminal number. Unlike staining intensity which may relate to the strength of synaptic contacts, fractional area of immunostaining relates to the number of synaptic contacts in a given region.

III.2.D. Statistical Analysis

For analysis of dentate gyrus regions of interest in immunostained sections, mean intensity of immunostaining was first compared between diagnostic groups in each limb of the granule cell layer as a whole, using a t-test. Significant results were followed up by a comparison across the five granule cell sublayers of the limb using a repeated measures analysis of variance (ANOVA) with diagnosis as a main effect and sublayer as a within-subject repeated measure. Where a significant interaction was indicated, post-hoc t-tests were calculated for each sublayer.

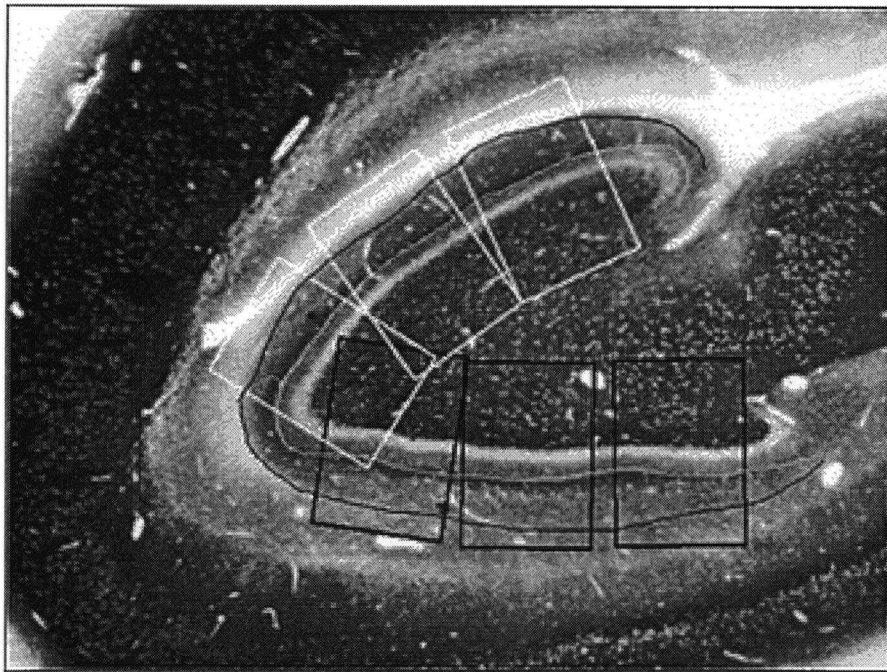


Figure III-1

Example of a SNAP-25 immunostained human hippocampus showing the regions (boxes) sampled at 20x microscope magnification. The full extent of the granule cell layer was sampled by obtaining images from both the ventral limb (black boxes) and the lateral limb (white boxes) of the dentate gyrus.

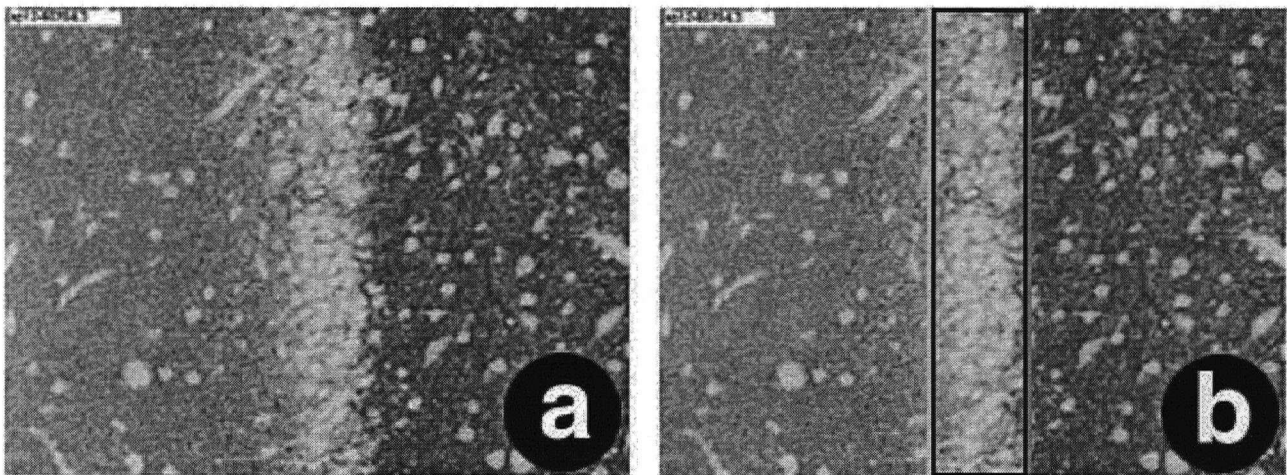


Figure III-2

Example of a SNAP-25 immunostained human hippocampus showing the raw image of the granule cell layer (A) sampled at 20x microscope magnification from the external limb of the dentate gyrus. The granule cell layer was manually outlined (B) and the image orientated such that the molecular border was to the left of the granule cell layer, the polymorph border to the right.

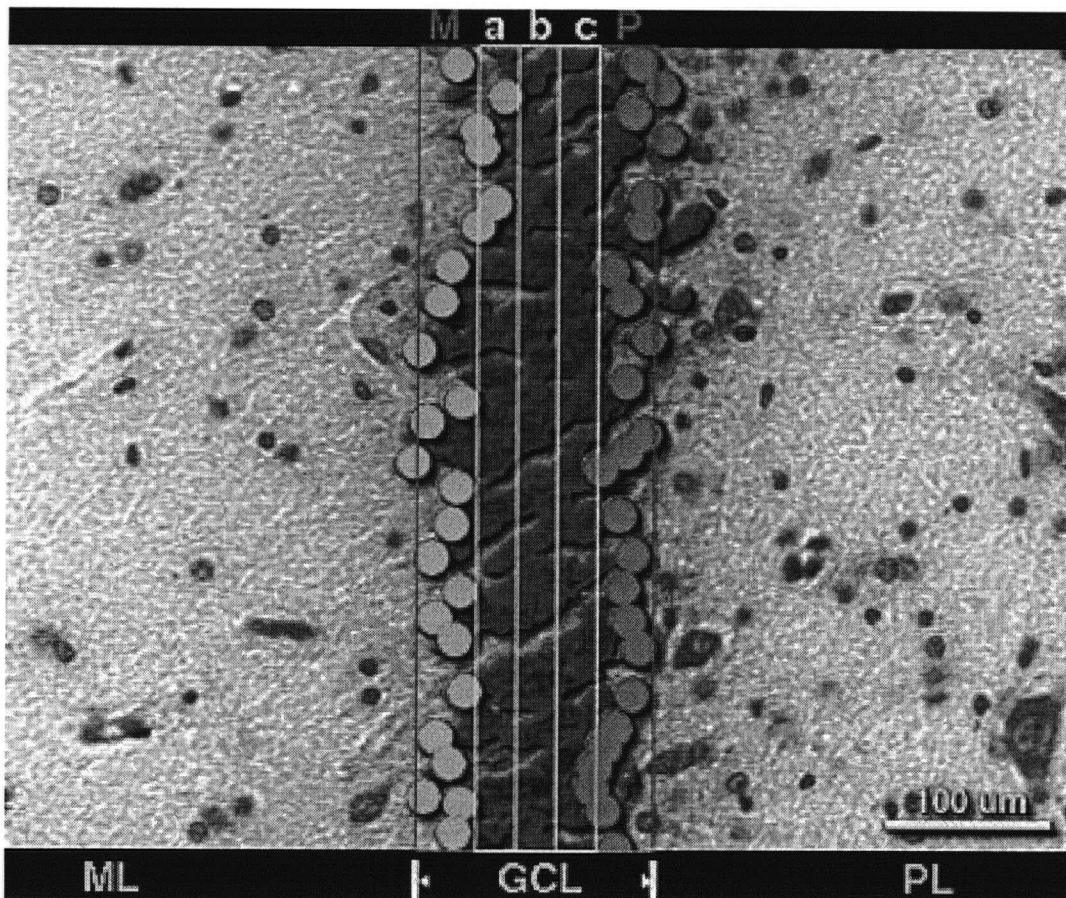


Figure III-3

Example of a Nissl stained section demonstrating the subdivision of the granule cell layer (GCL) into five parts: two border regions (molecular [M] and polymorph [P]) and three regions in-between [a,b,c]. Granule cells in the molecular border segment are highlighted in yellow; granule cells in the polymorph border segment are highlighted in green. The granule cell layer [GCL] is bordered by the molecular layer [ML] and the polymorph layer [PL].

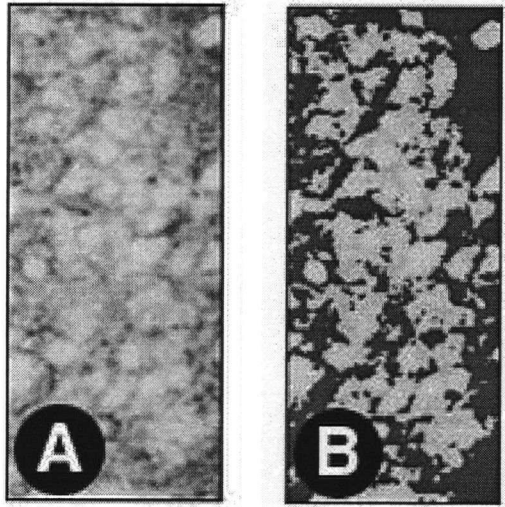


Figure III-4

Example of SNAP-25 immunostained span of the granule cell layer (A) segmented by the Otsu filter into stained/unstained regions (B: staining in red, unstained in white).

III.3. RESULTS

At higher magnification, section to section variability for synaptophysin and SNAP-25 was 7% and 8% for fractional area stained, 27% and 11% for staining intensity, and 10% and 14% for width measurements, respectively.

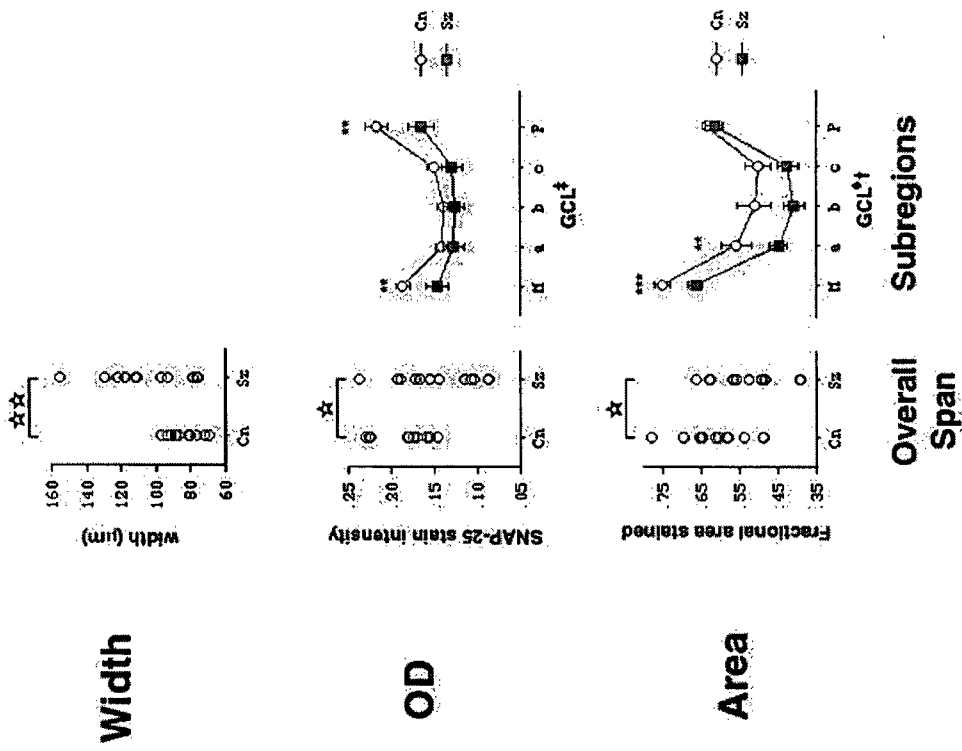
High magnification images of the granule cell layer were used for more detailed assessment of synaptic immunoreactivity. Initial analyses indicated no significant correlations between SNAP-25 immunoreactivity (area and intensity of immunostaining) and age or postmortem interval. No correlations between synaptophysin immunoreactivity (area and intensity of immunostaining) and postmortem interval were observed. A significant negative correlation between synaptophysin intensity of immunostaining and age was observed for the "P" polymorph segment in the lateral limb only ($r = 0.44$, $P = 0.05$). Significant positive correlations were observed for fractional area stained by synaptophysin and age ($r = 0.44-0.68$, $P = 0.005-0.05$, uncorrected for multiple comparisons). No significant correlations between granule cell width and postmortem interval or age were observed except in the external limb where a significant negative correlation between granule cell width and postmortem interval was observed ($r = 0.47$, $P = 0.03$).

Statistical analyses were performed with fractional area of synaptophysin immunostaining covaried with age.

Results for SNAP-25 and synaptophysin are seen in **Figure III-5** and **Figure III-6**, respectively.

SNAP-25 IMMUNOREACTIVITY IN THE DENTATE GYRUS OF SCHIZOPHRENIA

A. External Limb



B. Internal Limb

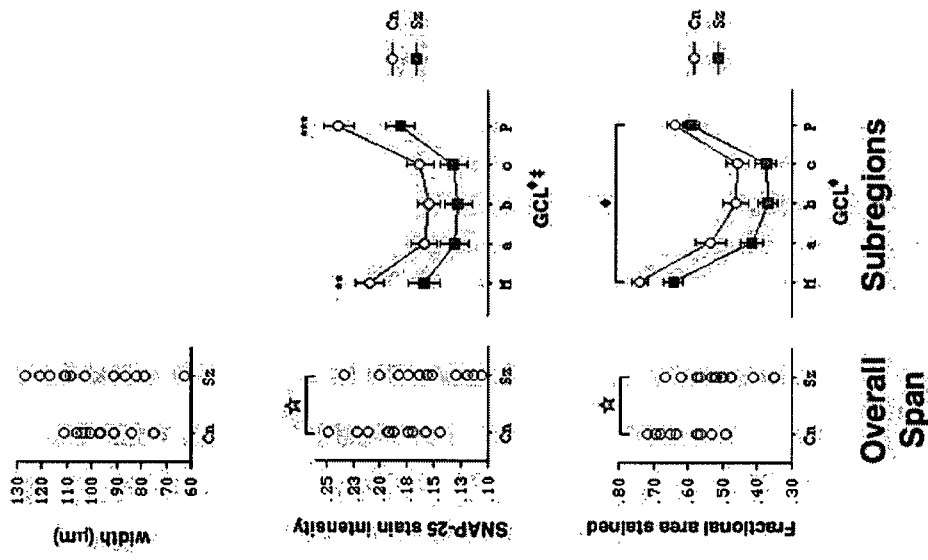
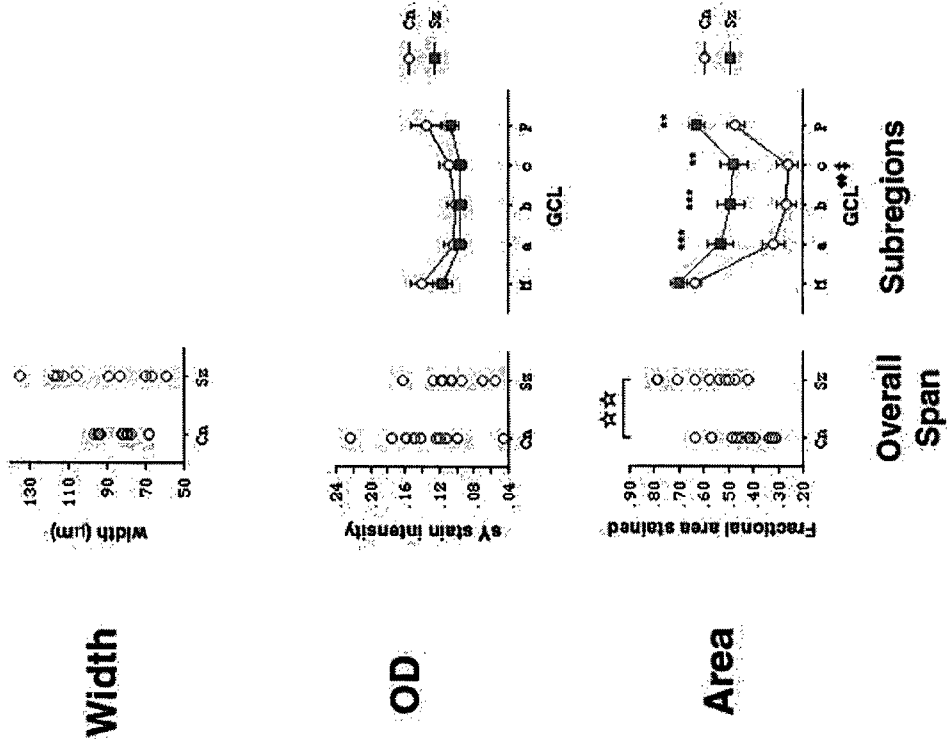


Figure III-5 In overall images of SNAP-25 immunostained dentate gyrus, the width of the external limb was significantly increased in schizophrenia (☆☆p < 0.01) while SNAP-25 stain intensity and fractional area stained were decreased (☆p < 0.05). Repeated measures analysis of variance showed similar decreases in stain area and intensity (main effect of diagnosis on SNAP-25 immunoreactivity: ♦ p < 0.05) and in individual subregions of the granule cell layer (significant interactions between diagnosis and subregion: †p < 0.05, ‡p < 0.001; subregion significance: **p < 0.025, ***p < 0.001).

SYNAPTOPHYSIN IMMUNOREACTIVITY IN THE DENTATE GYRUS OF SCHIZOPHRENIA

A. External Limb



B. Internal Limb

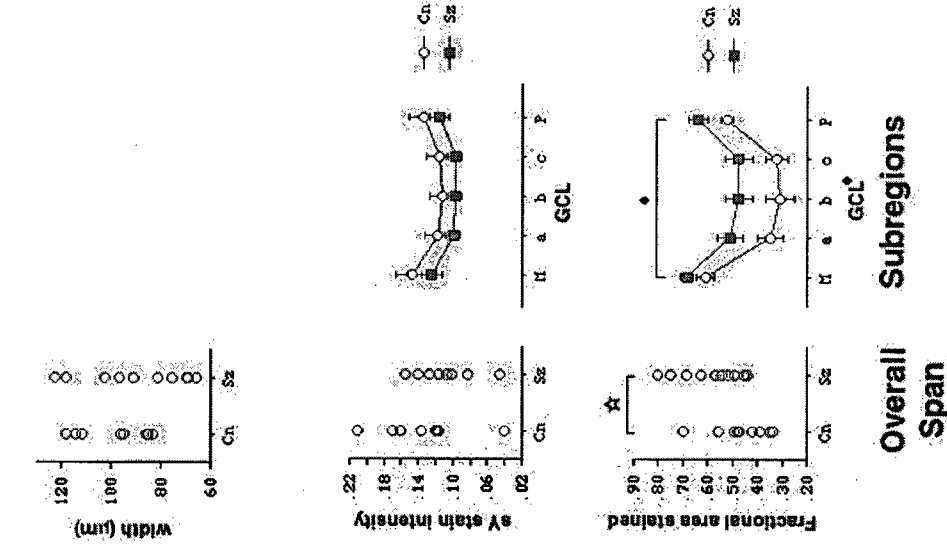


Figure III-6 In overall images of synaptophysin immunostained dentate gyrus, width and staining intensity were unchanged in both limbs while staining area was increased in both limbs ($\star p < 0.05$, $\star\star p < 0.01$). Repeated measures analysis of variance showed similar increases in staining area (main effect of diagnosis on synaptophysin immunoreactivity: $\blacklozenge p < 0.05$, $\blacklozenge p < 0.01$) and in individual subregions of the granule cell layer (significant interactions between diagnosis and subregion: $\ddagger p < 0.001$; subregion significance: $\star\star p < 0.01$, $\star\star\star p < 0.005$).

III.3.A.External Limb:

III.3.A.i. External Limb: Width

The width of the granule cell layer in the external limb in schizophrenia as gauged by SNAP-25 immunoreactivity showed a significant 27% increase compared with controls ($t=2.928$, $df=21$, $p=.0080$).

III.3.A.ii. External Limb: Mean intensity of immunostaining

For the overall span of the granule cell layer in this limb, mean intensity of SNAP-25 immunoreactivity was reduced 18.58% in schizophrenia ($t=2.153$, $df=21$, $p=.0431$). Repeated measures analysis of variance demonstrated no main effect of diagnosis ($F=3.265$, $df=1$, 84 , $p=.0851$), and significant main effects of layer ($F=108.026$, $df=4$, 84 , $p=.0001$) and a layer by diagnosis interaction ($F=12.983$, $df=4$, 84 , $p=.0001$), indicating all layers were not equally affected. In schizophrenia, intensity of immunoreactivity was decreased by 21.37% in the region [M] adjacent to the molecular layer ($t=2.539$, $df=21$, $p=.0191$) and by 23.96% in the region [P] adjacent to the polymorph layer ($t=2.691$, $df=21$, $p=.0137$).

For the overall span of the granule cell layer in this limb, mean intensity of synaptophysin immunoreactivity was reduced by 19.40% in schizophrenia, however this was not statistically significant ($t=1.506$, $df=19$, $p=.1484$).

III.3.A.iii. External Limb: Mean fractional area stained

For the overall span of the granule cell layer in this limb, mean percent area of SNAP-25 immunostaining was reduced 11.45% in schizophrenia ($t=2.261$, $df=21$, $p=.0345$). Repeated

measures analysis of variance demonstrated main effects of diagnosis ($F=4.907$, $df=1$, 84 , $p=.0379$), of layer ($F=115.605$, $df=4$, 84 , $p=.0001$) and a layer by diagnosis interaction ($F=2.965$, $df=4$, 84 , $p=.0242$), indicating all layers were not equally affected. In schizophrenia, percent area of immunoreactivity was decreased by 11.70% in the region [M] adjacent to the molecular layer ($t=3.203$, $df=21$, $p=.0043$) and by 19.75% in the next adjoining ["a"] layer ($t=2.408$, $df=21$, $p=.0253$).

For the overall span of the granule cell layer in this limb, mean percentage area of synaptophysin immunostaining was increased 35.93% ($F=9.386$, $df=1$, $p=.0067$). Repeated measures analysis of variance demonstrated main effects of diagnosis ($F=10.047$, $df=1$, 72 , $p=.0053$), of layer ($F=19.679$, $df=4$, 72 , $p=.0001$) and a layer by diagnosis interaction ($F=7.018$, $df=4$, 72 , $p=.0001$), indicating all layers were not equally affected. In schizophrenia, percent area of immunoreactivity was increased by 67.72% in region [a] ($F=11.346$, $df=1$, 18 , $p=.0034$), 85.61 % in the next adjoining region ["b"] ($F=10.786$, $df=1$, 18 , $p=.0041$), 83.46 % in region ["c"] layer ($F=10.017$, $df=1$, 18 , $p=.0054$), and 33.12 % in the region adjacent to the polymorph ["P"] layer ($F=9.216$, $df=1$, 18 , $p=.0071$).

III.3.B. Internal limb:

III.3.B.i. Internal Limb: Width

No difference in width of the granule cell layer in the internal limb was seen in schizophrenia and controls.

III.3.B.ii. Internal Limb: Mean intensity of immunostaining

For the overall span of the granule cell layer in this limb, mean intensity of SNAP-25 immunostaining was reduced 19.47% in schizophrenia ($t=2.383$, $df=20$, $p=.0272$). Repeated measures analysis of variance demonstrated main effects of diagnosis ($F=4.818$, $df=1$, 80 , $p=.0401$), of layer ($F=103.090$, $df=4$, 80 , $p=.0001$) and a layer by diagnosis interaction ($F=5.500$, $df=4$, 80 , $p=.0006$), indicating all layers were not equally affected. In schizophrenia, mean intensity of immunostaining was decreased by 22.45% in the region adjacent to the molecular layer ($t=2.488$, $df=20$, $p=.0218$) and by 22.62% in the region adjacent to the polymorph layer ($t=2.852$, $df=20$, $p=.0099$).

For the overall span of the granule cell layer in this limb, mean intensity of synaptophysin immunoreactivity was reduced 16.06% in schizophrenia, however this was not statistically significant ($t=1.174$ $df=17$, $p=.2528$).

III.3.B.iii. Internal Limb: Mean fractional area stained

For the overall span of the granule cell layer in this limb, mean percent area of SNAP-25 immunostaining was reduced 13.62% in schizophrenia ($t=2.283$, $df=20$, $p=.0335$). Repeated measures analysis of variance demonstrated main effects of diagnosis ($F=4.967$, $df=1$, 80 , $p=.0375$), of layer ($F=135.209$, $df=4$, 80 , $p=.0001$), with no significant interaction between layer and diagnosis. The range of reduction in percent area of SNAP-25 immunostaining in schizophrenia across the sublayers was 7-22%.

For the overall span of the granule cell layer in this limb, mean percentage area of synaptophysin immunostaining was increased 26.18 % in schizophrenia ($F=5.673$, $df=1, 17$, $p=.0300$). Repeated measures analysis of variance demonstrated main effects of diagnosis ($F=5.536$, $df=1, 64$, $p=.0318$), of layer ($F=10.086$, $df=4, 64$, $p=.0001$), and with no significant interaction between layer and diagnosis. The range of increases in percentage area of synaptophysin immunostaining in schizophrenia across the sublayers was 12-53%.

III.4. CONCLUSION

In this chapter, some differences in the effects of schizophrenia on the external compared with the internal limb of the granule cell layer were observed. The internal limb was greater affected than the external limb in schizophrenia in terms of fractional area stained for both presynaptic proteins; namely, decreased SNAP-25 and increased synaptophysin were observed in all subregions of the internal limb. In contrast, in the external limb only the two regions [M and "a"] adjacent to the molecular border were affected for SNAP-25 and all regions except the region [M] adjacent to the molecular border were affected for synaptophysin. The granule cell width of the external limb (as gauged by SNAP-25 immunoreactivity) was increased in schizophrenia.

In both limbs, decreased intensity of SNAP-25 immunostaining was observed in the marginal sublayers.

The present data supports my hypothesis for a pattern of abnormal synaptic change in subregions of the dentate gyrus. Before drawing further conclusions, the possible effects of antipsychotic drug treatment must be considered as an explanation for these findings.

Chapter IV ANTI-PSYCHOTIC DRUG TREATMENT

IV.1. OVERVIEW

Since the symptoms of schizophrenia can be ameliorated and treated by antipsychotic drugs (APDs), nearly all patients with schizophrenia have been exposed to APDs. The possible effects of APD treatment must be considered as an explanation for the findings of altered presynaptic protein immunoreactivities in schizophrenia. Past studies showed unchanged hippocampal presynaptic protein immunoreactivity after APD exposure (Eastwood, Burnet et al. 1995; Eastwood, Heffernan et al. 1997). I hypothesised that higher resolution studies of typical APD treatment might evince a pattern of presynaptic protein levels in the rat hippocampus different from the pattern of changes in schizophrenia, thereby supporting the conclusion that altered presynaptic protein levels in schizophrenia are not likely to be attributable to APD exposure.

Using optimised immunohistochemical image analysis, I studied presynaptic proteins (synaptophysin and SNAP-25) in APD treated rats:

4. at the level of the whole hippocampus (regions and layers) and;
5. at the level of the subregions of the dentate gyrus (limbs and GCL span).

These approaches to analysis parallel those used for the studies of schizophrenia in chapters 2 and 3.

IV.2. MATERIALS & METHODS

IV.2.A. Drug dosage and duration

Regarding the typical antipsychotic drugs (haloperidol, chlorpromazine, and trifluoperazine), the doses used in the present study were carefully chosen as being representative of those typically used within the field of pre-clinical studies. The animals received a daily dose of neuroleptic sufficient to produce mild sedation, but insufficient to generate severe motor

impairments suggesting that these doses bear similar behavioral effects to those used in humans. Haloperidol is the most widely used of three antipsychotic drugs that I investigated, both in animal and human studies. The current dose of haloperidol (1.0 mg/kg) is in the range of doses used to demonstrate putative antipsychotic properties in various rodent models of schizophrenia. These models include the neonatal ventral hippocampal lesion model (Al-Amin, Weinberger et al. 2000), reversal of phencyclidine-induced sensorimotor gating deficit in rats (Pietraszek and Ossowska 1998), and enhancement of latent inhibition (Dunn, Atwater et al. 1993). The current dose of haloperidol is also widely used to induce changes in neurotransmission (measured through *in vivo* techniques such as microdialysis and electrochemistry) in neural substrates that are hypothesised to underlie the therapeutic effects of antipsychotics. For example, a similar dose of haloperidol was shown to modify dopaminergic neurotransmission in both cortical and subcortical region in freely moving, conscious rats (Moghaddam and Bunney 1990).

Regarding duration of drug administration, sub-chronic administration of haloperidol and chlorpromazine (i.e. 14 days or more) at similar dosages has been used to determine the effects of antipsychotic drugs on various molecular markers in the brain. Both of these neuroleptics, after sub-chronic administration, produce widespread changes in the levels of cortical receptors, such as the 5-HT₂ receptor (Buckland, D'Souza et al. 1997). After 21 days of administration, both drugs induced decreased PKC activity in similar brain regions (Dwivedi and Pandey 1999). Of more pertinence, doses of haloperidol and chlorpromazine in the present study were very similar to the ones used by Eastwood and Harrison (2000; (Eastwood, Burnet et al. 2000)) to investigate changes in the mRNA levels of synaptic proteins in various brain regions, including frontal cortex, striatum and hippocampus.

IV.2.B. Drug administration in animals

Twenty-four adult male Sprague-Dawley rats (250-275 grams; Animal Care Centre, University of British Columbia, Vancouver, BC) were maintained in a colony room at 20°C ($\pm 1^\circ\text{C}$) on a 12 hour light-dark cycle (lights on 7 am to 7 pm) with unlimited access to water and food (Purina Rat Chow). Four randomly derived groups (n=6) received daily i.p. injections of either haloperidol (HAL: 1 mg/kg dissolved in 0.3% tartaric acid), chlorpromazine (CPZ: 10 mg/kg dissolved in distilled water), trifluoperazine (TFP: 6 mg/kg dissolved in distilled water), or vehicle (0.3% tartaric acid) over three weeks. After the last injection, animals were deeply anaesthetised with chloral hydrate, transcardially perfused with 200 mL PBS and 200 mL neutral buffered formalin (4% NBF), and sacrificed by decapitation. The brains were removed, fixed in NBF for 48 hours at 4°C, and then stored in TBS-azide (1% azide) at 4°C until use. All experimental procedures were conducted in accordance with the guidelines provided by the Canadian Council on Animal Care and the University of British Columbia Animal Care Committee.

Blocks of fixed tissue 1-2 mm thick were cut in the the coronal plane at levels corresponding to the brain areas of interest (atlas of Paxinos and Watson (1986)) for paraffin embedding prior to cutting sections 3 μm thick. Three sequential coronal sections from the same rat brain were placed on individual slides. Monoclonal antibodies reactive with synaptophysin (SP15) and SNAP-25 (SP12) were used to immunostain the paraffin sections of the dorsal hippocampus using methods as described previously (see II.2.A).

IV.2.C. Image Analysis

IV.2.C.i. Immunohistochemical image analysis of the whole hippocampus

Images of the whole hippocampus were collected blinded to drug treatment using my Sony CCD video camera, Nikon lens, and a Northern Light constant source lightbox. As per 2.1.A., imaging conditions were optimised to ensure appropriate compliance with the Beer-Lambert Law; namely, a single wavelength filter (Lee Chromalux Light Blue) centred around 450 nm and a custom designed series of monochrome slides for calibrating grey scale intensities to OD values were utilised.

Hippocampal regions of interest were demarcated (**Figure IV-1**) using an atlas (Paxinos and Watson (1986): (Paxinos and Watson 1986)). Ammon's horn subregions were defined by characteristics of the pyramidal cell layer including width and terminations of afferent projections such as the mossy fibres (synaptic immunostained sections). The CA1 and CA2 regions were combined as a single CA1+2 region. Regions were outlined using NIH Image v.1.61 (Rasband 1996) and the mean pixel intensity was calculated. For synaptophysin, white matter values were subtracted from grey matter image values on the same section. Since SNAP-25 is present in axons to a small but variable extent, this correction was not applied to SNAP-25 immunostaining. Instead, the background value from the negative control section was subtracted from the image values.

IV.2.C.ii. Immunohistochemical image analysis of the sublayers of the dentate gyrus

Images of the granule cell layer of the dentate gyrus from immunostained sections were collected using the 40x objective of an Olympus microscope (**Figure IV-2**) and using similar procedures as described (2.1.B.iii.). The granule cell layer of both limbs of the dentate gyrus in each section was sampled by obtaining images avoiding areas with convolutions. The granule cell layer in both limbs was outlined manually (**Figure IV-3**) and the span of the layer divided into five segments: two border regions (molecular and polymorph) and three regions in-between (a,b,c). For analysis, the Otsu filter was used to automatically determine the appropriate threshold for each image, allowing subtraction of unstained areas such as blood vessels and cell somas.

The total area of the granule cell layer, the width of the granule cell layer, immunostained area and mean intensity of immunostained pixels were determined for each image for each staining fraction.

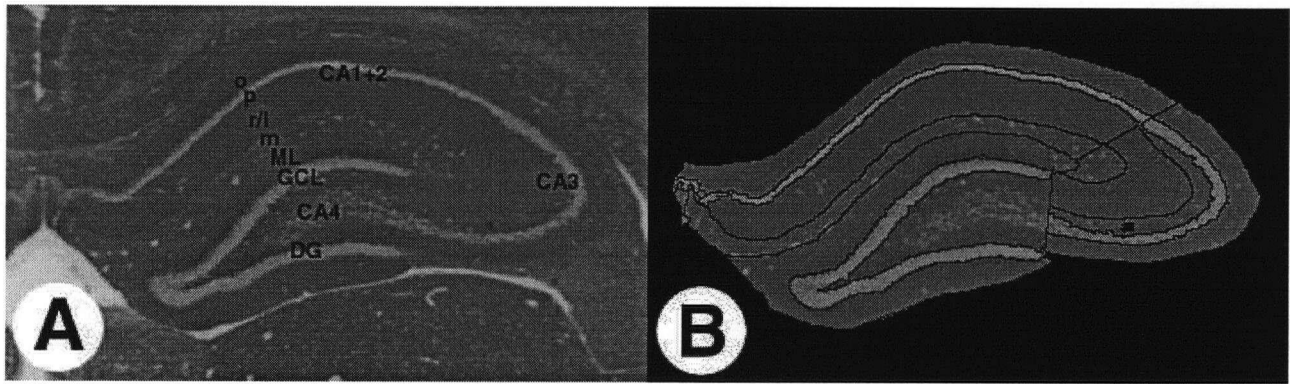


Figure IV-1

Example of a SNAP-25 immunostained rat hippocampus (A). Regions and layers were demarcated (B) with the aid of a brain atlas (Paxinos and Watson 1986).

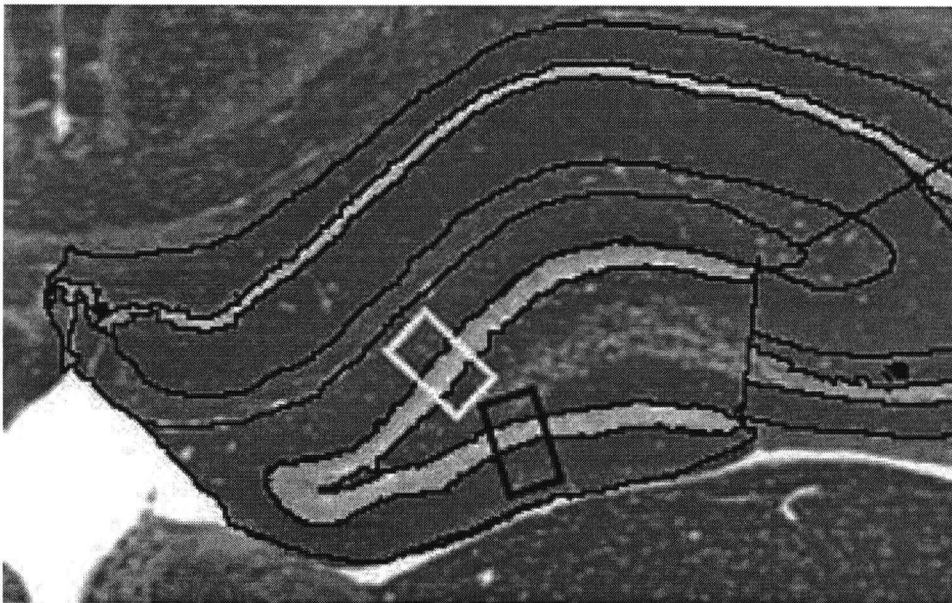


Figure IV-2

Example of a SNAP-25 immunostained rat hippocampus showing the regions (boxes) sampled at 40x microscope magnification. The granule cell layer was sampled by obtaining images from both the external limb (white boxes) and the internal limb (black boxes) of the dentate gyrus.

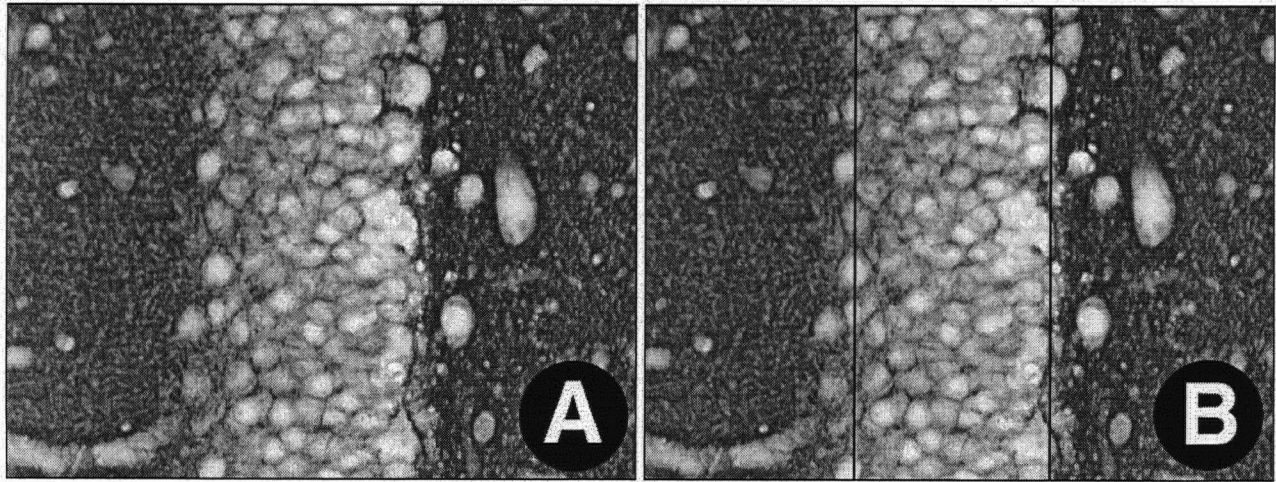


Figure IV-3

Example of a SNAP-25 immunostained rat hippocampus showing the raw image of the granule cell layer (A) sampled at 40x microscope magnification from the external limb of the dentate gyrus. The granule cell layer was manually outlined (B).

IV.2.D. Statistical Analysis

IV.2.D.i. Whole Hippocampus

For analysis of hippocampal regions of interest on immunostained sections, repeated-measures analysis of variance (ANOVA) was used for data sets obtained from CA1+2, CA3, and the dentate gyrus to study significant effects of antipsychotic drug and significant interactions between drug and subregion. Bonferroni corrections were applied for multiple comparisons (four initial regions [CA1+2, CA3, CA4 and the dentate gyrus], followed by four [in the CA1+2: oriens, pyramidal, radiatum/lacunosum, and the molecular layer] or five [in the CA3: oriens, pyramidal, radiatum/lacunosum, mossy fibre termination zone, and the molecular layer] or two subregions [in the dentate gyrus: the molecular and the granule cell layer] for significant interaction effects).

IV.2.D.ii. Sublayers of dentate gyrus

For analysis of dentate gyrus regions of interest in immunostained sections, parameters of immunostaining (mean intensity and mean fractional area) were first compared between paired groups (vehicle versus each among the APDs) in each limb of the granule cell layer as a whole, using a t-test. Significant results were followed up by a comparison across the five granule cell sublayers of the limb using a repeated measures analysis of variance (ANOVA) with drug as a main effect and sublayer as a within-subject repeated measure. Where a significant interaction was indicated, post-hoc t-tests were calculated for each sublayer.

IV.3. RESULTS

For measures of the whole hippocampus, slice to slice variability in staining intensity of sections from the same case was 2% for both synaptophysin and SNAP-25. At higher magnifications, slice to slice variability for synaptophysin and SNAP-25 was 6% and 5% for fractional area stained, 11% and 9% for staining intensity, and 3% and 4% for width measurements, respectively.

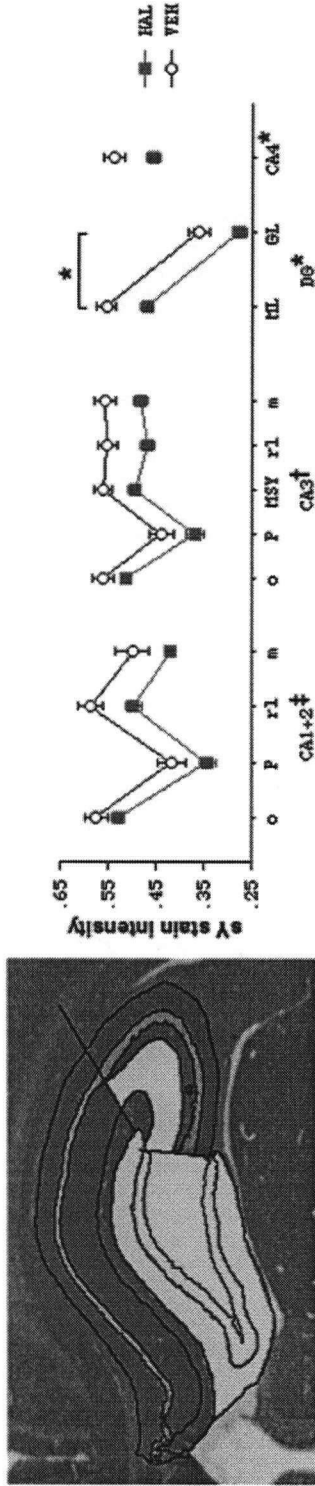
IV.3.A. Whole Hippocampus (Regions and Layers)

In haloperidol treated rats, significant reductions of the mean intensity of synaptophysin immunoreactivity were observed compared to controls in the CA4 region ($F=11.467$, $df=1$, $p=.0080$) and dentate gyrus ($F=9.839$, $df=1$, $p=.0120$); significant level set at 0.05/4, or $p=.0125$ for four comparisons. Within the subregions of the dentate gyrus, reduced synaptophysin immunoreactivity was also seen in both the (inner and outer) molecular layer ($F=12.922$, $df=1$, $p=.0058$) and the granule cell layer ($F=10.110$, $df=1$, $p=.0112$) (**Figure IV-4A**); the significant level was set at 0.05/2, or $p=0.0250$ for the two subregions of the dentate gyrus. Haloperidol treatment produced a significant layer by drug interaction in CA1+2 ($F=5.024$, $df=3$, $p=.0068$) and CA3 ($F=3.517$, $df=4$, $p=.0160$) for synaptophysin, but ANOVAs on individual subregions revealed significant changes after Bonferroni correction only in the radiatum-lacunosum layer ($F=12.239$, $df=1$, $p=.0067$) of the CA3 region; significant level set at 0.05/5, or $p=0.01$ for the five subregions within the CA3 region. In images of the overall hippocampus, although mean SNAP-25 stain

intensity tended to be higher in most regions after haloperidol treatment, no significant differences were observed (**Figure IV-4B**). Both chlorpromazine (**Figure IV-5**) and trifluperazine (**Figure IV-6**) treatment produced no changes in immunostaining of either synaptophysin or SNAP-25. Chlorpromazine treatment produced a significant layer by drug interaction in CA1+2 ($F=3.427$, $df=3$, $p=.0311$) and CA3 ($F=3.850$, $df=4$, $p=.0105$) for SNAP-25, but ANOVAs on individual subregions revealed no significant changes after Bonferroni correction.

ALTERED PRESYNAPTIC-IR AFTER HALOPERIDOL TREATMENT

A. Synaptophysin Immunoreactivity



B. SNAP-25 Immunoreactivity

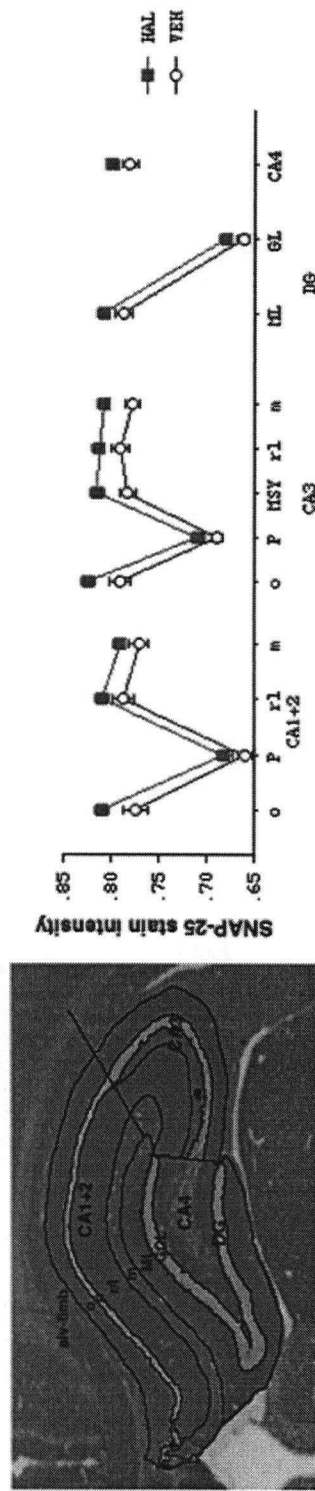


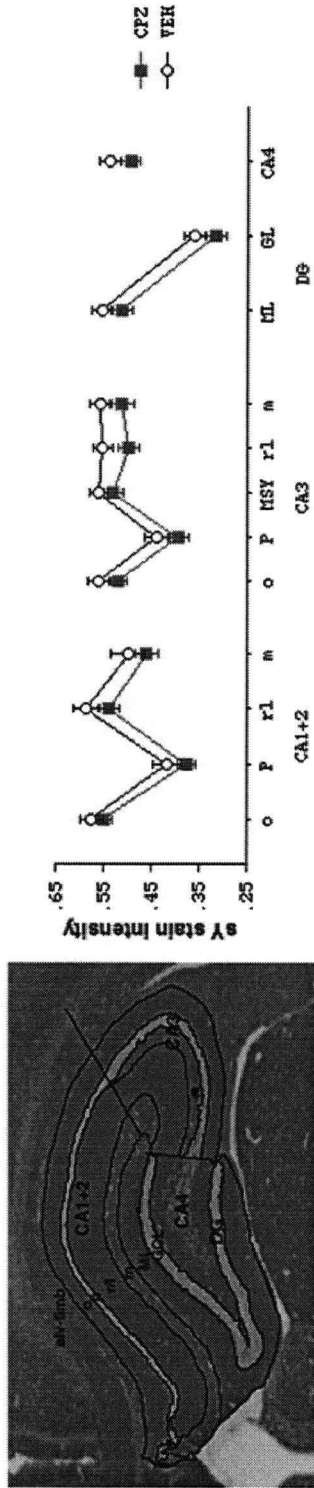
Figure IV-4 In images of the overall rat hippocampus, although mean SNAP-25 stain intensity tended to be higher in most regions in haloperidol treated animals (B), no significant differences were observed. Synaptophysin stain intensity was significantly reduced in the dentate gyrus and CA4 (main effect of haloperidol treatment on synaptophysin stain intensity: $*p < .05$) with prominent decreases in the individual layers of CA3 (significant interactions between haloperidol treatment and subregion: $†p < .025$, $‡p < .01$). The statistical significance of synaptophysin reductions is represented diagrammatically (diagram A).

Ammons region
oriens layer
pyramidal layer
radiatum-
molecular layer
Dentate gyrus
Molecular layer
granule cell layer

o
p
r1
m
DG
ML
GL

UNCHANGED PRESYNAPTIC-IR AFTER CHLORPROMAZINE TREATMENT

A. Synaptophysin Immunoreactivity



B. SNAP-25 Immunoreactivity

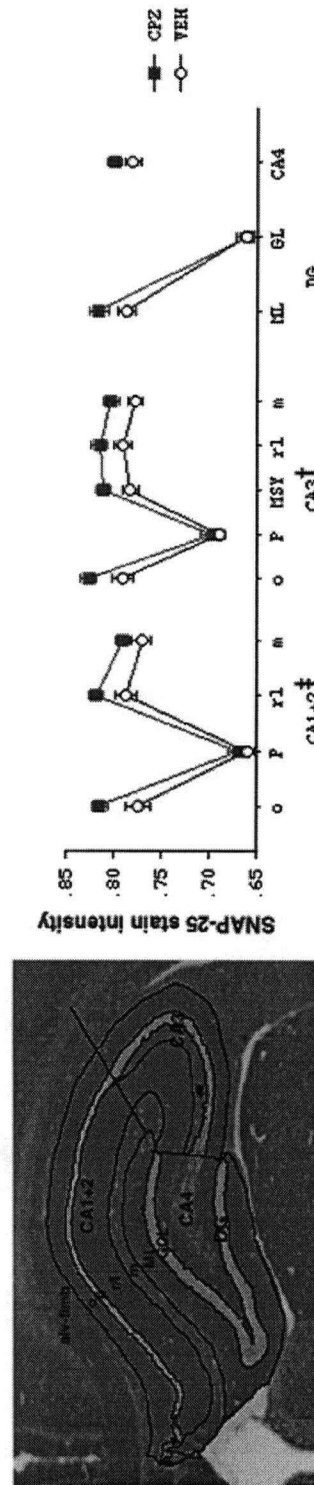
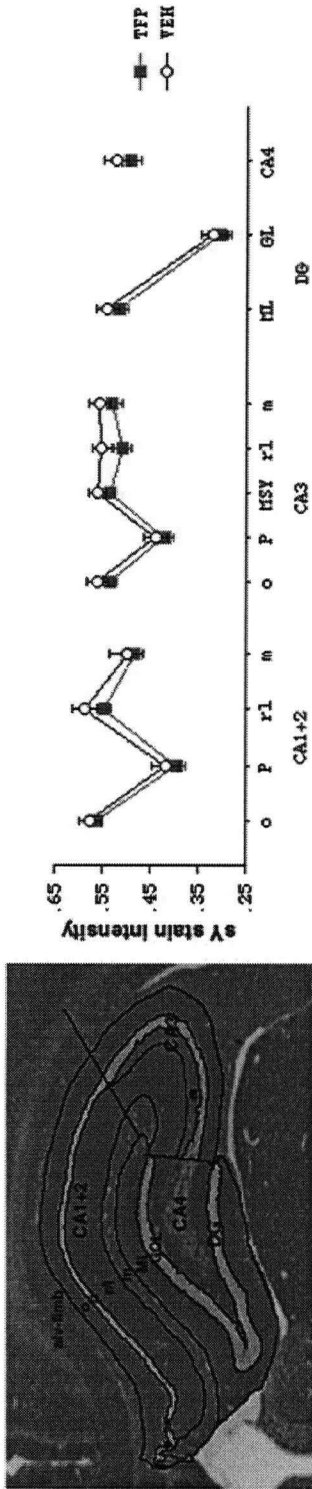


Figure IV-5 In images of the overall rat hippocampus, although mean synaptophysin (A) and SNAP-25 (B) stain intensity tended to be lower and higher in most regions, respectively, in chlorpromazine treated animals no significant differences were observed.

UNCHANGED PRESYNAPTIC-IR AFTER TRIFLUROPERAZINE TREATMENT

A. Synaptophysin Immunoreactivity



B. SNAP-25 Immunoreactivity

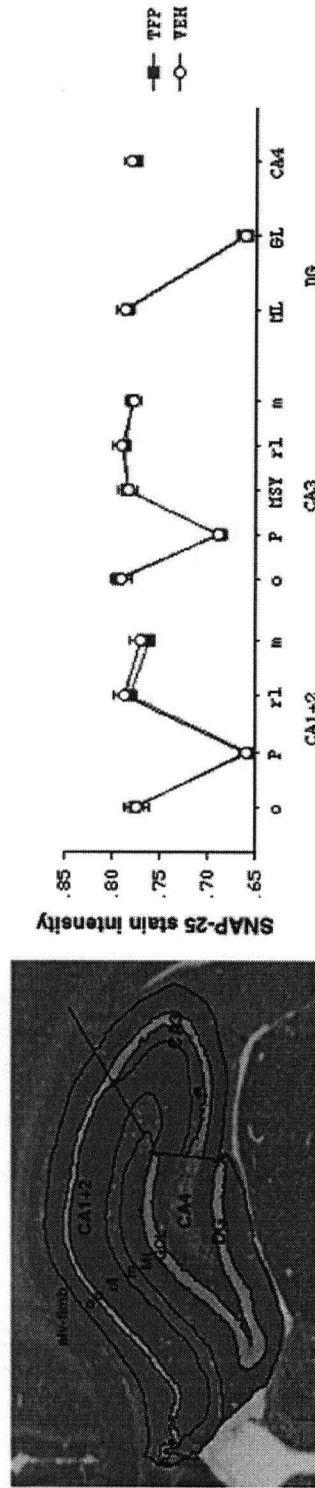
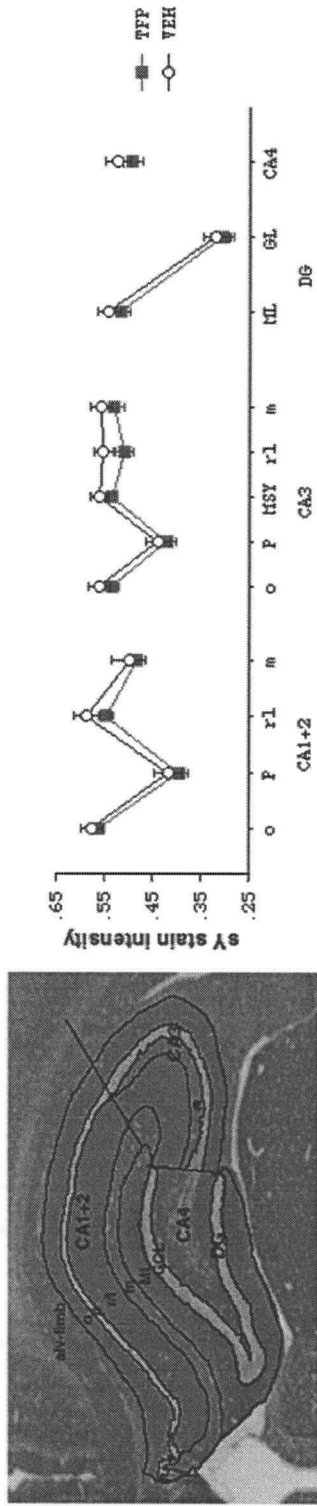


Figure IV-6 In images of the overall rat hippocampus, no significant differences were observed in mean synaptophysin (A) and SNAP-25 (B) stain intensity in any regions after exposure to trifluoroperazine.

UNCHANGED PRESYNAPTIC-IR AFTER TRIFLUPERAZINE TREATMENT

A. Synaptophysin Immunoreactivity



B. SNAP-25 Immunoreactivity

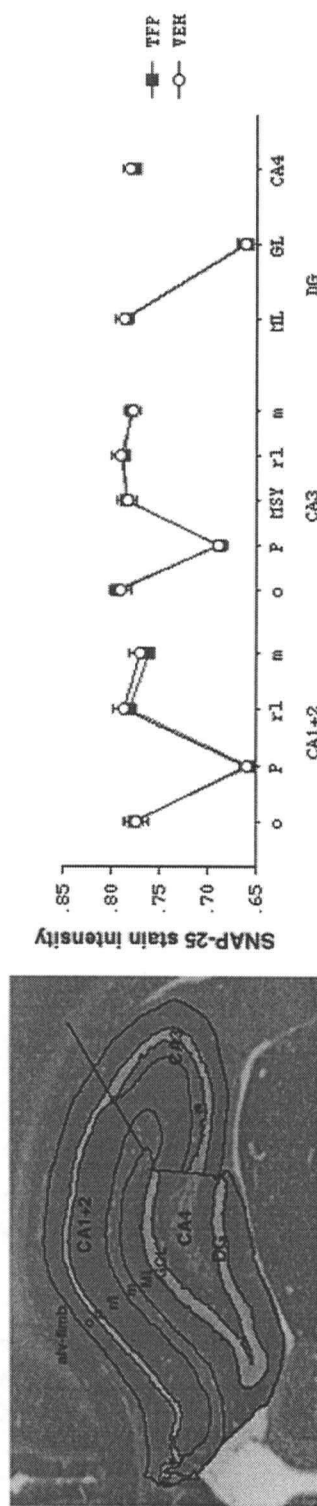


Figure IV-6 In images of the overall rat hippocampus, no significant differences were observed in mean synaptophysin (A) and SNAP-25 (B) stain intensity in any regions after exposure to trifluorphenazine.

IV.3.B.i.a.2. Haloperidol – External Limb: Mean fractional area stained

For the overall span of the granule cell layer in this limb, mean percent area of SNAP-25 immunostaining was increased 5.05% after haloperidol treatment ($t=2.260$, $df=9$, $p=.0501$).

Repeated measures analysis of variance demonstrated a trend for main effect of haloperidol treatment ($F=4.857$, $df=1, 36$, $p=.0550$), a significant effect of layer ($F=69.320$, $df=4, 36$, $p=.0001$) and no effect of layer by drug interaction ($F=.961$, $df=4, 36$, $p=.4406$). The range of increase in percentage area of immunostaining across sublayers was 1.69-7.00%.

For the overall span, in parallel with the effects on SNAP-25, mean percentage area of synaptophysin immunostaining was increased 6.48%, however this was a trend ($t=2.190$, $df=9$, $p=.0562$). Repeated measures analysis of variance demonstrated main effects of haloperidol treatment ($F=0.294$, $df=1, 36$, $p=.0294$), of layer ($F=211.492$, $df=4, 36$, $p=.0001$) and a layer by drug interaction ($F=4.035$, $df=4, 36$, $p=.0084$), indicating all layers were not equally affected. The percent area of immunoreactivity was increased in the middle subregions: 10.60% in region [a] ($t=2.637$, $df=9$, $p=.0270$), 14.67% in region [b] ($t=3.459$, $df=9$, $p=.0072$), and 16.67% in region [c] ($t=3.217$, $df=9$, $p=.0105$).

IV.3.B.i.b. Haloperidol – Internal Limb

IV.3.B.i.b.1. Haloperidol – Internal Limb: Mean intensity of immunostaining

For the overall span of the granule cell layer in this limb, mean intensity of SNAP-25 immunoreactivity was unchanged after haloperidol treatment. Repeated measures analysis of variance demonstrated no main effect of drug and a significant layer by drug interaction ($F=5.103$,

df=4, 36, p=.0023). After haloperidol treatment, mean intensity was decreased 11.82% in subregion [P] adjacent to the polymorph edge (F=2.806, df=9, p=.0205).

For the overall span, mean intensity of synaptophysin immunostaining was reduced 18.36% (t=3.224, df=9, p=.0104). Repeated measures analysis of variance demonstrated main effects of haloperidol treatment (F=7.889, df=1, 36, p=.0204), of layer (F=10.089, df=4, 36, p=.0001) and a layer by drug interaction (F=6.242, df=4, 36, p=.0006). After haloperidol treatment, mean intensity of immunostaining was decreased in subregions nearest the polymorph border: 17.96% in region [b] (t=2.471, df=9, p=.0355), 15.61% in region [c] (t=2.254, df=9, p=.0507), and 24.45% in region [P] (t=5.465, df=9, p=.0004).

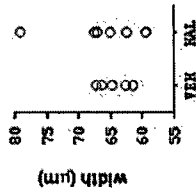
IV.3.B.i.b.2. Haloperidol – Internal Limb: Mean fractional area stained

For the overall span of the granule cell layer in this limb, mean percent area of SNAP-25 immunostaining was increased 7.76% after haloperidol treatment (t=4.713, df=9, p=.0011). Repeated measures analysis of variance demonstrated main effects of haloperidol treatment (F=8.000, df=1, 36, p=.0022) with no significant interaction between layer and drug. The range of increase in percent area of immunostaining in schizophrenia across the sublayers was 4.61-11.31%.

For the overall span, mean percent area of synaptophysin immunostaining was unchanged after haloperidol. Repeated measures analysis of variance demonstrated no main effect of haloperidol treatment and no interaction between layer and drug.

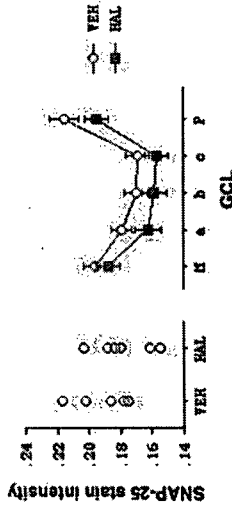
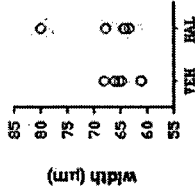
SNAP-25 Ir IN THE DENTATE GYRUS AFTER HALOPERIDOL TREATMENT

A. External Limb

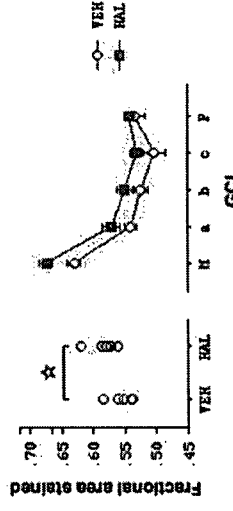
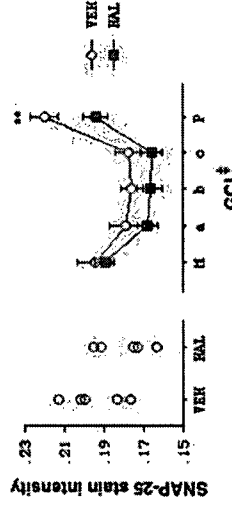


Width

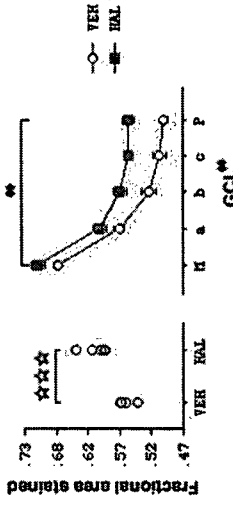
B. Internal Limb



OD



Area



Overall GCL regions Span

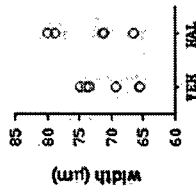
Overall GCL regions Span

Figure IV-7 In overall images of SNAP-25 immunostained dentate gyrus, the width and staining intensity were unchanged in both limbs while staining area was increased in both limbs (☆p = 0.05, ☆☆☆p < 0.001) Repeated measures analysis of variance showed:

- no change in external limb stain area;
- increase in internal limb stain area (main effect of drug exposure on SNAP-25 immunoreactivity: ♦ p = 0.005);
- increase in internal limb stain intensity for a particular subregion of the granule cell layer (significant interactions between drug exposure and subregion: † p < 0.005; subregion significance: ** p < 0.025).

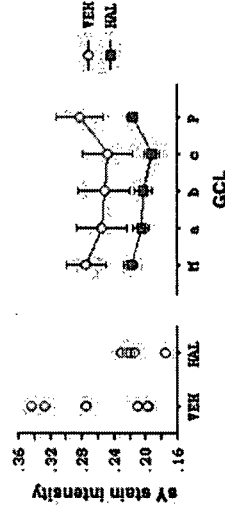
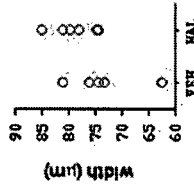
SYNAPTOPHYSIN ir IN THE DENTATE GYRUS AFTER HALOPERIDOL TREATMENT

A. External Limb

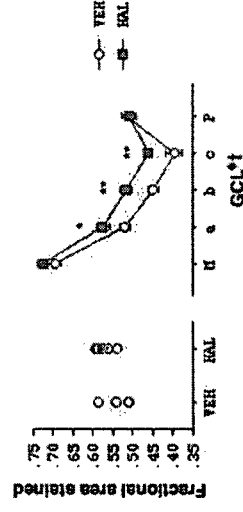
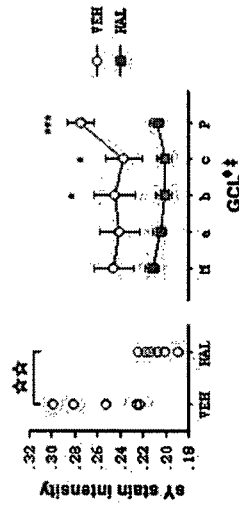


Width

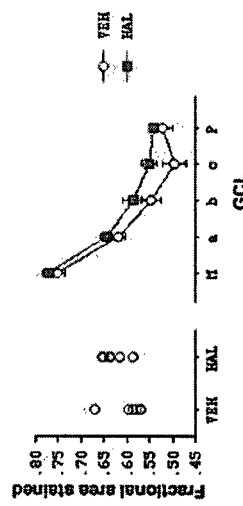
B. Internal Limb



OD



Area



Overall GCL regions Span

Overall GCL regions Span

Figure IV-8 In overall images of synaptophysin immunostained dentate gyrus, the width was unchanged in both limbs while staining intensity was decreased in the internal limb only (☆☆ $p < 0.01$). Repeated measures analysis of variance showed similar decreases in staining intensity in the internal limb only, but also revealed an increase in area of staining in the external limb only (main effect of drug exposure on synaptophysin immunoreactivity: ♦ $p = 0.05$) and changes in individual subregions of the granule cell layer (significant interactions between drug exposure and subregion: † $p < .01$, ‡ $p < 0.001$; subregion significance: * $p = 0.05$, ** $p < 0.01$, *** $p < 0.001$).

IV.3.B.ii. CHLORPROMAZINE

IV.3.B.ii.a. Chlorpromazine – External Limb

IV.3.B.ii.a.1. Chlorpromazine – External Limb: Mean intensity of immunostaining

For the overall span of the granule cell layer in this limb, mean intensity of SNAP-25 and synaptophysin immunoreactivity was unchanged after chlorpromazine treatment. Repeated measures analysis of variance demonstrated no main effects of chlorpromazine treatment or layer by drug interaction.

IV.3.B.ii.a.2. Chlorpromazine – External Limb: Mean fractional area stained

For the overall span, mean percent area of SNAP-25 immunostaining was increased 3.06% after chlorpromazine treatment, however this was not statistically significant ($t=1.386$, $df=9$, $p=.1991$). Repeated measures analysis of variance demonstrated no main effect of drug and a significant layer by drug interaction ($F=3.644$, $df=4, 36$, $p=.0136$). After chlorpromazine treatment, the fractional area of immunostaining was increased in subregions nearest molecular border: 6.52% in region [M] ($t=3.335$, $df=9$, $p=.0087$) and 5.91% in region [a] ($t=2.433$, $df=9$, $p=.0378$).

Similarly, for the overall span, mean fractional area of synaptophysin was increased 4.81% after chlorpromazine treatment, however this too was not statistically significant ($t=1.771$, $df=9$, $p=.1104$). Repeated measures analysis of variance also demonstrated no main effect of drug and a significant layer by drug interaction ($F=4.908$, $df=4, 36$, $p=.0029$). After chlorpromazine treatment, the fractional area of immunostaining was increased in subregions nearest molecular border: 5.32%

in region [M] ($t=2.310$, $df=9$, $p=.0463$), 9.06% in region [a] ($t=3.178$, $df=9$, $p=.0112$), and 11.56% in region [b] ($t=3.100$, $df=9$, $p=.0127$).

For both SNAP-25 and synaptophysin, chlorpromazine exposure resulted in a reversal of fractional area stained as one moved across the granule cell layer from the molecular to the polymorph border. The magnitude of initial increases (near the molecular edge) grows smaller, reaches its nadir at the "c" layer, and becomes decreased in fractional area stained relative to vehicle at the region [P] adjacent to the polymorph border.

IV.3.B.ii.b. Chlorpromazine – Internal Limb

IV.3.B.ii.b.1. Chlorpromazine – Internal Limb: Mean intensity of immunostaining

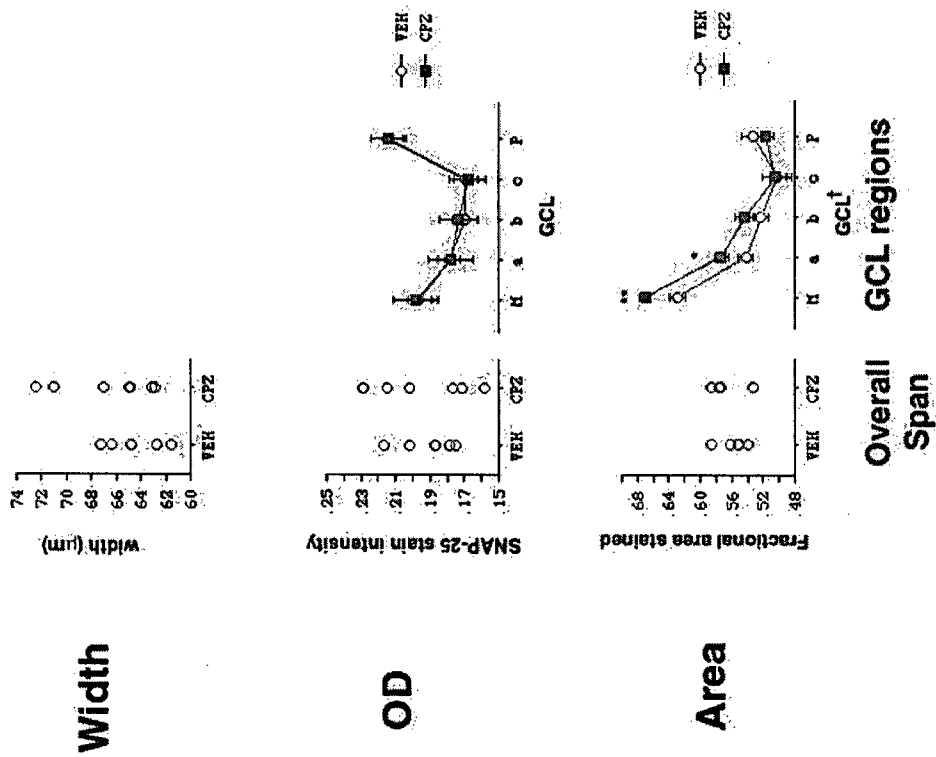
For the overall span of the granule cell layer in this limb, mean intensity of SNAP-25 and synaptophysin immunoreactivity was unchanged after chlorpromazine treatment. Repeated measures analysis of variance also demonstrated no main effects of chlorpromazine treatment or layer by drug interaction.

IV.3.B.ii.b.2. Chlorpromazine – Internal Limb: Mean fractional area stained

For the overall span, mean fractional area of SNAP-25 and synaptophysin immunoreactivity was unchanged after chlorpromazine treatment. No main effects of chlorpromazine treatment or layer by drug interaction were found with repeated measures analysis of variance.

SNAP-25 in the Dentate Gyrus after Chlorpromazine Treatment

A. External Limb



B. Internal Limb

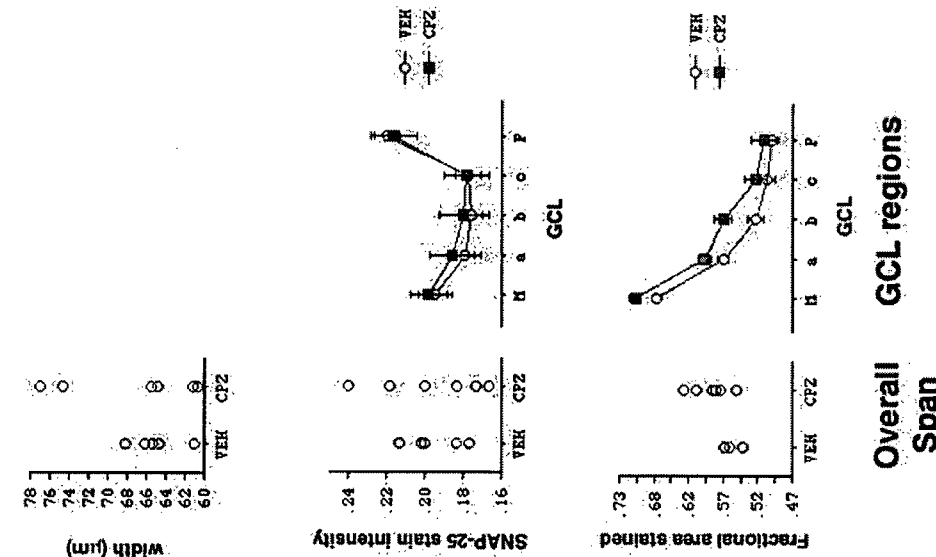
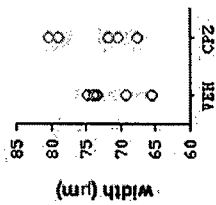


Figure IV-9 In overall images of SNAP-25 immunostained dentate gyrus, the width, staining intensity and staining area were unchanged in both limbs. Repeated measures analysis of variance showed, however, increased stain area in the external limb for a particular subregion only (significant interactions between drug exposure and subregion: [†]p < 0.01; subregion significance: *p = 0.05, **p < 0.01). A transition occurs in degree of area stained at the regions [c and P] near the polymorph border of the external limb.

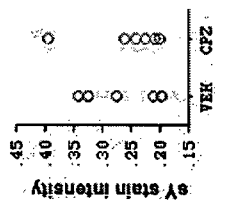
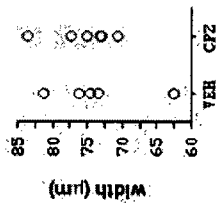
SYNAPTOPHYSIN ir IN THE DENTATE GYRUS AFTER CHLORPROMAZINE TREATMENT

A. External Limb

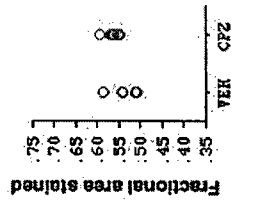
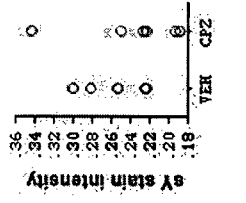


Width

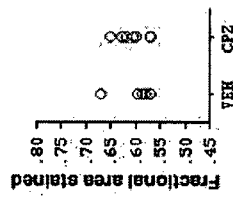
B. Internal Limb



OD



Area



Overall GCL regions Span

Overall GCL regions Span

Figure IV-10 In overall images of synaptophysin immunostained dentate gyrus, the width, staining intensity and staining area were unchanged in both limbs. Repeated measures analysis of variance showed, however, increased stain area in the external limb for a particular subregion only (significant interactions between drug exposure and subregion: †p < 0.005; subregion significance: *p = 0.05, **p < 0.01). A transition occurs in degree of area stained at the regions [c and P] near the polymorph border of the external limb.

IV.3.B.iii. TRIFLUPERAZINE

IV.3.B.iii.a. Trifluperazine – External Limb

IV.3.B.iii.a.1. Trifluperazine – External Limb: Mean intensity of immunostaining

For the overall span of the granule cell layer, mean intensity of SNAP-25 and synaptophysin immunoreactivity was unchanged after trifluperazine treatment. No main effects of trifluperazine treatment or layer by drug interaction were found with repeated measures analysis of variance.

IV.3.B.iii.a.2. Trifluperazine – External Limb: Mean fractional area stained

For the overall span, trifluperazine treatment resulted in no change in mean fractional area of SNAP-25 immunoreactivity. Similarly, repeated measures analysis of variance demonstrated no main effects of trifluperazine treatment or layer by drug interaction

For the overall span, mean fractional area of synaptophysin was nonsignificantly increased by 2.59% after trifluperazine treatment ($t=.766$, $df=8$, $p=.4655$). Repeated measures analysis of variance demonstrated no main effect of drug, however a significant layer by drug interaction was observed ($F=6.018$, $df=4, 32$, $p=.0010$). After trifluperazine treatment, the fractional area of immunostaining was increased in the middle subregions nearest the molecular border: 5.32% in region [a] ($t=2.926$, $df=8$, $p=.0191$) and 9.06% in region [b] ($t=2.839$, $df=8$, $p=.0218$).

Trifluperazine exposure resulted in a reversal of fractional area stained similar to chlorpromazine except only synaptophysin showed this effect for trifluperazine while both presynaptic proteins showed this effect for chlorpromazine. To reiterate, initial increases in

fractional area stained (near the molecular edge) gradually become decreases in fractional area stained during a transition at the layers [c and P] nearest the polymorph border.

IV.3.B.iii.b. Trifluperazine – Internal Limb

IV.3.B.iii.b.1. Trifluperazine – Internal Limb: Mean intensity of immunostaining

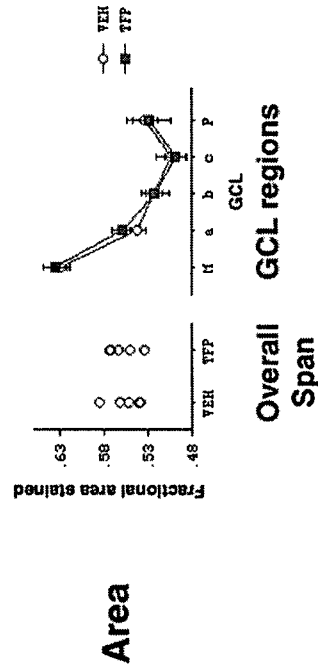
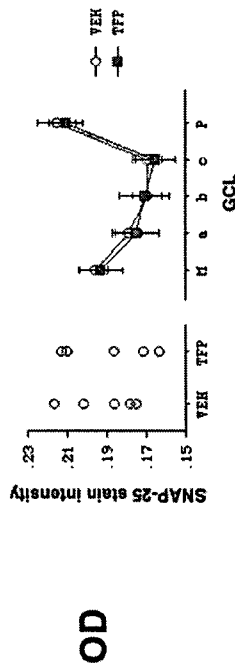
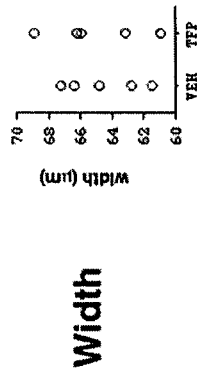
For the overall span of the granule cell layer in this limb, mean intensity of SNAP-25 and synaptophysin immunoreactivity was unchanged after trifluperazine treatment. Repeated measures analysis of variance demonstrated no main effects of trifluperazine treatment or layer by drug interaction.

IV.3.B.iii.b.2. Trifluperazine – Internal Limb: Mean fractional area stained

For the overall span, mean fractional area of SNAP-25 and synaptophysin immunoreactivity was unchanged after trifluperazine treatment. Repeated measures analysis of variance demonstrated no main effects of trifluperazine treatment or layer by drug interaction.

SNAP-25 ir IN THE DENTATE GYRUS AFTER TRIFLUPERAZINE TREATMENT

A. External Limb



B. Internal Limb

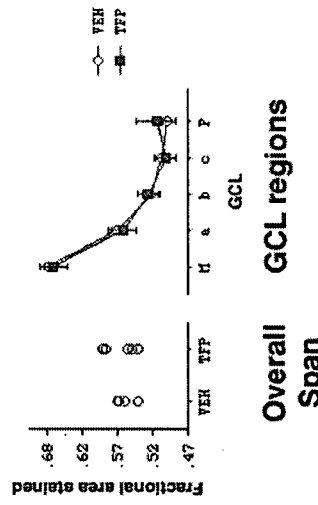
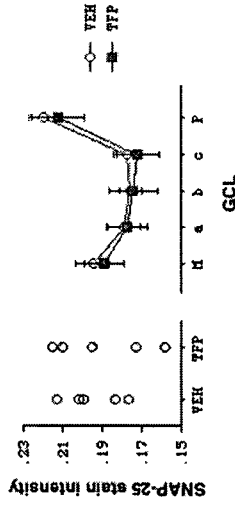
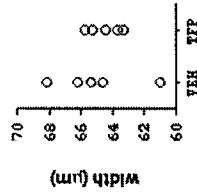
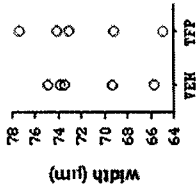


Figure IV-11 In overall images of SNAP-25 immunostained dentate gyrus, the width, staining intensity and staining area were unchanged in both limbs. Repeated measures analysis of variance also showed that these parameters were unchanged in both limbs.

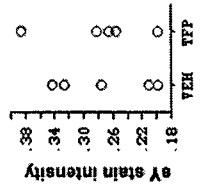
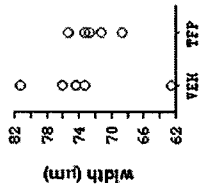
SYNAPTOPHYSIN ir IN THE DENTATE GYRUS AFTER TRIFLUPERAZINE TREATMENT

A. External Limb

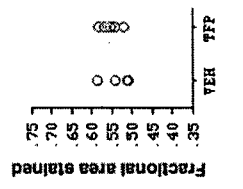
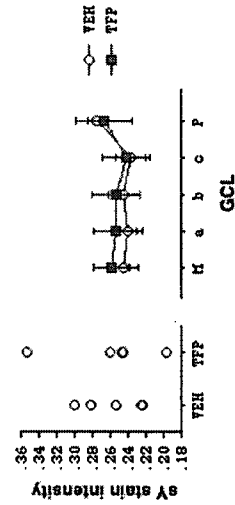


Width

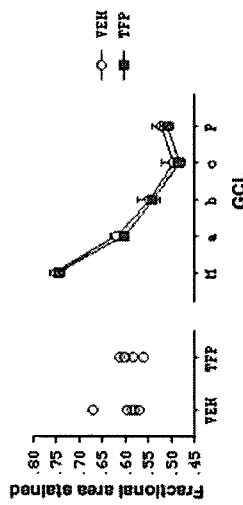
B. Internal Limb



OD



Overall GCL regions Span



Overall GCL regions Span

Figure IV-12 In overall images of synaptophysin immunostained dentate gyrus, the width, staining intensity and staining area were unchanged in both limbs. Repeated measures analysis of variance showed, however, increased stain area in the external limb for a particular subregion only (significant interactions between drug exposure and subregion: †p < 0.001; subregion significance: *p = 0.025). A reversal of fractional area stained occurs from layers [c and P] nearest the polymorph edge of the external limb.

IV.4. CONCLUSION

In this chapter, analyses of the overall hippocampus after antipsychotic exposure showed that haloperidol – but not chlorpromazine nor trifluoperazine – produced changes in synaptic connectivity. Haloperidol treatment resulted in no change in SNAP-25 immunostain intensity with a concomitant reduction of synaptophysin immunostain intensity specific to the CA4 region and the dentate gyrus (molecular and granule cell layer) – unlike the analyses of the overall hippocampus in schizophrenia which showed decreased SNAP-25 and no change in synaptophysin immunostain intensity.

Analyses of the span and the granule cell layer limbs in the dentate gyrus revealed changes in synaptic connectivity both common and unique among the typical antipsychotic drugs used in this study. Common to all the typical APDs used, fractional area of synaptophysin staining was increased in the external limb and unchanged in the internal limb – the former parallels the increases seen in schizophrenia in the same region while the latter is unlike the findings in schizophrenia, suggesting that schizophrenia results in synaptic changes of a particular limb, the internal limb.

Unique to a particular APD, haloperidol exposure showed changes in SNAP-25 levels specific to the internal limb: an increased fractional area of staining and a decrease in staining intensity in regions nearest the polymorph border – both results are unlike the findings in schizophrenia, suggesting once again that schizophrenia results in synaptic changes peculiar to the

internal limb. Chlorpromazine exposure showed an increased SNAP-25 area of staining in the external limb – unlike the findings in schizophrenia.

The present data partially supports my hypothesis that typical APD treatment produces a pattern of presynaptic protein levels in the rat hippocampus different from the pattern of changes in schizophrenia. While the pattern of SNAP-25 immunoreactivity is clearly different, a subset of the changes in synaptophysin seen in schizophrenia may be similar to those seen in rats exposed to typical APDs.

Chapter V DISCUSSION

V.1. OVERVIEW

Analyses of the overall hippocampus revealed a reduction in SNAP-25 (and no change in synaptophysin) immunostaining intensity in perforant pathway termination zones (subiculum, the molecular layer of CA1 and CA2, and the outer molecular layer of the dentate gyrus) in schizophrenia suggesting that (a subset of) circuits from the entorhinal cortex to the hippocampus is disconnected in schizophrenia (**Table V-1**).

Table V-1

Summary: Overall Hippocampus Analyses

	OVERALL HIPPOCAMPUS							
	SYNAPTOPHYSIN				SNAP-25			
	SZ	HAL	CPZ	TFP	SZ	HAL	CPZ	TFP
CA1+2	-	-	-	-	↓	-	-	-
CA3	-	-	-	-	-	-	-	-
CA4	-	↓	-	-	-	-	-	-
DG	-	↓	-	-	↓	-	-	-

A closer examination of the dentate gyrus [DG] revealed some differences in the effects of schizophrenia on the external compared with the internal limb of the granule cell layer (unaccounted for by antipsychotic treatment) – decreased fractional area of SNAP-25

immunostaining throughout the entire internal limb with reductions in some parts of the external limb; increased fractional area of synaptophysin immunostaining throughout the entire internal limb with increases in some parts of the external limb; increased granule cell width (as gauged by SNAP-25 immunoreactivity) – suggesting a neurodevelopmental defect in schizophrenia (**Table V-2**).

Table V-2

Summary: Dentate Gyrus Analyses for External and Internal Limbs

EXTERNAL LIMB								
SYNAPTOPHYSIN					SNAP-25			
	SZ	HAL	CPZ	TFP	SZ	HAL	CPZ	TFP
Width	-	-	-	-	↑	-	-	-
OD	-	-	-	-	↓	-	-	-
Area	↑	↑	↑	↑	↓	↑ (trend)	↑	-

INTERNAL LIMB								
SYNAPTOPHYSIN					SNAP-25			
	SZ	HAL	CPZ	TFP	SZ	HAL	CPZ	TFP
Width	-	-	-	-	-	-	-	-
OD	-	↓	-	-	↓	-	-	-
Area	↑	-	-	-	↓	↑	-	-

An investigation of typical antipsychotic treatment on synaptic connectivity showed changes in synaptophysin immunoreactivity (increased fractional area stained in the external limb) after typical APD exposure, changes similar to those found in schizophrenia. Haloperidol and chlorpromazine exposure also resulted in changes in SNAP-25 immunoreactivity (increased fractional area in the internal limb for the former, the external limb for the latter) different from changes seen in schizophrenia. These results suggest that part of the mechanism of APD's therapeutic effects could be related to compensatory changes in SNAP-25 levels.

V.1.A. Entorhinal-Hippocampal circuit

In analyses of the overall hippocampus, the effect of schizophrenia and haloperidol treatment resulted in different synaptic changes in the termination zones of the entorhinal→hippocampal circuit.

Schizophrenia demonstrated reduced SNAP-25 in the termination zones of all ERC projections – the perforant, alvear, and dentate gyrus pathways – leaving CA3 and CA4 unchanged; synaptophysin was ubiquitously unchanged. In contrast, haloperidol treatment resulted in reduced synaptophysin mainly in the perforant pathway terminal regions with no change in SNAP-25. As well, previous studies of synaptophysin levels in the schizophrenic hippocampus reported no overall change (Browning, Dudek et al. 1993; Eastwood, Burnet et al. 1995) or a decrease (Eastwood and Harrison 1995; Vawter, Howard et al. 1999).

V.1.B. Human Pathologies: Comparison with Alzheimer disease

Cytoarchitectural studies provide some support for the possibility of an abnormal entorhinal→hippocampal circuit in schizophrenia. In schizophrenia, studies have found an overall reduced ERC volume(Falkai, Bogerts et al. 1988) and cytoarchitectural changes throughout the ERC layers (see **Table V-3**), mainly in layer II and III(Jakob and Beckmann 1986; Jakob and Beckmann 1989; Arnold, Hyman et al. 1991; Jakob and Beckmann 1994; Arnold, Franz et al. 1995; Arnold, Ruscheinsky et al. 1997; Falkai, Honer et al. 1999; Falkai, Schneider-Axmann et al. 2000) – although this was not confirmed in all studies(Heinsen, Gossmann et al. 1996; Akil and Lewis 1997; Krimer, Herman et al. 1997). As well, while the human entorhinal→ hippocampal connection is established as early as 19 weeks of gestation(Hevner and Kinnery 1996), myelination of the perforant and alvear pathway occurs in late adolescence from 16 to 20 years of age(Benes 1989; Arnold and Trojanowski 1996), a time when onset of symptoms in schizophrenia typically occurs.

Table V-3

ERC cytoarchitectural changes in schizophrenia

E R C	II	Altered arrangement of clusters(Jakob and Beckmann 1986; Jakob and Beckmann 1989; Arnold, Hyman et al. 1991; Jakob and Beckmann 1994; Arnold, Franz et al. 1995; Arnold, Ruscheinsky et al. 1997; Falkai, Schneider-Axmann et al. 2000) Reduced pyramidal cell number and size(Jakob and Beckmann 1986; Jakob and Beckmann 1989; Jakob and Beckmann 1994; Arnold, Franz et al. 1995) Increased effective size of layer(Arnold, Ruscheinsky et al. 1997)	Perforant path →
-------------	----	---	------------------

III	Reduced pyramidal cell number and size(Jakob and Beckmann 1986; Jakob and Beckmann 1989; Jakob and Beckmann 1994) Abnormal patchy appearance(Arnold, Hyman et al. 1991)	Perforant path → Alvear path →
IV-VI	Reduced pyramidal number and size(Jakob and Beckmann 1994) Abnormal pyramidal orientation(Arnold, Hyman et al. 1991)	Novel DG path →

The altered cytoarchitecture of the entire ERC in schizophrenia may lead to a defect in all three output pathways to the hippocampus. Rat entorhinal lesion studies evinced reduced synaptophysin(Cabalka, Hyman et al. 1992) and reduced SNAP-25(Geddes, Hess et al. 1990) in the perforant pathway termination zones with a concomitant SNAP-25 increase in the dentate inner molecular layer. Given that complete denervation of the ERC → hippocampus connection results in a coupled decrease of synaptophysin and SNAP-25, the ERC abnormalities in schizophrenia are probably subtle and comprise partial denervation, a disconnection in a subcomponent of all three output pathways from the ERC → hippocampus since only SNAP-25 (which is concentrated in a subset of synapses) and not synaptophysin (which is found in all synapses) showed changes.

In comparison, unlike the subtle ERC changes in schizophrenia, AD involves a grossly altered ERC with neurofibrillary tangles and senile plaque involvement along with profound neuron loss throughout all layers, leading to a dramatic denervation of the ERC → hippocampal circuit(Hyman, Van Hoesen et al. 1984; Hyman, Van Hoesen et al. 1986). AD evinced reduced synaptophysin in the perforant termination zones with a concomitant increase in the dentate inner molecular layer suggestive of reinnervation(Hamos, DeGennaro et al. 1989; Goto and Hirano 1990;

Honer, Dickson et al. 1992) and reduced SNAP-25 in the CA1 region and a reduced OML:IML ratio for SNAP-25(Wakabayashi, Honer et al. 1994). This differential pattern of synaptic components corresponds with Western blot analyses showing a 30% decrease in synaptophysin and only a 10% decrease in SNAP-25 with synaptophysin (and syntaxin) reductions correlating with reduced cognitive function in AD(Wakabayashi, Honer et al. 1994; Shimohama, Kamiya et al. 1997; Sze, Bi et al. 2000). While the pattern of synaptic change in schizophrenia differs markedly from AD, a differential pattern of synaptic components is seen in schizophrenia and a comparable investigation into whether SNAP-25 reduction correlates with cognitive function in schizophrenia is indicated.

The increased SNAP-25 in the IML after entorhinal lesions reflects reinnervation and stresses the role of SNAP-25 in brain development, axonal growth, and neurite elongation(Osen-Sand, Catsicas et al. 1993). The decreased hippocampal SNAP-25 in the schizophrenia may represent reflect impaired synaptogenesis.

SNAP-25 IR

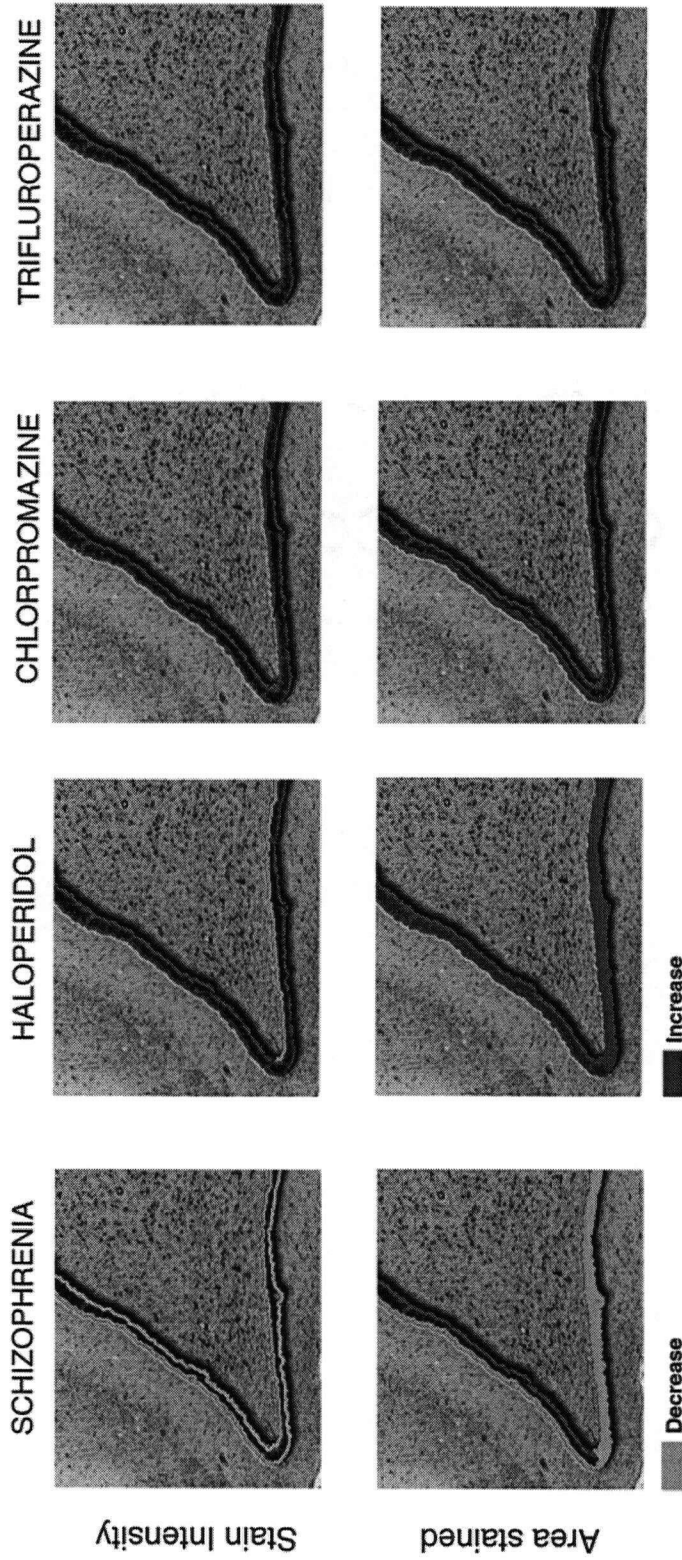


Figure V-1

Differential effect of schizophrenia and APD treatment on SNAP-25 ir in the dentate gyrus. Intensity of SNAP-25 ir was decreased in the marginal zones of both limbs in schizophrenia and also decreased in the polymorph border of the internal limb after haloperidol exposure. Fractional area of SNAP-25 ir was decreased across the entire span of the internal limb and in limited regions ("M" and "a") of the external limb in schizophrenia, increased across the span of both limbs after haloperidol exposure, and increased in limited regions ("M" and "a") of the external limb after chlorpromazine exposure.

V.2. ASPECTS OF DENTATE DEVELOPMENT: LIMBS AND GRANULE CELLS

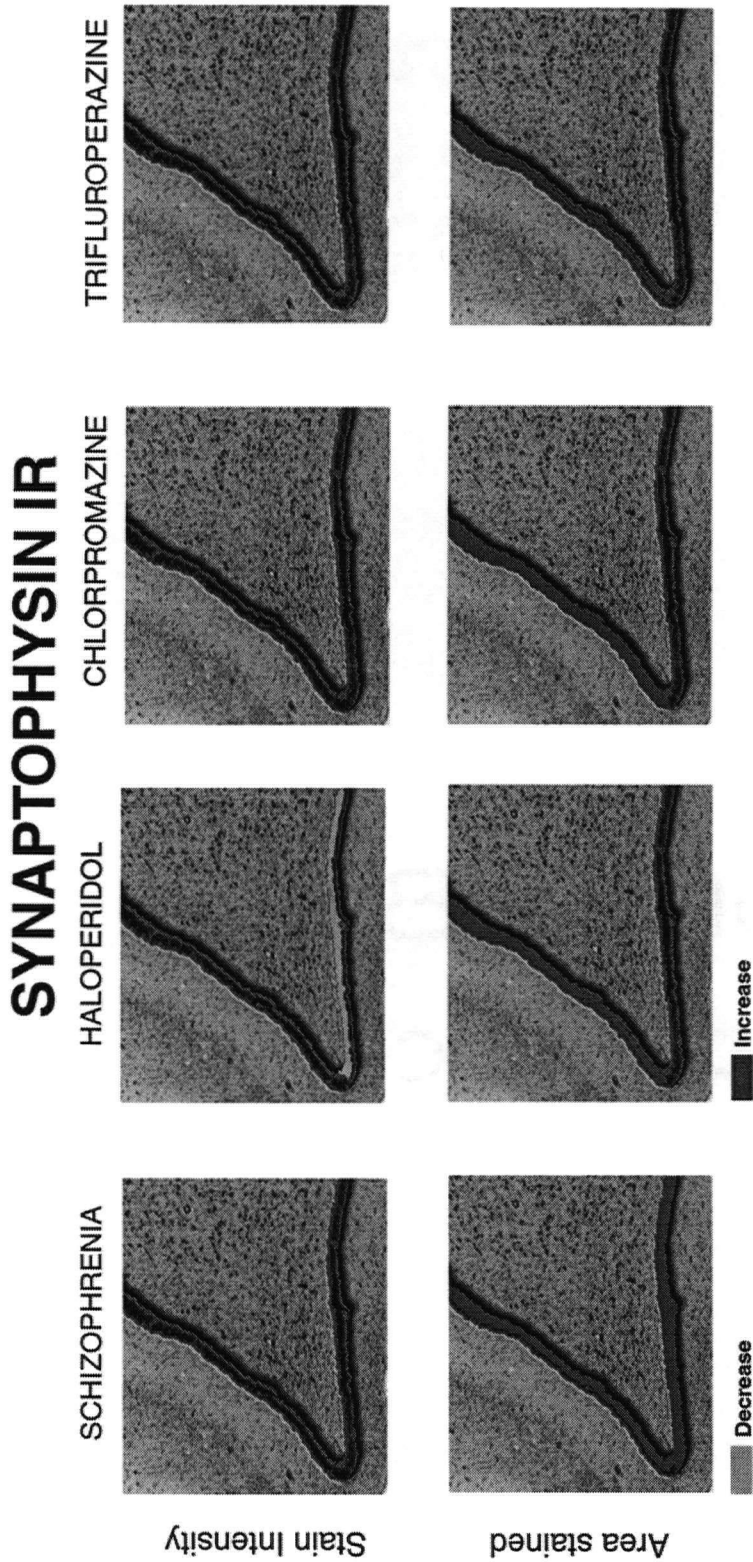


Figure 5-2

Effects of schizophrenia and APD treatment on synaptophysin ir in the dentate gyrus. Intensity of synaptophysin ir was unchanged in both limbs in schizophrenia and decreased in most subregions of the internal limb after haloperidol exposure. Ifractional area of synaptophysin ir was increased in both limbs in schizophrenia and increased in most subregions of the external limb after exposure to each of the antipsychotic drugs, suggesting that the increases in the internal limb in schizophrenia may be specific to this pathology while the increases in the external limb in schizophrenia may be attributed to APD treatment.

The neurodevelopmental aspect of schizophrenia was investigated with the hypothesis that if schizophrenia is a problem of abnormal prenatal development, then one would expect a different pattern of connectivity in the two limbs of the dentate gyrus, while a predominantly postnatal problem would show differences in the span of the granule cell layer.

In the development of the human fetal dentate gyrus, two developmental gradients are apparent: the limbs of the granule cell layer [GCL] evince differences in cell density and organisation prenatally (Arnold and Trojanowski 1996), while the span of the GCL continues to develop postnatally (Rakic and Nowakowski 1981; Eckenhoff and Rakic 1988; Eriksson, Perfilieva et al. 1998). The two limbs are initially anatomically different early in gestation with the (early forming) external limb being more condensed and more organised than the (later forming) internal limb. From the first appearance of the granule cell layer at the 13th fetal week (Humphrey 1967), there is a progressive condensation of each limb, a lack of immature cells by 32-34 weeks, and a decrease in neuronal density in both limbs thereafter (Arnold and Trojanowski 1996). The limbs become anatomically identical and exhibit a cytoarchitecture similar to that seen in the adult by 39-40 weeks gestational age. Meanwhile, another neurogenic gradient exists across the span of the GCL where early-born granule cells reside in the superficial portion of the GCL (toward the molecular border) and later-born granule cells occupy the deeper portion of the layer (toward the polymorph border). Studies in rodents have shown that connections into the limbs of the GCL closely follow the pattern of granule cell neurogenesis, although temporally delayed, with

connections occurring first in the early forming external limb followed by connections to the later forming internal limb (Gall, Brecha et al. 1984; Slomianka and Geneser 1997).

In a closer examination of the dentate gyrus, one effect of schizophrenia was a decrease in SNAP-25 immunoreactivity (intensity and area stained) in both limbs which cannot be attributed to APD exposure since haloperidol produced an opposite effect, an increase in SNAP-25. In both limbs, reduced SNAP-25 stain intensity was evident in the marginal sublayers for schizophrenia.

A difference in the limbs, however, was evident in measurements of width (as gauged by SNAP-25 staining) and of area stained (by both synaptophysin and SNAP-25). Schizophrenia showed an elevation of synaptophysin in both limbs. The increase in the external limb may be due to APD exposure since all three APDs produced similar increases in synaptophysin in this limb. The increase in the internal limb cannot, however, be attributed to APD exposure since synaptophysin levels are unchanged in this limb after APD treatment, suggesting that the internal limb is greater affected in schizophrenia. While decreased area of SNAP-25 staining was seen in both limbs, the entire span of the (later forming) internal limb was affected while only the subregions adjacent to the molecular border of the (early forming) external limb showed effects. In addition, the increased width in only the external limb provides further evidence for the possibility of a prenatal development defect in schizophrenia.

An alternative explanation to the changes seen in the limbs in schizophrenia is that the differences could relate to different properties between the limbs. Postnatal influences can also produce differential changes between the two dentate limbs. Limbs differences in terms of number

of proliferating granule cells have been shown to occur after haloperidol exposure (Dawirs, personal communication) and after performing spatial learning tasks(Ambrogini, Cuppini et al. 2000).

Induction of LTP results in a preferential increase of syntaxin mRNA levels in the internal limb of the dentate gyrus(Hicks, Davis et al. 1997). In essence, the dentate limb differences seen in schizophrenia may relate to either postnatal or prenatal problems since both limbs are differentially affected postnatally and develop differentially prenatally.

V.2.A. SNAP-25 Limb differences: Width of overall GCL

That only the external limb showed a significant increase in width (as gauged by SNAP-25 immunoreactivity) in schizophrenia suggests a possible defect in condensation of the external limb (putting the timing before 32-34 weeks when granule cells mature and hold their position). Given that a morphometric study of the GCL indicated reduced overall volume in schizophrenia, with a non-significant reduction in mean granule cell number(Falkai and Bogerts 1986), one would have expected a decrease in GCL width in schizophrenia. That the external limb width was unchanged as gauged by synaptophysin immunoreactivity suggests that my finding of increased width of SNAP-25 immunostaining may be an artifact since the GCL was determined by its non-staining profile contrasted against a sea of positive immunoreactivity which is prone to methodological variability. Alternatively, the increased width of SNAP-25 immunostaining may be a specific effect on SNAP-25 connections of perhaps unchanged neurons or neuronal width.

V.2.B. SNAP-25 and Synaptophysin Limb differences: Staining Pattern across GCL subdivisions

That a differential pattern of SNAP-25 reductions and synaptophysin increases between the limbs occurs in schizophrenia places the timing of a possible defect at 39-40 weeks gestational age (or earlier) when the two limbs should be identical. The two limbs demonstrated differences in connectivity across the span of their granule cell layer pointing to a possible defect in GABAergic interneurons in individual limbs.

V.2.C. Symmetrical GABAergic inhibitory synapses predominate in the GCL

Generally, superficial early born granule cells [GC] located near the molecular border receive nearly twice the density of axo-somatic and axo-axonal synapses than the deep, later generated GCs found near the polymorph border (Lee, Gerbrandt et al. 1982; Kosaka 1996). Of the two parameters measured (staining intensity and fractional area of staining), fractional area of staining consistently showed a higher area stained in the superficial region adjacent to the molecular border ["M"] compared to the deeper region adjacent to the polymorph border ["P"] in both human controls and in vehicle treated rats, suggesting that fractional area stained is an indicator of number of synapses – while the intensity of staining may be a better indicator of synaptic strength.

Electron microscope studies in rats have shown that of the total number of axo-somatic synapses, 80% are symmetrical and 20% asymmetrical, and that of the total axo-axonal synapses, the majority are overwhelmingly symmetrical and rarely ($\leq 1\%$ of total) asymmetrical. The pattern of GABA-like immunoreactivity (GABA-ir) also follows the neurogenic gradient seen in the GCL where more GABA-ir terminals contact superficial GCs than deeper GCs (Woodson, Nitecka et al.

1989). As well, superficial GCs have greater dendritic length which may reflect greater synaptic input into those GCs(Seress and Pokorny 1981; Green and Juraska 1985).

In contrast to rats, electron microscope studies in nonhuman primates and humans have shown that of the total number of axo-somatic synapses, the majority are overwhelmingly symmetrical and rarely asymmetrical(Schlander, Thomalske et al. 1987; Seress and Ribak 1990; Seress and Ribak 1992). Similarly, a lower frequency of GAD-positive neurons is found in the dentate gyrus of nonhuman primates than in rats(Babb, Pretorius et al. 1988).

Compared to the rat, the lower number of inhibitory symmetric axosomatic synapses with the somata of GCs and the existence of monosynaptic ERC excitatory circuits to basal (and promixal) dendrites of GCs, strongly argues for a higher susceptibility of the human GC for synchronized bursting activity(Seress 1992) and, therefore, disruption of normal hippocampal function when inhibitory circuits are impaired.

Table V-4

Characteristics of Superficial versus Deep GCs

	Superficial GC Near molecular border	Deep GC Near polymorph border
# axo-somatic synapses (rodent: 80% symm, 20% asymm(Lee, Gerbrandt et al. 1982; Kosaka, Hama et al. 1984; Seress and Ribak 1985; Kosaka 1996); non-human primate: mainly symm, rarely asymm(Seress and Ribak 1990; Seress and Ribak 1992)	2x that found in Deep	
# axo-axonal synapses (most symm, ≤ 1% asymm)(Lee, Gerbrandt et al.	2x that found in Deep	

1982; Kosaka, Hama et al. 1984; Kosaka 1996)		
Dendritic parameters (material, number, branch length, fields)(Seress and Pokorny 1981; Green and Juraska 1985)	More dendritic material, wider dendritic fields	Less dendritic material, narrower dendritic field
GABA-ir(Woodson, Nitecka et al. 1989)	More GABA-ir	Less GABA-ir

EM GABA-ir studies in rat have shown that the local GABAergic innervation of granule cells originates from two interneuron types(Halasy and Somogyi 1993): one, basket cells with soma at the polymorph border which send their main axon towards the IML and innervate the GCL with secondary collaterals; the other, hilar chandelier cells which make axo-axonal synapses on initial segments of GC and of hilar cells.

A recent rat study(Dupuy-Davies and Houser 1999) combining BrdU and GAD67 expression (mRNA and protein) found that superficial early-appearing GABA neurons (many of which are basket cells) situated near the molecular border gradually alter their position to become the deeper mature GABA neurons along the polymorph border. There is a gradual shift in the concentration of GAD-labeled terminals from above the GCL near the molecular border to within the GCL and towards the polymorph border during development of the DG. The early-appearing GABA neurons at the molecular border could help to establish and maintain the outer border of the GCL, help stimulate outgrowth of GC dendrites and, through a series of events, promote neuronal development(Ben-Ari, Tseeb et al. 1994; Dupuy-Davies and Houser 1999).

Given that symmetric GABAergic inhibitory synapses predominate within the nonhuman primate GCL, the elevated fractional area of synaptophysin immunoreactivity and reduced

fractional area of SNAP-25 staining across the entire span of the internal limb in schizophrenia could reflect an increase in GABAergic terminals with a loss in a specific subset throughout this limb. APD exposure resulted in no change in synaptophysin in the internal limb (all APDs) and increased SNAP-25 (haloperidol in the internal limb, chlorpromazine in the external limb) fractional area. Medication thus seems an unlikely cause of the changes in synaptophysin and SNAP-25 reported here in schizophrenia. As well, schizophrenia showed increased fractional area of synaptophysin ir across the span of the granule cell layer with reduced fractional area of SNAP-25 ir in only the regions adjacent to the molecular border ("M" and "a") in the external limb. It is tempting to speculate that schizophrenia involves, in part, an early developmental defect affecting early-appearing GABA neurons and/or early-born GCs since a disruption in either (or both) would probably lead to altered synaptic connectivity in these regions ("M" and "a"). The reduced intensity of SNAP-25 ir in the marginal borders in both limbs may indicate reduced synaptic strength of GABA terminals in these areas and may represent an early developmental defect (at "M") coupled with a problem occurring in later development (at "P"). Alternatively, such changes in presynaptic proteins in schizophrenia could reflect a postnatal defect or response given the plasticity of the dentate limbs throughout life.

V.2.D. Human Pathologies: Comparison with Temporal lobe epilepsy

Since there are temporal differences in the maturation of granule neurons and of GABAergic neurons across the span of the GCL, the reduced SNAP-25 ir (stain intensity and fractional area stained) and increased synaptophysin ir (fractional area stained) of the GCL in schizophrenia could

point to a disturbed synaptic circuitry originating from improper development of granule neurons and/or GABAergic neurons. Supporting this idea of disturbed development is a quantitative immunohistochemistry and western blot study of the schizophrenic dentate gyrus which found decreased levels of the embryonic highly polysialylated isoform of NCAM (PSA-NCAM)(Barbeau, Liang et al. 1995), critical for many neurodevelopmental processes including neurulation, axonal outgrowth, and the establishment of neuronal connectivity.

The pattern of denervation (decreased SNAP-25 ir) and reinnervation (increased synaptophysin ir) in the GCL of schizophrenics may point to aberrant synaptic reorganisation in the pathophysiology of schizophrenia(Stevens 1992). In comparison, temporal lobe epilepsy [TLE] is thought to be a developmental disorder involving a grossly altered dentate gyrus with denervation (severe neuronal cell loss accompanied by a severe loss of synapses) and aberrant reinnervation (synaptic reorganisation by aberrant neural sprouting of the granule cell's mossy fibres). In TLE, while synaptophysin is decreased in the CA1 and CA4 hippocampal fields, synaptophysin is increased in the (inner) molecular layer of the dentate gyrus indicating probable synaptic reorganization(Honer, Beach et al. 1994; Davies, Schweitzer et al. 1998; Looney, Dohan et al. 1999; Proper, Oestreicher et al. 2000). Interestingly, a subset of patients with TLE also manifest a schizophrenic-like psychosis(Ardila and Gomez 1988; Kan, Mori et al. 1989; Bruton, Stevens et al. 1994), suggesting that aberrant synaptic reorganisation of the hippocampus may underlie the psychosis in schizophrenia.

V.2.E. Integrity of GCs

Recent investigations have demonstrated abnormalities in dentate granule cells and innervation of granule cells in schizophrenia. An immunohistochemical study(Mizukami, Sasaki et al. 2000) found GABA(B) receptor stain intensity was decreased in granule cells and unchanged in interneurons of the GCL while a quantitative autoradiographic study(Benes, Khan et al. 1996) found increased GABA(A) receptor binding in the GCL. Synaptophysin mRNA in the granule cell layer was reported to be decreased(Harrison, McLaughlin et al. 1991; Eastwood and Harrison 1995). A quantitative autoradiographic study(Freedman, Hall et al. 1995) of schizophrenic patients found fewer nicotinic receptors in the dentate gyrus, a condition which may lead to failure of cholinergic activation of inhibitory interneurons and manifest clinically as decreased gating of response to sensory stimulation. As well, mRNA studies of the dentate gyrus demonstrated unchanged levels of 5HT1A receptor mRNA and reduced levels of GluR1 and GluR2 mRNA, implying a functional abnormality of the granule cells(Harrison, McLaughlin et al. 1991; Eastwood, McDonald et al. 1995). Timm staining studies of the mossy fiber projections from granule cells showed either a reduction or no change in the hilus, CA4, and CA3 regions in schizophrenia(Adams, DeMasters et al. 1995; Goldsmith and Joyce 1995). Ligand-binding studies found abnormalities of beta-adrenergic, seroternergic and glutamatergic receptors of the granule cells in schizophrenia(Kerwin, Patel et al. 1990; Joyce, Lexow et al. 1992; Joyce, Shane et al. 1993). Finally, dentate granule cell dendrites are the targets of the perforant pathway projection. As described previously, I found a deficit in the presynaptic, SNAP-25 component of this pathway in schizophrenia. Interestingly,

neonatal rats subjected to X-irradiation targeting the developing limbs of the dentate gyrus resulted in a more severe GC loss in the later-developing internal limb (since later forming cells are more susceptible to X-irradiation) with a resulting decrease in numbers of ERC neurons in layer II (55-58% loss) and layer III (20-25% loss) and slight (nonsignificant) increase in layer IV-VI (Lewis and Cotman 1980). While it appears that granule cells play an important role in determining the density of their innervation, the implication for schizophrenia is that a subtle disturbance of GCs in early development may possibly initiate the aberrant cytoarchitecture seen in the schizophrenic ERC.

V.3. SYNAPTIC CHANGES FROM APD TREATMENT .

Of the few studies that have looked at the effects of APDs on synaptic proteins in the hippocampus, no changes in synaptophysin levels were found (Eastwood, Burnet et al. 1995; Eastwood, Heffernan et al. 1997). I found, however, decreases in synaptophysin (stain intensity) after haloperidol treatment in studies of the whole hippocampus in the CA4 region, the radiatum-lacunosum of the CA3 region, and the dentate gyrus, suggesting haloperidol is decreasing synaptic strength in some hippocampal circuits. I also found in higher resolution studies increases in synaptophysin and SNAP-25 levels (area stained) in the span of the GCL after exposure to APDs, suggesting that APD could be acting to induce sprouting of GABAergic terminals in this area. (Todtenkopf and Benes 1998) looked at the relationship between APD exposure (CPZ) and the density of GABAergic terminals in the schizophrenic hippocampus. He found that drug-naïve patients had the lowest density of terminals while the density of GABAergic terminals increased with CPZ exposure, supporting the notion that APD could be inducing GABAergic terminal sprouting in the hippocampus. The proliferation of terminals may also coincide with a proliferation of granule cells since adult gerbils exposed to haloperidol showed increased dentate granule cell proliferation (Dawirs, Hildebrandt et al. 1998).

I found that the proliferation of terminals (increased fractional area of synaptophysin) after APD exposure was specific to the external limb. Similarly, the number of BrdU-positive cells in adult rats is increased preferentially in the external limb of the dentate gyrus after haloperidol exposure (Dawirs, personal communication) and after performing spatial learning tasks (Ambrogini,

Cuppini et al. 2000). Interestingly, the survival of newborn cells is enhanced by learning(Ambrogini, Cuppini et al. 2000), leading to speculation that haloperidol may also have a neuroprotective role. Other agents such as chronic exposure to the synthetic cannabinoid WIN 55,212-2 resulted in increased MAP-2 immunoreactivity in only the internal blade of the dentate gyrus(Lawston, Borella et al. 2000). Taken together, these findings suggest that the two limbs are different sites of pharmaco-behavioural action and that the therapeutic effects of APD in schizophrenia may in part be related to elevated synaptic terminal number: an increase in a subset of (SNAP-25 ir) terminals in both limbs and a global increase of (synaptophysin ir) terminals in the external limb. LIMITATIONS

The methodological limitations in neuropathological studies of the schizophrenic hippocampus(Benes 1988; Casanova and Kleinman 1990; Harrison 1996) include:

Flaws in experimental design:

- Use of inappropriate controls (such as patient with neurological disease)
- Inaccurate diagnosis of schizophrenia
- Lack of blind quantitation
- Improper cytoarchitectural divisions of the hippocampus
- Exposure to neuroleptics (and other somatic treatments)

Peri-mortem factors

- Hypoxic insult prior to death (or agonal state)
- Post-mortem interval
- Duration of tissue fixation

V.4. LIMITATIONS

V.4.A. Flaws in experimental design

This thesis attempted to avoid each of the potential confounds when performing neuropathological studies of the schizophrenic hippocampus: the control subjects were free of neurological disease; diagnoses were made according to DSM-III-R criteria following chart review by a research psychiatrist; all quantitation was performed blind to diagnosis; hippocampal regions and layers were demarcated with the help of a neuropathologist; and, to address the role of neuroleptic exposure, I studied the effects of APD exposure in rats.

The correspondence between giving APDs to normal rats and giving APDs to ill people is, however, problematic since species differences may exclude proper comparison. As mentioned previously in the discussion, the synaptic circuitry within the granule cell layer of nonhuman primates and humans is different from rats.

Since APDs seem to evince a differential limb effect (preferentially changing synaptic connectivity in the external limb), one can interpret the limb differences in connectivity in schizophrenia as being attributed to purely APD targetting the external limb.

V.4.B. Peri-mortem factors

An EM study of the molecular layer of the motor-sensory cortex in rats showed decreased synaptic density and decreased number of synaptic vesicles per synapse with increasing PMI, reaching significance at 8 hours and becoming marked by 15 hours (Petit and LeBoutillier 1990).

While the mean postmortem interval in my study was 8.6 ± 6.7 hours for schizophrenics and $13.6 \pm$

5.3 hours for controls, I found no correlation between synaptophysin immunoreactivity and PMI at the level of the gross hippocampus and of the dentate GCL. While SNAP-25 immunoreactivity did not correlate with PMI at the level of the dentate GCL, a significant correlation was observed in the gross hippocampus (in the presubiculum and the pyramidal layers of CA1 and CA2).

Unexpectedly, a positive correlation was found for SNAP-25 and PMI. This may be attributed to false positive findings since it was uncorrected for multiple comparisons – although, conceivably, the increased proteolysis with longer PMI may be exposing more epitopes for the SNAP-25 antibody.

One study (Hoog, Gould et al. 1988) found that ability of the synaptophysin (SY38) antibody to recognize the epitope of the synaptophysin antigen can be compromised with prolonged formalin fixation. I used another synaptophysin antibody (EP10 in humans (Honer, Kaufmann et al. 1992) and SP15 in rat (Honer, Hu et al. 1993) studies) for immunohistochemistry.

Other studies have found that with increasing subject age, synaptophysin mRNA in the temporal lobe of schizophrenics declined (Tcherepanov and Sokolov 1997) and synaptophysin staining (area) in the frontal cortex declined (Masliah, Mallory et al. 1993). My study found, however, that with increasing age there is an increase in fractional area of synaptophysin immunostaining in the dentate GCL. It may be that because of the unique nature of the mammalian GCL in its ability to continue to generate new granule neurons postnatally, my high resolution study is detecting authentic increases in synaptic terminals in this region and that there may be an increase with age.

V.4.C. Presynaptic protein ir: Markers of synaptic density or of vesicles?

In addition to the possible confounds inherent in studying in the postmortem schizophrenic hippocampus, the use of presynaptic protein-ir as a marker of synaptic density can also be criticised. Although synaptophysin and SNAP-25 can be used as a measure of synaptic density, the changes in presynaptic protein-ir could be due to (as possibly in synaptophysin, a vesicular protein) an alteration in size or number of vesicles per terminal, or due to (as possibly in SNAP-25, a plasma membrane protein) a structural abnormality of the presynaptic region. Changes in size or number of vesicles would probably affect the intensity of staining (but not fractional area of staining) for synaptophysin (a vesicular protein) and conceivably have little affect on SNAP-25 (a plasma membrane protein) in terms of stain intensity and area stained. An option to using presynaptic proteins as an indicator of synaptic density is measuring postsynaptic components such as PSD-25 and gephyrin which are proteins associated specifically with glutamate and GABA postsynaptic sites, respectively.

V.5. SUMMARY

This thesis has contributed a body of new observations on the pathogenesis of schizophrenia and on the effects of typical APD exposure. Among these, the following are considered to be the most salient, and have implications for my understanding of schizophrenia as noted:

- A subset of ERC→hippocampus circuits (as assessed by SNAP-25 ir) is disconnected in schizophrenia, confirming the hypothesis that an abnormal ERC in schizophrenia would be associated with changes in the perforant pathway termination zones of the hippocampus.
- Schizophrenia evinces a differential pattern of synaptic circuitry in the two limbs of dentate GCL with more prominent changes seen in the internal limb. This indicates a possible prenatal developmental defect at 39-40 weeks gestational age (or earlier) when the two limbs should be identical.
- APD treatment on the whole results in a pattern of synaptic change different from those seen in schizophrenia, suggesting the previous observations (#1 and #2) are specific to schizophrenia and not due to neuroleptic exposure.
- Common to all typical APDs used in this study, typical APD exposure results in increased terminal number preferentially in the external limb of the dentate gyrus, possibly indicating a common site of pharmacological action in typical APDs.

REFERENCES

- Adams, C. E., B. K. DeMasters, et al. (1995). "Regional zinc staining in postmortem hippocampus from schizophrenic patients." Schizophrenia Research **18**(1): 71-7.
- Akil, M. and D. A. Lewis (1997). "Cytoarchitecture of the entorhinal cortex in schizophrenia." American Journal of Psychiatry **154**(7): 1010-2.
- Al-Amin, H., D. Weinberger, et al. (2000). "Exaggerated MK-801-induced motor hyperactivity in rats with the neonatal lesion of the ventral hippocampus." Behavioural Pharmacology **11**(3-4): 269-78.
- Alder, J., H. Kanki, et al. (1995). "Overexpression of synaptophysin enhances neurotransmitter secretion at *Xenopus* neuromuscular synapses." Journal of Neuroscience **15**(1 Pt 2): 511-9.
- Alder, J., B. Lu, et al. (1992). "Calcium-dependent transmitter secretion reconstituted in *Xenopus* oocytes: requirement for synaptophysin." Science **257**(5070): 657-61.
- Alder, J., Z. P. Xie, et al. (1992). "Antibodies to synaptophysin interfere with transmitter secretion at neuromuscular synapses." Neuron **9**(4): 759-68.
- Altshuler, L. L., M. F. Casanova, et al. (1990). "The hippocampus and parahippocampus in schizophrenia, suicide, and control brains [published erratum appears in Arch Gen Psychiatry 1991 May;48(5):422]." Archives Of General Psychiatry **47**(11): 1029-34.
- Altshuler, L. L., A. Conrad, et al. (1987). "Hippocampal pyramidal cell orientation in schizophrenia. A controlled neurohistologic study of the Yakovlev collection." Archives Of General Psychiatry **44**(12): 1094-8.
- Ambrogini, P., R. Cuppini, et al. (2000). "Spatial learning affects immature granule cell survival in adult rat dentate gyrus." Neuroscience Letters **286**(1): 21-4.
- Andreasen, N. C., V. W. d. Swayze, et al. (1990). "Ventricular enlargement in schizophrenia evaluated with computed tomographic scanning. Effects of gender, age, and stage of illness [see comments]." Archives Of General Psychiatry **47**(11): 1008-15.
- Ardila, A. and J. Gomez (1988). "Complex partial status and schizophrenia." International Journal of Neuroscience **39**(3-4): 235-44.

- Arnold, S. and J. Trojanowski (1996). "Human fetal hippocampal development: I. Cytoarchitecture, myeloarchitecture, and neuronal morphological features." Journal of Comparative Neurology **367**: 274-292.
- Arnold, S. E., B. R. Franz, et al. (1995). "Smaller neuron size in schizophrenia in hippocampal subfields that mediate cortical-hippocampal interactions." American Journal of Psychiatry **152**(5): 738-48.
- Arnold, S. E., B. R. Franz, et al. (1996). "Glial fibrillary acidic protein-immunoreactive astrocytosis in elderly patients with schizophrenia and dementia." Acta Neuropathologica **91**(3): 269-77.
- Arnold, S. E., B. T. Hyman, et al. (1991). "Some cytoarchitectural abnormalities of the entorhinal cortex in schizophrenia." Archives Of General Psychiatry **48**(7): 625-32.
- Arnold, S. E., V. M. Lee, et al. (1991). "Abnormal expression of two microtubule-associated proteins (MAP2 and MAP5) in specific subfields of the hippocampal formation in schizophrenia." PNAS **88**(23): 10850-4.
- Arnold, S. E., D. D. Ruschinsky, et al. (1997). "Further evidence of abnormal cytoarchitecture of the entorhinal cortex in schizophrenia using spatial point pattern analyses." Biological Psychiatry **42**(8): 639-47.
- Babb, T. L., J. K. Pretorius, et al. (1988). "Distribution of glutamate-decarboxylase-immunoreactive neurons and synapses in the rat and monkey hippocampus: light and electron microscopy." Journal of Comparative Neurology **278**: 121-138.
- Barbeau, D., J. J. Liang, et al. (1995). "Decreased expression of the embryonic form of the neural cell adhesion molecule in schizophrenic brains." PNAS **92**(7): 2785-9.
- Bark, I. C. (1993). "Structure of the chicken gene for SNAP-25 reveals duplicated exon encoding distinct isoforms of the protein." Journal of Molecular Biology **233**(1): 67-76.
- Bark, I. C., K. M. Hahn, et al. (1995). "Differential expression of SNAP-25 protein isoforms during divergent vesicle fusion events of neural development." PNAS **92**(5): 1510-4.
- Bark, I. C. and M. C. Wilson (1994). "Human cDNA clones encoding two different isoforms of the nerve terminal protein SNAP-25." Gene **139**(2): 291-2.

- Beauregard, M. and J. Bachevalier (1996). "Neonatal insult to the hippocampal region and schizophrenia: a review and a putative animal model." Canadian Journal of Psychiatry. Revue Canadienne de Psychiatrie **41**(7): 446-56.
- Ben-Ari, Y., V. Tseeb, et al. (1994). "γ-aminobutyric acid (GABA): a fast excitatory transmitter which may regulate the development of hippocampal neurones in early postnatal life." Prog Brain Res **102**: 261-273.
- Benes, F. M. (1988). "Post-mortem Structural Analyses of Schizophrenic Brain: Study Designs and the Interpretation of Data." Psychiatric Development **3**: 213-226.
- Benes, F. M. (1989). "Myelination of cortical-hippocampal relays during late adolescence." Schizophrenia Bulletin **15**(4): 585-93.
- Benes, F. M., J. Davidson, et al. (1986). "Quantitative cytoarchitectural studies of the cerebral cortex of schizophrenics." Archives Of General Psychiatry **43**(1): 31-5.
- Benes, F. M., Y. Khan, et al. (1996). "Differences in the subregional and cellular distribution of GABAA receptor binding in the hippocampal formation of schizophrenic brain." Synapse **22**(4): 338-49.
- Benes, F. M., E. W. Kwok, et al. (1998). "A reduction of nonpyramidal cells in sector CA2 of schizophrenics and manic depressives." Biological Psychiatry **44**(2): 88-97.
- Benes, F. M., R. Majocha, et al. (1987). "Increased vertical axon numbers in cingulate cortex of schizophrenics." Archives Of General Psychiatry **44**(11): 1017-21.
- Benes, F. M., J. McSparren, et al. (1991). "Deficits in small interneurons in prefrontal and cingulate cortices of schizophrenic and schizoaffective patients." Archives Of General Psychiatry **48**(11): 996-1001.
- Benes, F. M., P. A. Paskevich, et al. (1985). "The effects of haloperidol on synaptic patterns in the rat striatum." Brain Res. **329**: 265-274.
- Benes, F. M., P. A. Paskevich, et al. (1985). "Synaptic re-arrangements in medial prefrontal cortex of haloperidol-treated rats." Brain Res **348**: 15-20.
- Benes, F. M., P. A. Paskevich, et al. (1983). "Haloperidol-induced plasticity of axon terminals in rat substantia nigra." Science **221**: 969-971.

- Benes, F. M., I. Sorensen, et al. (1991). "Reduced neuronal size in posterior hippocampus of schizophrenic patients." Schizophrenia Bulletin **17**(4): 597-608.
- Benes, F. M., I. Sorensen, et al. (1992). "Increased density of glutamate-immunoreactive vertical processes in superficial laminae in cingulate cortex of schizophrenic brain." Cerebral Cortex **2**(6): 503-12.
- Bertoni-Freaddari, C., P. Fattoretti, et al. (1989). "Computer-assisted morphometry of synaptic plasticity during aging and dementia." Pathol Res Pract **185**: 799-802.
- Bertoni-Freddari, C., P. Fattoretti, et al. (1989). "Computer-assisted morphometry of synaptic plasticity during aging and dementia." Pathol Res Pract **185**: 799-802.
- Biegon, A. and M. Wolff (1986). "Quantitative histochemistry of actylcholinesterase in rat and human brain postmortem." Journal of Neuroscience Methods **16**(39-45).
- Bilder, R. M., B. Bogerts, et al. (1995). "Anterior hippocampal volume reductions predict frontal lobe dysfunction in first episode schizophrenia." Schizophrenia Research **17**(1): 47-58.
- Binz, T., J. Blasi, et al. (1994). "Proteolysis of snap-25 by types e and a botulinal neurotoxins." Journal of Biological Chemistry **269**(3): 1617-1620.
- Blasi, J., E. R. Chapman, et al. (1993). "Botulinum neurotoxin A selectively cleaves the synaptic protein SNAP-25 [see comments]." Nature **365**(6442): 160-3.
- Bleuler, E. (1950). Dementia praecox of the group of schizophrenias (translated by J. Zinkin). New York, International University Press.
- Bogerts, B., M. Ashtari, et al. (1990). "Reduced temporal limbic structure volumes on magnetic resonance images in first episode schizophrenia." Psychiatry Research **35**(1): 1-13.
- Bogerts, B., P. Falkai, et al. (1990). "Post-mortem volume measurements of limbic system and basal ganglia structures in chronic schizophrenics. Initial results from a new brain collection." Schizophrenia Research **3**(5-6): 295-301.
- Bogerts, B., E. Meertz, et al. (1985). "Basal ganglia and limbic system pathology in schizophrenia. A morphometric study of brain volume and shrinkage." Archives Of General Psychiatry **42**(8): 784-91.

- Borison, R. L. and B. I. Diamond (1978). "A new animal model for schizophrenia: interactions with adrenergic mechanisms." Biological Psychiatry **13**(2): 217-25.
- Brennwald, P., B. Kearns, et al. (1994). "sec9 is a snap-25-like component of a yeast snare complex that may be the effector of sec4 function in exocytosis." Cell **79**(2): 245-258.
- Brown, R., N. Colter, et al. (1986). "Postmortem evidence of structural brain changes in schizophrenia. Differences in brain weight, temporal horn area, and parahippocampal gyrus compared with affective disorder." Archives Of General Psychiatry **43**(1): 36-42.
- Browning, M. D., E. M. Dudek, et al. (1993). "Significant reductions in synapsin but not synaptophysin specific activity in the brains of some schizophrenics." Biological Psychiatry **34**(8): 529-35.
- Bruton, C. J., T. J. Crow, et al. (1990). "Schizophrenia and the brain: a prospective clinico-neuropathological study." Psychological Medicine **20**(2): 285-304.
- Bruton, C. J., J. R. Stevens, et al. (1994). "Epilepsy, psychosis, and schizophrenia: clinical and neuropathologic correlations." Neurology **44**(1): 34-42.
- Buckland, P., U. D'Souza, et al. (1997). "The effects of antipsychotic drugs on the mRNA levels of serotonin 5HT2A and 5HT2C receptors." Molecular Brain Research **48**(1): 45-52.
- Buckley, K. M., E. Floor, et al. (1987). "Cloning and sequence analysis of cDNA encoding p38, a major synaptic vesicle protein." Journal of Cell Biology **105**(6 Pt 1): 2447-56.
- Bunney, B. G., S. G. Potkin, et al. (1995). "New morphological and neuropathological findings in schizophrenia: a neurodevelopmental perspective." Clinical Neuroscience **3**(2): 81-8.
- Buzsaki, G., M. Penttonen, et al. (1995). "Possible physiological role of the perforant path-CA1 projection." Hippocampus **5**: 141-146.
- Cabalka, L. M., B. T. Hyman, et al. (1992). "Alteration in the pattern of nerve terminal protein immunoreactivity in the perforant pathway in Alzheimer's disease and in rats after entorhinal lesions." Neurobiology of Aging **13**(2): 283-91.
- Calhoun, M. E., M. Jucker, et al. (1996). "Comparative evaluation of synaptophysin-based methods for quantification of synapses." Journal of Neurocytology **25**(12): 821-8.

- Calverly, R., K. Bedi, et al. (1988). "Estimation of the numerical density of synapses in rat neocortex comparison of the "dissector" with an "unfolding" method." J Neurosci Methods **23**: 195.
- Cannon, T. D., S. A. Mednick, et al. (1994). "Developmental brain abnormalities in the offspring of schizophrenic mothers II. Structural brain characteristics of schizophrenia and schizotypal personality disorder." Archives Of General Psychiatry **51**: 995-962.
- Casanova, M. F. and J. E. Kleinman (1990). "The Neuropathology of Schizophrenia: A Critical Assessment of Research Methodologies." Biol. Psychiatry **27**: 353-362.
- Casanova, M. F., J. R. Stevens, et al. (1987). "Gliosis in schizophrenia [letter]." Biological Psychiatry **22**(9): 1172-5.
- Catsicas, S., D. Larhammar, et al. (1991). "Expression of a conserved cell-type-specific protein in nerve terminals coincides with synaptogenesis." PNAS **88**(3): 785-9.
- Chambers, R. A., J. Moore, et al. (1996). "Cognitive effects of neonatal hippocampal lesions in a rat model of schizophrenia." Neuropsychopharmacology **15**(6): 587-94.
- Christison, G. W., M. F. Casanova, et al. (1989). "A quantitative investigation of hippocampal pyramidal cell size, shape, and variability of orientation in schizophrenia." Archives Of General Psychiatry **46**(11): 1027-32.
- Chua, S. E. and P. J. McKenna (1995). "Schizophrenia--a brain disease? A critical review of structural and functional cerebral abnormality in the disorder." British Journal of Psychiatry **166**(5): 563-82.
- Colter, N., S. Battal, et al. (1987). "White matter reduction in the parahippocampal gyrus of patients with schizophrenia [letter]." Archives Of General Psychiatry **44**(11): 1023.
- Conrad, A. J., T. Abebe, et al. (1991). "Hippocampal pyramidal cell disarray in schizophrenia as a bilateral phenomenon." Archives Of General Psychiatry **48**(5): 413-7.
- Cotter, D., R. Kerwin, et al. (1997). "Alterations in hippocampal non-phosphorylated MAP2 protein expression in schizophrenia." Brain Research **765**(2): 238-46.

- Cotter, D., S. Wilson, et al. (2000). "Increased dendritic MAP2 expression in the hippocampus in schizophrenia." Schizophrenia Research **41**(2): 313-23.
- Cowan, D., M. Linial, et al. (1990). "Torpedo synaptophysin: evolution of a synaptic vesicle protein." Brain Research **509**(1): 1-7.
- Crow, T. J., J. Ball, et al. (1989). "Schizophrenia as an anomaly of development of cerebral asymmetry. A postmortem study and a proposal concerning the genetic basis of the disease." Archives Of General Psychiatry **46**(12): 1145-50.
- David, A. S., A. Malmberg, et al. (1997). "IQ and risk for schizophrenia: population-based cohort study." Psychol Med **27**: 1311-1323.
- Davies, C., D. Mann, et al. (1987). "A quantitative morphometric analysis of the neuronal and synaptic content of the frontal and temporal cortex in patients with Alzheimer's disease." Brain Res **517**: 69-75.
- Davies, K. G., J. B. Schweitzer, et al. (1998). "Synaptophysin immunohistochemistry densitometry measurement in resected human hippocampus: implication for the etiology of hippocampal sclerosis." Epilepsy Research **32**(3): 335-44.
- Dawirs, R. R., K. Hildebrandt, et al. (1998). "Adult treatment with haloperidol increases dentate granule cell proliferation in the gerbil hippocampus." J. Neural Transmission **105**: 317-327.
- Degreef, G., M. Ashtari, et al. (1991). "Follow up MRI study in first episode schizophrenia." Schizophrenia Research **5**(3): 204-6.
- DeGroot, D. and E. Bierman (1986). "Synapsin I: a synaptic-vesicle associated neuronal phosphoprotein." Biochem Pharmacol **35**: 4349.
- Deicken, R. F., M. Pegues, et al. (1999). "Reduced hippocampal N-acetylaspartate without volume loss in schizophrenia." Schizophrenia Research **37**(3): 217-23.
- DeKosky, S. and S. Scheff (1990). "Synaptic loss in frontal cortex biopsies in Alzheimer's diseases: correlation with disease severity." Ann Neurol **27**: 457-464.
- Deller, T., G. Adelman, et al. (1996). "The alvear pathway of the rat hippocampus." Cell Tissue Res **286**: 293-303.

- Deller, T., A. Martinez, et al. (1996). "A novel entorhinal projection to the rat dentate gyrus: direct innervation of proximal dendrites and cell bodies of granule cells and GABAergic neurons." Journal of Neuroscience **16**(10): 3322-3333.
- Done, D. J., T. J. Crow, et al. (1994). "Childhood antecedents of schizophrenia and affective illness: social adjustment at ages 7 and 11." BMJ **309**: 699-703.
- Dunn, L., G. Atwater, et al. (1993). "Effects of antipsychotic drugs on latent inhibition: sensitivity and specificity of an animal behavioral model of clinical drug action." Psychopharmacology **112**(2-3): 315-23.
- Dupuy-Davies, S. and C. R. Houser (1999). "Evidence for changing positions of GABA neurons in the developing rat dentate gyrus." Hippocampus **9**: 186-199.
- Dwivedi, Y. and G. Pandey (1999). "Effects of treatment with haloperidol, chlorpromazine, and clozapine on protein kinase C (PKC) and phosphoinositide-specific phospholipase C (PI-PLC) activity and on mRNA and protein expression of PKC and PLC isozymes in rat brain." J Pharmacol Exp Ther **291**(2): 688-704.
- Dwork, A. J. (1997). "Postmortem studies of the hippocampal formation in schizophrenia." Schizophrenia Bulletin **23**(3): 385-402.
- Eastwood, S. and P. Harrison (2000). "Hippocampal synaptic pathology in schizophrenia, bipolar disorder and major depression: a study of complexin mRNAs." Molecular Psychiatry **5**(4): 425-32.
- Eastwood, S. L., P. W. Burnet, et al. (1994). "Striatal synaptophysin expression and haloperidol-induced synaptic plasticity." Neuroreport **5**(6): 677-80.
- Eastwood, S. L., P. W. Burnet, et al. (1995). "Altered synaptophysin expression as a marker of synaptic pathology in schizophrenia." Neuroscience **66**(2): 309-19.
- Eastwood, S. L., P. W. Burnet, et al. (2000). "Expression of complexin I and II mRNAs and their regulation by antipsychotic drugs in the rat forebrain." Synapse **36**(3): 167-77.
- Eastwood, S. L. and P. J. Harrison (1995). "Decreased synaptophysin in the medial temporal lobe in schizophrenia demonstrated using immunohistochemistry." Neuroscience **69**(2): 339-43.

- Eastwood, S. L. and P. J. Harrison (1995). "Decreased synaptophysin in the medial temporal lobe in schizophrenia demonstrated using immunautoradiography." Neuroscience **69**(2): 339-343.
- Eastwood, S. L. and P. J. Harrison (1999). "Detection and quantification of hippocampal synaptophysin messenger RNA in schizophrenia using autoclaved, formalin-fixed, paraffin wax-embedded sections." Neuroscience **93**(1): 99-106.
- Eastwood, S. L., J. Heffernan, et al. (1997). "Chronic haloperidol treatment differentially affects the expression of synaptic and neuronal plasticity-associated genes." Molecular Psychiatry **2**(4): 322-9.
- Eastwood, S. L., B. McDonald, et al. (1995). "Decreased expression of mRNAs encoding non-NMDA glutamate receptors GluR1 and GluR2 in medial temporal lobe neurons in schizophrenia." Brain Research. Molecular Brain Research **29**(2): 211-23.
- Eckenhoff, M. F. and P. Rakic (1988). "Nature and fate of proliferative cells in the hippocampal dentate gyrus during the life span of the rhesus monkey." Journal of Neuroscience **8**(8): 2729-47.
- Edelmann, L., P. I. Hanson, et al. (1995). "Synaptobrevin binding to synaptophysin: a potential mechanism for controlling the exocytotic fusion machine." Embo journal **14**(2): 224-31.
- Eriksson, P. S., E. Perfilieva, et al. (1998). "Neurogenesis in the adult human hippocampus [see comments]." Nature Medicine **4**(11): 1313-7.
- Erlenmeyer-Kimling, L., U. H. Adamo, et al. (1997). "The New York High Risk Project: prevalence and comorbidity of axis I disorders in offspring of schizophrenia parents at 25 year follow-up." Archives Of General Psychiatry **54**: 1096-1102.
- Erlenmeyer-Kimling, L. and B. A. Cornblatt (1992). "A summary of attentional findings in the New York High-Risk Project." J. Psychiatr Res **26**: 405-426.
- Erlenmeyer-Kimling, L., E. Squires-Wheeler, et al. (1995). "The New York High Risk Project, psychoses and clust A personality disorders in offspring of schizophrenia parents at 23 years of follow-up." Archives Of General Psychiatry **52**: 857-865.
- Falkai, P. and B. Bogerts (1986). "Cell loss in the hippocampus of schizophrenics." European Archives of Psychiatry and neurological sciences **236**(3): 154-61.

- Falkai, P., B. Bogerts, et al. (1988). "Limbic pathology in schizophrenia: the entorhinal region--a morphometric study." Biological Psychiatry **24**(5): 515-21.
- Falkai, P., W. G. Honer, et al. (1999). "No evidence for astrogliosis in brains of schizophrenic patients. A post-mortem study." Neuropathology and Applied Neurobiology **25**(1): 48-53.
- Falkai, P., T. Schneider-Axmann, et al. (2000). "Entorhinal cortex pre-alpha cell clusters in schizophrenia: quantitative evidence of a developmental abnormality." Biol Psychiatry **47**(11): 937-43.
- Fernandez-Chacon, R. and T. C. Sudhof (1999). "Genetics of synaptic vesicle function: Toward the complete functional anatomy of an organelle." Annual Review of Physiology **61**: 753-776.
- Fish, B. (1977). "Neurobiologic antecedents of schizophrenia in children." Archives Of General Psychiatry **34**: 1297-1313.
- Fish, B., J. Marcus, et al. (1992). "Infants at risk for schizophrenia: sequelae of a genetic neurointegrative defect." Archives Of General Psychiatry **49**: 221-235.
- Fisman, M. (1975). "The brain stem in psychosis." British Journal of Psychiatry **126**: 414-22.
- Fog, R., H. Pakkenberg, et al. (1976). "High dose treatment of rats with perphenazine enanthate." Psychopharmacology **50**: 305-307.
- Freedman, R., M. Hall, et al. (1995). "Evidence in postmortem brain tissue for decreased numbers of hippocampal nicotinic receptors in schizophrenia." Biological Psychiatry **38**(1): 22-33.
- Friston, K. J. and C. D. Frith (1995). "Schizophrenia: a disconnection syndrome?" Clinical Neuroscience **3**(2): 89-97.
- Gall, C., N. Brecha, et al. (1984). "Ontogeny of enkephalin-like immunoreactivity in the rat hippocampus." Neuroscience **11**(2): 359-79.
- Garcia, E. P., P. S. McPherson, et al. (1995). "rbSec1A and B colocalize with syntaxin 1 and SNAP-25 throughout the axon, but are not in a stable complex with syntaxin." Journal of Cell Biology **129**(1): 105-20.
- Geddes, J. W., E. J. Hess, et al. (1990). "Lesions of hippocampal circuitry define synaptosomal-associated protein-25 (SNAP-25) as a novel presynaptic marker." Neuroscience **38**(2): 515-25.

- Goldberg, T. E., E. F. Torrey, et al. (1994). "Relations between neuropsychological performance and brain morphological and physiological measures in monozygotic twins discordant for schizophrenia." Psychiatry Research **55**(1): 51-61.
- Goldsmith, S. K. and J. N. Joyce (1995). "Alterations in hippocampal mossy fiber pathway in schizophrenia and Alzheimer's disease." Biological Psychiatry **37**(2): 122-6.
- Goto, S. and A. Hirano (1990). "Neuronal inputs to hippocampal formation in Alzheimer's disease and in parkinsonism-dementia complex on Guam." Acta Neuropathologica **79**(5): 545-50.
- Green, E. J. and J. M. Juraska (1985). "The dendritic morphology of hippocampal dentate granule cells varies with their position in the granule cell layer: a quantitative Golgi study." Experimental Brain Research **59**(3): 582-6.
- Gruzelier, J., K. Seymour, et al. (1988). "Impairments on neuropsychologic tests of temporohippocampal and frontohippocampal functions and word fluency in remitting schizophrenia and affective disorders." Archives Of General Psychiatry **45**(7): 623-9.
- Halasy, K. and P. Somogyi (1993). "Subdivisions in the multiple GABAergic innervation of granule cells in the dentate gyrus of the rat hippocampus." European Journal of Neuroscience **5**: 411-429.
- Hamos, J. E., L. J. DeGennaro, et al. (1989). "Synaptic loss in Alzheimer's disease and other dementias." Neurology **39**(3): 355-61.
- Hare, E. H. (1987). "Epidemiology of schizophrenia and affective psychoses." British Medical Bulletin **43**(3): 514-530.
- Harrison, P. (1996). "Advances in post mortem molecular neurochemistry and neuropathology: examples from schizophrenia research." British Medical Bulletin **52**(3): 527-538.
- Harrison, P. J. (1995). "On the neuropathology of schizophrenia and its dementia: neurodevelopmental, neurodegenerative, or both?" Neurodegeneration **4**(1): 1-12.
- Harrison, P. J. (1999). "The neuropathological effects of antipsychotic drugs." Schizophrenia Research **40**(2): 87-99.

- Harrison, P. J. (1999). "The neuropathology of schizophrenia. A critical review of the data and their interpretation." Brain **122** (Pt 4): 593-624.
- Harrison, P. J. and S. L. Eastwood (1998). "Preferential involvement of excitatory neurons in medial temporal lobe in schizophrenia [see comments] [published erratum appears in Lancet 1999 Jan 9;353(9147):154]." Lancet **352**(9141): 1669-73.
- Harrison, P. J., D. McLaughlin, et al. (1991). "Decreased hippocampal expression of a glutamate receptor gene in schizophrenia." Lancet **337**(8739): 450-2.
- Heckers, S., H. Heinsen, et al. (1991). "Hippocampal neuron number in schizophrenia. A stereological study." Archives Of General Psychiatry **48**(11): 1002-8.
- Heckers, S., H. Heinsen, et al. (1990). "Limbic structures and lateral ventricle in schizophrenia. A quantitative postmortem study [see comments]." Archives Of General Psychiatry **47**(11): 1016-22.
- Heinonen, O., H. Soininen, et al. (1995). "Loss of synaptophysin-like immunoreactivity in the hippocampal formation is an early phenomenon in Alzheimer's disease." Neuroscience **64**(2): 375-84.
- Heinsen, H., E. Gossmann, et al. (1996). "Variability in the human entorhinal region may confound neuropsychiatric diagnoses." Acta Anatomica **157**(3): 226-37.
- Hess, D. T., T. M. Slater, et al. (1992). "The 25 kDa synaptosomal-associated protein SNAP-25 is the major methionine-rich polypeptide in rapid axonal transport and a major substrate for palmitoylation in adult CNS." Journal of Neuroscience **12**(12): 4634-41.
- Hess, E. J., K. A. Collins, et al. (1994). "Deletion map of the coloboma (Cm) locus on mouse chromosome 2." Genomics **21**: 257-261.
- Hess, E. J., H. A. Jinnah, et al. (1992). "Spontaneous locomotor hyperactivity in a mouse mutant with a deletion including the Snap gene on chromosome 2." Journal of Neuroscience **12**(7): 2865-74.
- Hevner, R. F. and H. C. Kinnery (1996). "Reciprocal entorhinal-hippocampal connections established by human fetal midgestation." Journal of Comparative Neurology **372**: 384-394.

- Heyser, C. J., M. C. Wilson, et al. (1995). "Coloboma hyperactive mutant exhibits delayed neurobehavioral developmental milestones." Brain Research. Developmental Brain Research **89**(2): 264-9.
- Hicks, A., S. Davis, et al. (1997). "Synapsin I and syntaxin 1B: key elements in the control of neurotransmitter release are regulated by neuronal activation and long-term potentiation in vivo." Neuroscience **79**(2): 329-40.
- Honer, W., T. Beach, et al. (1994). "Hippocampal synaptic pathology in patients with temporal lobe epilepsy." Acta Neuropathologica **87**: 202-210.
- Honer, W. G., D. W. Dickson, et al. (1992). "Regional synaptic pathology in Alzheimer's disease." Neurobiology of Aging **13**(3): 375-82.
- Honer, W. G., L. Hu, et al. (1993). "Human synaptic proteins with a heterogeneous distribution in cerebellum and visual cortex." Brain Research **609**(1-2): 9-20.
- Honer, W. G., C. A. Kaufmann, et al. (1992). "Characterization of a synaptic antigen of interest in neuropsychiatric illness." Biological Psychiatry **31**(2): 147-58.
- Hoog, A., V. E. Gould, et al. (1988). "Tissue fixation methods alter the immunohistochemical demonstrability of synaptophysin." Ultrastructural Pathology **12**(6): 673-8.
- Hsu, S.-M., L. Raine, et al. (1981). "Use of avidin-biotin-peroxidase complex (ABC) in immunoperoxidase techniques: a comparison between ABC and unlabeled antibody (PAP) procedures." Journal of Histochemistry and Cytochemistry **29**: 577-580.
- Huang, X., S. Chen, et al. (1996). "Immunocytochemical detection of regional protein changes in rat brain sections using computer-assisted image analysis." Journal of Histochemistry and Cytochemistry **44**(9): 981-987.
- Humphrey, T. (1967). "The development of the hippocampal fissure." Journal of Anatomy **101**: 655-676.
- Hyman, B., G. Van Hoesen, et al. (1986). "Perforant pathway changes and the memory impairment of Alzheimer's disease." Ann. Neurol. **20**: 472-481.
- Hyman, B. T., G. W. Van Hoesen, et al. (1984). "Alzheimer's disease: cell-specific pathology isolates the hippocampal formation." Science **225**: 1168-1170.

- Ihara, Y., M. Sato, et al. (1986). "Morphological changes in rat striatal boutons after chronic methamphetamine and haloperidol treatment." Neurosci. Res. **3**: 403-410.
- Illowsky, B. P., D. M. Juliano, et al. (1988). "Stability of CT scan findings in schizophrenia: results of an 8 year follow-up study." Journal of Neurology, Neurosurgery and Psychiatry **51**(2): 209-13.
- Jago, R., J. H. Steel, et al. (1991). "Observer variation in quantification of immunocytochemistry by image analysis." Histochemical Journal **23**: 541-547.
- Jahn, R., W. Schiebler, et al. (1984). "A quantitative dot-immunobinding assay for proteins using nitrocellulose membrane filters." PNAS(USA) **81**: 1684.
- Jakob, H. and H. Beckmann (1986). "Prenatal developmental disturbances in the limbic allocortex in schizophrenics." Journal of Neural Transmission **65**(3-4): 303-26.
- Jakob, H. and H. Beckmann (1989). "Gross and histological criteria for developmental disorders in brains of schizophrenics." Journal of the Royal Society of Medicine **82**(8): 466-9.
- Jakob, H. and H. Beckmann (1994). "Circumscribed malformation and nerve cell alterations in the entorhinal cortex of schizophrenics. Pathogenetic and clinical aspects." Journal of Neural Transmission. general section **98**(2): 83-106.
- Jeste, D. V. and J. B. Lohr (1989). "Hippocampal pathologic findings in schizophrenia. A morphometric study." Archives Of General Psychiatry **46**(11): 1019-24.
- Jeste, D. V., J. B. Lohr, et al. (1998). "Adverse neurobiological effects of long-term use of neuroleptics: human and animal studies." J. Psychiatr. Res. **32**: 201-214.
- Jeste, D. V., J. b. Lohr, et al. (1992). "Study of neuropathological changes in the striatum following 4, 8, and 12 months of treatment with fluphenazine in rats." Psychopharmacology **106**: 154-160.
- Jones, P. B. and D. J. Dones (1997). From birth to onset: a developmental perspective of schizophrenia in two national birth cohorts. Neurodevelopment and adult psychopathology. M. S. Keshavan and R. M. Murray. Cambridge, Cambridge University Press: 119-136.

- Jones, P. B., B. Rodgers, et al. (1994). "Childhood developmental risk factors for adult schizophrenia in the British 1946 birth cohort." Lancet **334**: 1398-1402.
- Jonsson, S. A., A. Luts, et al. (1997). "Hippocampal pyramidal cell disarray correlates negatively to cell number: implications for the pathogenesis of schizophrenia." European Archives of Psychiatry and Clinical Neuroscience **247**(3): 120-7.
- Joyce, J. N., N. Lexow, et al. (1992). "Distribution of beta-adrenergic receptor subtypes in human post-mortem brain: alterations in limbic regions of schizophrenics." Synapse **10**(3): 228-46.
- Joyce, J. N., A. Shane, et al. (1993). "Serotonin uptake sites and serotonin receptors are altered in the limbic system of schizophrenics [see comments]." Neuropsychopharmacology **8**(4): 315-36.
- Kan, R., Y. Mori, et al. (1989). "A case of temporal lobe astrocytoma associated with epileptic seizures and schizophrenia-like psychosis." Japanese Journal of Psychiatry and Neurology **43**(1): 97-103.
- Kelley, J. J., X. M. Gao, et al. (1997). "The effect of chronic haloperidol treatment on dendritic spines in the rat striatum." Exp. Neurol. **146**: 471-478.
- Kerwin, R., S. Patel, et al. (1990). "Quantitative autoradiographic analysis of glutamate binding sites in the hippocampal formation in normal and schizophrenic brain post mortem." Neuroscience **39**(1): 25-32.
- Kirkby, D. L. and G. A. Higgins (1998). "Characterization of perforant path lesions in rat models of memory and attention." European Journal of Neuroscience **10**: 828-838.
- Knable, M. B. and D. R. Weinberger (1995). "Are mental diseases brain diseases? The contribution of neuropathology to understanding of schizophrenic psychoses." European Archives of Psychiatry and Clinical Neuroscience **245**(4-5): 224-30.
- Knaus, P., B. Marqueze-Pouey, et al. (1990). "Synaptoporin, a novel putative channel protein of synaptic vesicles." Neuron **5**(4): 453-62.
- Kosaka, T. (1996). "Synapses in the granule cell layer of the rat dentate gyrus: serial-sectioning study." Experimental Brain Research **112**: 237-243.

- Kosaka, T., K. Hama, et al. (1984). "GABAergic synaptic boutons in the granule cell layer of rat dentate gyrus." Brain Research **293**: 353-359.
- Kovelman, J. A. and A. B. Scheibel (1984). "A neurohistological correlate of schizophrenia." Biological Psychiatry **19**(12): 1601-21.
- Kovelman, J. A. and A. B. Scheibel (1986). "Biological substrates of schizophrenia." Acta Neurologica Scandinavica **73**(1): 1-32.
- Kraepelin, E., R. M. Barclay, et al. (1919). Dementia praecox and paraphrenia. Edinburgh, E&S Livingstone.
- Krimer, L. S., M. M. Herman, et al. (1997). "A qualitative and quantitative analysis of the entorhinal cortex in schizophrenia." Cerebral Cortex **7**(8): 732-9.
- Lawrie, S. M. and S. S. Abukmeil (1998). "Brain abnormality in schizophrenia. A systematic and quantitative review of volumetric magnetic resonance imaging studies [see comments]." British Journal of Psychiatry **172**: 110-20.
- Lawrie, S. M. and S. S. Abukmeil (1998). "Brain abnormality in schizophrenia: a systemic and quantitative review of volumetric magnetic resonance imaging studies." British Journal of Psychiatry **172**: 110-120.
- Lawston, J., A. Borella, et al. (2000). "Changes in hippocampal morphology following chronic treatment with the synthetic cannabinoid WIN 55,212-2." Brain Research **877**: 407-410.
- Lee, K. S., L. Gerbrandt, et al. (1982). "Axo-somatic synapses in the normal and X-irradiated dentate gyrus: factors affecting the density of afferent innervation." Brain Research **249**: 51-56.
- Leube, R. E. (1994). "Expression of the synaptophysin gene family is not restricted to neuronal and neuroendocrine differentiation in rat and human." Differentiation **56**(3): 163-71.
- Leube, R. E., U. Leimer, et al. (1994). "Sorting of synaptophysin into special vesicles in nonneuroendocrine epithelial cells." Journal of Cell Biology **127**(6 Pt 1): 1589-601.
- Lewis, E. R. and C. W. Cotman (1980). "Factors specifying the development of synapse number in the rat dentate gyrus: effects of partial target loss." Brain Research **191**: 35-52.

- Lichtman, J., J. Sunderland, et al. (1989). "High-resolution imaging of synaptic structure with a simple confocal microscope." New Biologist **1**: 75.
- Lipska, B. K., G. E. Jaskiw, et al. (1992). "Ibotenic acid lesion of the ventral hippocampus differentially affects dopamine and its metabolites in the nucleus accumbens and prefrontal cortex in the rat." Brain Research **585**(1-2): 1-6.
- Lipska, B. K., G. E. Jaskiw, et al. (1993). "Postpubertal emergence of hyperresponsiveness to stress and to amphetamine after neonatal excitotoxic hippocampal damage: a potential animal model of schizophrenia." Neuropsychopharmacology **9**(1): 67-75.
- Lipska, B. K., N. R. Swerdlow, et al. (1995). "Neonatal excitotoxic hippocampal damage in rats causes post-pubertal changes in prepulse inhibition of startle and its disruption by apomorphine." Psychopharmacology **122**(1): 35-43.
- Looney, M. R., F. C. J. Dohan, et al. (1999). "Synaptophysin immunoreactivity in temporal lobe epilepsy-associated hippocampal sclerosis." Acta Neuropathologica **98**(2): 179-85.
- Malmberg, A., G. Lewis, et al. (1998). "Premorbid adjustment and personality in people with schizophrenia." British Journal of Psychiatry **172**: 308-313.
- Marcus, J., J. Auerbach, et al. (1981). "Infants at risk for schizophrenia: the Jerusalem infant development study." Archives Of General Psychiatry **38**: 703-713.
- Marin, C. and E. Tolosa (1997). "Striatal synaptophysin levels are not indicative of dopaminergic supersensitivity." neuropharmacology **36**(8): 1115-7.
- Masliah, E., M. Ellisman, et al. (1992). "Three-dimensional analysis of the relationship between synaptic pathology and neuropil threads in Alzheimer disease." Journal of Neuropathology and Experimental Neurology **51**: 404-414.
- Masliah, E., A. M. Fagan, et al. (1991). "Reactive synaptogenesis assessed by synaptophysin immunoreactivity is associated with GAP-43 in the dentate gyrus of the adult rat." experimental Neurology **113**(2): 131-42.
- Masliah, E., M. Mallory, et al. (1993). "Quantitative synaptic alterations in the human neocortex during normal aging." Neurology **43**(1): 192-7.

- Masliah, E., R. D. Terry, et al. (1990). "Quantitative immunohistochemistry of synaptophysin in human neocortex: an alternative method to estimate density of presynaptic terminals in paraffin sections." Journal of Histochemistry and Cytochemistry **38**(6): 837-44.
- Masliah, E., R. D. Terry, et al. (1991). "Cortical and subcortical patterns of synaptophysinlike immunoreactivity in Alzheimer's disease." American Journal of Pathology **138**(1): 235-46.
- Masliah, E., R. D. Terry, et al. (1989). "Immunohistochemical quantification of the synapse-related protein synaptophysin in Alzheimer disease." Neuroscience Letters **103**(2): 234-9.
- Masliah, E., R. D. Terry, et al. (1990). "Diffuse plaques do not accentuate synapse loss in Alzheimer's disease." American Journal of Pathology **137**(6): 1293-7.
- Mayanil, C. S. and P. A. Knepper (1993). "Synaptic vesicle and synaptic membrane glycoproteins during pre- and postnatal development of mouse cerebral cortex, cerebellum and spinal cord." Developmental Neuroscience **15**(2): 133-45.
- McCarley, R. W., C. G. Wible, et al. (1999). "MRI anatomy of schizophrenia." Biol Psychiatry **45**(9): 1099-119.
- McKinney, W. T. and E. C. Moran (1981). "Animal models of schizophrenia." American Journal of Psychiatry **138**(4): 478-83.
- McLardy, L. T. (1975). "Hippocampal zinc and structural deficit in brains from chronic alcoholics and some schizophrenics." Journal of Orthomolecular Psychiatry **4**(1): 32-38.
- McMahon, H. T., V. Y. Bolshakov, et al. (1996). "synaptophysin, a major synaptic vesicle protein, is not essential for neurotransmitter release." Proc. Natl. Acad. Sci. U.s.a. **93**(10): 4760-4764.
- Melloni, R. H. J., L. M. Hemmendinger, et al. (1993). "Synapsin I gene expression in the adult rat brain with comparative analysis of mRNA and protein in the hippocampus." Journal of Comparative Neurology **327**(4): 507-20.
- Meshul, C. K., A. Janowsky, et al. (1992). "Coadministration of haloperidol and SCH-23390 prevents the increase in 'perforated' synapses due to either drug alone." Neuropsychopharmacology **7**: 285-293.
- Millar, D. A. and E. D. Williams (1982). "A step-wedge standard for the quantification of immunoperoxidase techniques." Histochem. J. **14**: 609-620.

- Mize, R. R., R. N. Holdefer, et al. (1988). "Quantitative immunocytochemistry using an image analyzer. I. Hardware evaluation, image processing, and data analysis." Journal of Neuroscience Methods **26**(1): 1-23.
- Mizukami, K., M. Sasaki, et al. (2000). "Immunohistochemical localization of gamma-aminobutyric acid(B) receptor in the hippocampus of subjects with schizophrenia." Neurosci Lett **283**(2): 101-4.
- Moghaddam, B. and B. Bunney (1990). "Acute effects of typical and atypical antipsychotic drugs on the release of dopamine from prefrontal cortex, nucleus accumbens, and striatum of the rat: an in vivo microdialysis study." J. Neurochem **54**(5): 1755-60.
- Mossberg, K., U. Arvidsson, et al. (1990). "Computerized quantification of immunofluorescence-labeled axon terminals and analysis of co-localization of neurochemicals in axon terminals with a confocal scanning laser microscope." J. Histochem. Cytochem. **38**(2): 179-190 As...].
- Nabors, L. B., E. Songu-Mize, et al. (1988). "Quantitative immunocytochemistry using an image analyzer. II. Concentration standards for transmitter immunocytochemistry." Journal of Neuroscience Methods **26**(1): 25-34.
- Nakahara, T., K. Nakamura, et al. (1998). "Effect of chronic haloperidol treatment on synaptic protein mRNAs in the rat brain." Brain Research. Molecular Brain Research **61**(1-2): 238-42.
- Nasrallah, H. A., N. C. Andreasen, et al. (1986). "A controlled magnetic resonance imaging study of corpus callosum thickness in schizophrenia." Biological Psychiatry **21**(3): 274-82.
- Nasrallah, H. A., M. McCalley-Whitters, et al. (1983). "A histological study of the corpus callosum in chronic schizophrenia." Psychiatry Research **8**(4): 251-60.
- Navone, F., R. Jahn, et al. (1986). "Protein p38: an integral membrane protein specific for small vesicles of neurons and neuroendocrine cells." Journal of Cell Biology **103**(6 Pt 1): 2511-27.
- Nestor, P. G., M. E. Shenton, et al. (1993). "Neuropsychological correlates of MRI temporal lobe abnormalities in schizophrenia [see comments]." American Journal of Psychiatry **150**(12): 1849-55.
- Nielsen, C. B. and M. Lyon (1978). "Evidence for cell loss in corpus striatum after long-term treatment with neuroleptic drug (flupenthixol) in rats." Psychopharmacology **59**: 85-89.

Osen-Sand, A., M. Catsicas, et al. (1993). "Inhibition of axonal growth by SNAP-25 antisense oligonucleotides in vitro and in vivo [see comments]." Nature **364**(6436): 445-8.

Otsu, N. (1979). "A threshold selection method from gray-level histograms." IEEE Transactions on Systems, Man, and Cybernetics **9**(1): 62-66.

Oyler, G. A., G. A. Higgins, et al. (1989). "The identification of a novel synaptosomal-associated protein, SNAP-25, differentially expressed by neuronal subpopulations." Journal of Cell Biology **109**(6 Pt 1): 3039-52.

Oyler, G. A., J. W. Polli, et al. (1991). "Developmental expression of the 25-kDa synaptosomal-associated protein (SNAP-25) in rat brain." PNAS **88**(12): 5247-51.

Pakkenberg, B. (1990). "Pronounced reduction of total neuron number in mediodorsal thalamic nucleus and nucleus accumbens in schizophrenics." Archives Of General Psychiatry **47**(11): 1023-8.

Pakkenberg, H., R. Fog, et al. (1973). "The long term effect of perphenazine enanthate on the rat brain. Some metabolic and anatomical observations." Psychopharmacologia (Berl) **29**: 329-336.

Pappolla, M. (1988). "Computerized image-analysis microspectroscopy of tissue sections." Arch. Pathol. Lab Med **112**: 787-790.

Parikh, I., S. March, et al. (1974). "Topics in the Methodology of Substitution Reactions with Agarose." Methods in Enzymology **34**: 77-102.

Parnas, J., F. Schulsinger, et al. (1982). "Behavioural precursors of schizophrenia spectrum, a prospective study." Archives Of General Psychiatry **39**: 659-664.

Patanow, C. M., J. R. Day, et al. (1997). "Alterations in hippocampal expression of SNAP-25, GAP-43, stannin and glial fibrillary acidic protein following mechanical and trimethyltin-induced injury in the rat." Neuroscience **76**(1): 187-202.

Paxinos, G. and C. Watson (1986). The Rat Brain in Stereotaxic Coordinates 2nd Ed. San Diego, California, Academic Press, Inc.

- Penke, B., M. Zarandi, et al. (1986). "Targeted immobilization of neurotransmitters and neuropeptides on agarose and on Acrylex polymers." Journal of Chromatography **376**(307): 307-14.
- Perdahl, E., R. Adolfsson, et al. (1984). "Synapsin I (protein I) in different brain regions in senile dementia of Alzheimer type and in multiinfarct dementia." J Neural Transmission **6**: 133.
- Peretti-Renucci, R., C. Feuerstein, et al. (1991). "quantitative image analysis with densitometry for immunohistochemistry and autoradiography of receptor binding sites--methodological considerations." J. Neurosci. Res. **28**(4): 583-600.
- Petit, T. L. and J. C. LeBoutillier (1990). "Quantifying synaptic number and structure: effects of stain and post-mortem delay." Brain Research **517**: 269-275.
- Pietraszek, M. and K. Ossowska (1998). "Chronic treatment with haloperidol diminishes the phencyclidine-induced sensorimotor gating deficit in rats." Naunyn-Schmiedebergs Archives of Pharmacology **357**(4): 466-71.
- Pilowsky, L. S., R. W. Kerwin, et al. (1993). "Schizophrenia: a neurodevelopmental perspective." Neuropsychopharmacology **9**(1): 83-91.
- Pool, C. W., S. Madlener, et al. (1984). "Quantification of antiserum reactivity in immunocytochemistry: two new methods for measuring peroxidase activity on antigen-coupled beads incubated according to an immunocytoperoxidase method." J. Histochem. Cytochem. **32**: 921-928.
- Porath, J. and R. Axen (1976). "Immobilization of enzymes to agar, agarose, and Sephadex supports." Methods in Enzymology **44**(19): 19-45.
- Proper, E. A., A. B. Oestreicher, et al. (2000). "Immunohistochemical characterization of mossy fibre sprouting in the hippocampus of patients with pharmaco-resistant temporal lobe epilepsy." Brain **123** (Pt 1): 19-30.
- Raber, J., P. P. Mehta, et al. (1997). "Coloboma hyperactive mutant mice exhibit regional and transmitter-specific deficits in neurotransmission." Journal of Neurochemistry **68**(1): 176-86.
- Rakic, P. and R. S. Nowakowski (1981). "The time of origin of neurons in the hippocampal region of the rhesus monkey." Journal of Comparative Neurology **196**(1): 99-128.

- Rasband, W. (1996). NIH Image Program, Research Services Branch (RSB) of the National Institute of Mental Health (NIMH), part of the National Institutes of Health (NIH).
- Risinger, C., A. G. Blomqvist, et al. (1993). "Evolutionary conservation of synaptosome-associated protein 25 kDa (SNAP-25) shown by *Drosophila* and *Torpedo* cDNA clones." Journal of Biological Chemistry **268**(32): 24408-14.
- Risinger, C. and D. Larhammar (1993). "Multiple loci for synapse protein SNAP-25 in the tetraploid goldfish." PNAS **90**(22): 10598-602.
- Roberts, G. W., N. Colter, et al. (1986). "Gliosis in schizophrenia: a survey." Biological Psychiatry **21**(11): 1043-50.
- Roberts, G. W., N. Colter, et al. (1987). "Is there gliosis in schizophrenia? Investigation of the temporal lobe." Biological Psychiatry **22**(12): 1459-68.
- Roberts, R. C., L. A. Gaither, et al. (1995). "Ultrastructural correlates of haloperidol induced oral dyskinesia in rat striatum." Synapse **20**: 234-243.
- Rosoklija, G., G. Toomayan, et al. (2000). "Structural abnormalities of subicular dendrites in subjects with schizophrenia and mood disorders: preliminary findings." arch gen Psychiatry **57**(4): 349-56.
- Rubin, P., A. Holm, et al. (1995). "Neuropsychological deficit in newly diagnosed patients with schizophrenia or schizophreniform disorder." Acta Psychiatrica Scandinavica **92**(1): 35-43.
- Saykin, A. J., R. C. Gur, et al. (1991). "Neuropsychological function in schizophrenia. Selective impairment in memory and learning." Archives Of General Psychiatry **48**(7): 618-24.
- Saykin, A. J., D. L. Shtasel, et al. (1994). "Neuropsychological deficits in neuroleptic naive patients with first-episode schizophrenia." Archives Of General Psychiatry **51**(2): 124-31.
- Scheff, S. and D. Price (1993). "Synapse loss in the temporal lobe in Alzheimer's disease." Ann Neurol **33**: 190-199.
- Scheller, R. H. (1995). "Membrane trafficking in the presynaptic nerve terminal." Neuron **14**: 1-20.
- Schiavo, G., A. Santucci, et al. (1993). "Botulinum neurotoxins serotypes A and E cleave SNAP-25 at distinct COOH-terminal peptide bonds." FEBS Letters **335**(1): 99-103.

- Schipper, J., T. R. Werkman, et al. (1984). "Quantitative immunocytochemistry of corticotropin-releasing factor (CRF). Studies on nonbiological models and on hypothalamic tissues of rats after hypophysectomy, adrenalectomy and dexamethasone treatment." Brain Research **293**(1): 111-8.
- Schlacter, M., G. Thomalske, et al. (1987). "Fine structure of GABAergic neurons and synapses in the human dentate gyrus." Brain Research **401**(1): 185-9.
- Schmajuk, N. A. (1987). "Animal models for schizophrenia: the hippocampally lesioned animal." Schizophrenia Bulletin **13**(2): 317-27.
- Schneider, K. (1959). Clinical Psychopathology (Translated by M.W. Hamilton). New York, Grune & Stratton.
- Schnell, S. A., W. A. Staines, et al. (1999). "Reduction of Lipofuscin-like autofluorescence in fluorescently labeled tissue." Journal of Histochemistry and Cytochemistry **47**(6): 719-730.
- Schulz, S. C., M. M. Koller, et al. (1983). "Ventricular enlargement in teenage patients with schizophrenia spectrum disorder." American Journal of Psychiatry **140**(12): 1592-5.
- See, R. E., M. A. Chapman, et al. (1992). "Comparison of chronic intermittent haloperidol and raclopride effects on striatal dopamine release and synaptic ultrastructure in rats." Synapse **12**: 147-154.
- Seidman, L. J., D. Yurgelun-Todd, et al. (1994). "Relationship of prefrontal and temporal lobe MRI measures to neuropsychological performance in chronic schizophrenia." Biological Psychiatry **35**(4): 235-46.
- Selemon, L. D., M. S. Lidow, et al. (1999). "Increased volume and glial density in primate prefrontal cortex associated with chronic antipsychotic drug exposure." Biol Psychiatry **46**: 151-160.
- Seress, L. (1992). The Dentate Gyrus and Its Role in Seizures (Epilepsy Res. Suppl. 7). Morphological variability and Developmental aspects of monkey and human granule cells: differences between the rodent and primate dentate gyrus. C. E. Ribak, C. M. Gall and I. Mody, Elsevier Science Publishers: 3-28.

- Seress, L. and J. Pokorny (1981). "Structure of the granular layer of the rat dentate gyrus. A light microscopic and Golgi study." Journal of Anatomy **133**: 181-195.
- Seress, L. and C. E. Ribak (1985). "A substantial number of asymmetric axosomatic synapses is a characteristic of the granule cells of the hippocampal dentate gyrus." Neuroscience Letters **56**: 21-26.
- Seress, L. and C. E. Ribak (1990). "Postnatal development of the light and electron microscopic features of basket cells in the hippocampal dentate gyrus of the rat." Anat. Embryol. **181**: 547-565.
- Seress, L. and C. E. Ribak (1992). "Ultrastructural features of primate granule cell bodies show important differences from those of rats: axosomatic synapses, somatic spines and infolded nuclei." Brain Research **569**: 353-357.
- Shimohama, S., S. Kamiya, et al. (1997). "Differential involvement of synaptic vesicle and presynaptic plasma membrane proteins in Alzheimer's disease." Biochemical and Biophysical Research Communications **236**(2): 239-42.
- Slomianka, L. and F. A. Geneser (1997). "Postnatal development of zinc-containing cells and neuropil in the hippocampal region of the mouse." Hippocampus **7**(3): 321-40.
- Soares, J. C. and R. B. Innis (1999). "Neurochemical brain imaging investigations of schizophrenia." Biol Psychiatry **46**(5): 600-15.
- Sommer, L. (1989). Analytical absorption spectrophotometry in the visible and ultraviolet. The Principles, Elsevier Science Publishers.
- Stevens, C. D., L. L. Altshuler, et al. (1988). "Quantitative study of gliosis in schizophrenia and Huntington's chorea." Biological Psychiatry **24**(6): 697-700.
- Stevens, J. R. (1982). "Neuropathology of schizophrenia." Archives Of General Psychiatry **39**(10): 1131-9.
- Stevens, J. R. (1992). "Abnormal reinnervation as a basis for schizophrenia: a hypothesis [published erratum appears in Arch Gen Psychiatry 1992 Sep;49(9):708]." Archives Of General Psychiatry **49**(3): 238-43.

- Steward, O. and S. A. Scoville (1976). "Cells of origin of entorhinal cortical afferents to the hippocampus and fascia dentata of the rat." Journal of Comparative Neurology **169**: 347-370.
- Steward, O. and S. Vinsant (1983). "The process of reinnervation in the dentate gyrus of the adult rat: a quantitative electron microscopic analysis of terminal proliferation and reactive synaptogenesis." J Comp Neurol **214**: 370-386.
- Straughan, B. and S. Walker (1976). Absorption of Light by a Medium. Spectroscopy. B. Straughan and S. Walker. Great Britain, Chapman and Hall. **3**: 122-123.
- Streefkerk, J. G. and M. Van der Ploeg (1973). "Quantitative aspects of cytochemical peroxidase procedures investigated in a model system." J. Histochem. Cytochem. **21**: 715-722.
- Streefkerk, J. G., M. Van der Ploeg, et al. (1975). "Agarose beads as matrices for proteins in cytophotometric investigations of immunohistoperoxidase procedures." J. Histochem. Cytochem. **23**: 243-250.
- Stridsberg, M., G. Lundqvist, et al. (1994). "Development of polyclonal antibodies and evaluation of a sensitive radioimmunoassay for detection and measurement of synaptophysin." Acta Neuropathologica **87**(6): 635-41.
- Sudhof, T. C., F. Lottspeich, et al. (1987). "The cDNA and derived amino acid sequences for rat and human synaptophysin." Nucleic Acids Research **15**(22): 9607.
- Sudhof, T. C., F. Lottspeich, et al. (1987). "A synaptic vesicle protein with a novel cytoplasmic domain and four transmembrane regions." Science **238**(4830): 1142-4.
- Sze, C. I., H. Bi, et al. (2000). "Selective regional loss of exocytotic presynaptic vesicle proteins in Alzheimer's disease brains." Journal of the Neurological Sciences **175**(2): 81-90.
- Takeichi, M. (1985). "Electron microscopic morphometric studies on synaptic vesicles of long-term CPZ-administered rat striatum." Folia Psychiatr. Neurol. Jpn **39**: 185-192.
- Tamamaki, N. and Y. Nojyo (1993). "Projection of the entorhinal layer II neurons in the rat as revealed by intracellular pressure-injection of neurobiotin." Hippocampus **3**: 471-480.
- Taylor, C. R. (1978). "Immunoperoxidase techniques. Practical and theoretical aspects." Arch. Path. Lab. Med. **102**: 113-21.

- Tcherepanov, A. A. and B. P. Sokolov (1997). "Age-related abnormalities in expression of mRNAs encoding synapsin 1A, synapsin 1B, and synaptophysin in the temporal cortex of schizophrenics." Journal of Neuroscience Research **49**(5): 639-44.
- Terry, R. D., E. Masliah, et al. (1991). "Physical basis of cognitive alterations in alzheimer's disease: synapse loss is the major correlate of cognitive impairment." Ann. Neurol **30**: 572-580.
- Todtenkopf, M. S. and F. M. Benes (1998). "Distribution of glutamate decarboxylase65 immunoreactive puncta on pyramidal and nonpyramidal neurons in hippocampus of schizophrenic brain." Synapse **29**(4): 323-32.
- Trojanowski, J. Q., M. A. Obrocka, et al. (1983). "A comparison of eight different chromagen protocols for the demonstration of immunoreactive neurofilaments or glial filaments in rat cerebellum using the peroxidase-anti-peroxidase method and monoclonal antibodies." Journal of Histochemistry and Cytochemistry **31**: 1217-1223.
- Uranova, N. A., D. D. Orlovskaya, et al. (1991). "Morphometric study of synaptic patterns in the rat caudate nucleus and hippocampus under haloperidol treatment." Synapse **7**: 253-259.
- Valnes, K. and P. Brandtzaeg (1982). "Comparison of paired immunofluorescence and paired immunoenzyme staining methods based on primary antisera from the same species." J. Histochem. Cytochem **30**: 513-24.
- Varty, G. B., C. A. Marsden, et al. (1999). "Reduced synaptophysin immunoreactivity in the dentate gyrus of prepulse inhibition-impaired isolation-reared rats." Brain Research **824**(2): 197-203.
- Vawter, M. P., A. L. Howard, et al. (1999). "Alterations of hippocampal secreted N-CAM in bipolar disorder and synaptophysin in schizophrenia." Molecular Psychiatry **4**(5): 467-75.
- Velakoulis, D. and C. Pantelis (1996). "What have we learned from functional imaging studies in schizophrenia? The role of frontal, striatal and temporal areas." Australian and New Zealand Journal of Psychiatry **30**(2): 195-209.
- Vincent, S. L., J. McSparren, et al. (1991). "Evidence for ultrastructural changes in cortical axo-dendritic synapses following longterm treatment with haloperidol or clozapine." Neuropsychopharmacology **5**: 147-155.

- Vita, A., M. Dieci, et al. (1995). "Language and thought disorder in schizophrenia: brain morphological correlates." Schizophrenia Research **15**(3): 243-51.
- Vivino, M. *Fundamentals of Densitometry*. **2001**.
- Wakabayashi, K., W. G. Honer, et al. (1994). "Synapse alterations in the hippocampal-entorhinal formation in Alzheimer's disease with and without Lewy body disease." Brain Research **667**(1): 24-32.
- Walker, E. F., T. Savoie, et al. (1994). "Neuromotor precursors of schizophrenia." Schizophrenia Bulletin **20**: 441-445.
- Ward, K. E., L. Friedman, et al. (1996). "Meta-analysis of brain and cranial size in schizophrenia." Schizophrenia Research **22**: 197-223.
- Weinberger, D. R. (1999). "Cell biology of the hippocampal formation in schizophrenia." Biological Psychiatry **45**(4): 395-402.
- White, C., A. Simmons, et al. (1993). "Determination of synaptic density using an enzyme-linked immunosorbant assay (ELISA) and monoclonal antibody SY38 to synaptophysin." J. Neuropathol Exp Neurol **52**: 263.
- Wiedenmann, B. and W. W. Franke (1985). "Identification and localization of synaptophysin, an integral membrane glycoprotein of Mr 38,000 characteristic of presynaptic vesicles." Cell **41**(3): 1017-28.
- Wiedenmann, B., H. Rehm, et al. (1988). "Fractionation of synaptophysin-containing vesicles from rat brain and cultured PC12 pheochromocytoma cells." FEBS Letters **240**(1-2): 71-7.
- Wilchek, M. and T. Miron (1974). "Stable, high capacity and non charged agarose derivatives for immobilization of biologically active compounds and for affinity chromatography." Molecular & Cellular Biochemistry **4**(3): 181-7.
- Witter, M. P. and D. G. Amaral (1991). "Entorhinal cortex of the monkey. V. Projections to the dentate gyrus, hippocampus, and subicular complex." Journal of Comparative Neurology **307**: 437-459.
- Witter, M. P., F. G. Wouterlood, et al. (2000). "Anatomical organization of the parahippocampal-hippocampal network." Annals of the New York Academy of Sciences **911**: 1-24.

- Wolf, H. K., R. Buslei, et al. (1996). "NeuN: a useful neuronal marker for diagnostic histopathology." Journal of Histochemistry and Cytochemistry **44**(10): 1167-71.
- Woodman, P. G. (1997). "The roles of NSF, SNAPs, and SNAREs during membrane fusion." Biochimica et Biophysica Acta **1357**: 155-172.
- Woods, B. T., D. Yurgelun-Todd, et al. (1990). "Progressive ventricular enlargement in schizophrenia: comparison to bipolar affective disorder and correlation with clinical course." Biological Psychiatry **27**(3): 341-52.
- Woodson, W., L. Nitecka, et al. (1989). "Organisation of the GABAergic system in the rat hippocampal formation: a quantitative immunocytochemical study." Journal of Comparative Neurology **280**: 254-271.
- Wright, I. C., S. Rabe-Hesketh, et al. (2000). "Meta-analysis of regional brain volumes in schizophrenia." Am J Psychiatry **157**(1): 16-25.
- Wygant, M. D. and J. W. Nelson (2001). A Guide to Densitometer Evaluation (Technical Note #54). Sunnyvale, CA, Molecular Dynamics.
- Zaidel, D. W., M. M. Esiri, et al. (1997). "The hippocampus in schizophrenia: lateralized increase in neuronal density and altered cytoarchitectural asymmetry." Psychological Medicine **27**(3): 703-13.
- Zaidel, D. W., M. M. Esiri, et al. (1997). "Size, shape, and orientation of neurons in the left and right hippocampus: investigation of normal asymmetries and alterations in schizophrenia." American Journal of Psychiatry **154**(6): 812-8.
- Zhong, C. Z., D. J. Hayzer, et al. (1992). "Molecular cloning of a cDNA encoding a novel protein related to the neuronal vesicle protein synaptophysin." Biochimica et Biophysica Acta **1129**(2): 235-8.

APPENDIX I: Autofluorescence artifacts

Continued attempts to colocalise synaptophysin and SNAP-25 from normal human formalin fixed hippocampal tissue using epi-fluorescent and confocal microscopy showed unacceptably high autofluorescent background. Such autofluorescent artifacts are common to tissue that has been formalin fixed and to human tissue from older subjects. Since the only human tissues available were all fixed with neutral buffered formalin and were mainly from elderly patients, I tried protocols to reduce or eliminate the autofluorescence through chemical treatment.

A. The Basis of Autofluorescence & Attempts to block Autofluorescence

The fluorescent pigment lipofuscin accumulates with age in the cytoplasm of cells of the CNS. Because of its broad excitation and emission spectra, the presence of lipofuscin-like autofluorescence complicates the use of fluorescence microscopy. Recently, studies have shown substantial reductions of lipofuscin-like autofluorescence in CNS tissue sections after treatment with CuSO_4 or Sudan Black (Schnell, Staines et al. 1999). The latter was found to be especially good at eliminating lipofuscin-like autofluorescence in aged human CNS tissue.

A.1. Fluorescent immunohistochemistry

Monoclonal antibodies reactive with synaptophysin (SP15, mouse immunoglobulin M) and SNAP-25 (SP12, mouse immunoglobulin G) were used.

Normal human sections were deparaffinized by sequential immersion in xylene and decreasing concentrations of alcohol followed by TBS. This was followed by incubation in TBS plus 0.2% Triton X-100 for 30 min. Non-specific immunoreactivity was blocked by incubation in TBS-5% nonfat, powdered milk for 1 hr at RT. Slides were incubated with both presynaptic primary antibodies diluted 1:10 in milk against synaptophysin (SP15, mouse immunoglobulin M) and SNAP-25 (SP12, mouse immunoglobulin G) overnight at 4°C. Slides were then washed in TBS (three times for 10 min) at RT. Fluorescent secondary antibodies (Jackson Immunolabs) diluted 1:50 in TBS-milk were then added for 1 hr at RT. Following a TBS wash (three times for 10 min) at RT, sections were chemically treated to eliminate autofluorescence before coverslipping with glycerol. In addition, for cross-reactivity controls, two sections underwent all incubation steps and autofluorescent reduction procedures, but in which the primary antibody SP15 or SP12, respectively, were replaced by tissue culture medium conditioned by the parent, nonsecreting myeloma cell line; while for negative controls, another two sections only underwent CuSO₄ or Sudan Black treatment, respectively, lacking both primary antibody and fluorescent secondary antibody treatment.

A.2. Chemical treatment: Reducing Autofluorescence

Treatment A: Cupric Sulfate.

After fluorescent immunohistochemistry, the sections were dipped briefly in distilled H₂O, and treated with CuSO₄ (Fisher Scientific; Pittsburgh, PA) in ammonium acetate buffer (50 mM CH₃COONH₄, pH 5.0) for 60 min, dipped briefly in distilled H₂O, and coverslipped in glycerol.

Treatment B: Sudan Black.

After fluorescent immunohistochemistry, the sections were treated with a 1% solution of Sudan Black B (Allied Chemical; New York, NY) in 70% alcohol for 5 min. followed by sequential immersion in decreasing concentrations of alcohol, dipped briefly in distilled H₂O, and coverslipped in glycerol.

Even after either CuSO₄ or Sudan Black treatment, the negative controls showed unacceptably high background fluorescence suggesting that chemical treatment to reduce autofluorescence was ineffective for my formalin fixed aged human hippocampal tissue. Hampered by these results using fluorescent microscopy, I sought to develop a double immunostaining technique using simple light microscopy.